

Principles of c-di-GMP Signaling

Characterization of a Second Messenger System Orchestrating Bacterial Life Style

Inauguraldissertation

zur Erlangung der Würde eines Doktors der Philosophie

vorgelegt der

Philosophisch-Naturwissenschaftlichen Fakultät

Der Universität Basel

Von

Beat Christen aus Basel, Schweiz

Basel 2007

Genehmigt von der Philosophisch-Naturwissenschaftlichen Fakultät auf
Antrag von

- Prof. Dr. Urs Jenal
- Prof. Dr. Guy R. Cornelis
- Prof. Dr. Christoph. Dehio

Basel, den 13.2.2007

Prof. Dr. Hans-Peter Hauri

This work was performed in the laboratory of Prof. Dr. Urs Jenal in the division of molecular microbiology at the Biozentrum of the University of Basel and was supported by Swiss Science Foundation Fellowship 3100A0-108186 to U.J..

I would like to thank Prof Dr. Urs Jenal for giving me the opportunity to do my PhD thesis in his group.

Abstract

Bacteria are able to switch between two mutually exclusive lifestyles, motile single cells and sedentary multicellular communities, known as biofilms, that colonize surfaces. Recent studies demonstrated that the global bacterial second messenger c-di-GMP orchestrates the developmental transition between both lifestyles. In a wide variety of bacterial species high intracellular c-di-GMP levels provoke excretion of protective and adhesive exopolymeric substances and inhibit flagella and pili based cell motility. Synthesis and degradation of c-di-GMP is catalyzed by diguanylate cyclases (DGC's) and c-di-GMP-specific phosphodiesterases (PDE), respectively. Although the enzymes responsible for the synthesis of c-di-GMP have been recently identified, little information is available on general regulatory principles of the c-di-GMP signaling circuitry. Here we present genetic and biochemical approaches in combination with structural analysis to elucidate the molecular mechanisms of signal transduction, signal modulation and signal inactivation.

In (Christen and Christen et al 2007, PNAS) we describe the isolation of several c-di-GMP binding proteins from *Caulobacter crescentus* by affinity chromatography. One of these proteins, DgrA, is a PilZ homolog involved in mediating c-di-GMP-dependent control of *C. crescentus* cell motility. Biochemical and structural analysis of DgrA and homologs from *C. crescentus*, *Salmonella typhimurium* and *Pseudomonas aeruginosa* identified this protein family as the first class of specific diguanylate receptors. Our studies suggested a general mechanism for c-di-GMP binding and signal transduction whereby increased concentrations of c-di-GMP are sensed by DgrA through direct binding and induce conformational changes of the diguanylate receptor that block motility by interfering with motor function rather than flagellar assembly.

In (Christen and Christen et al 2006, JBC) we demonstrate that an allosteric binding site for c-di-GMP (I-site) is responsible for non-competitive product inhibition of DGC's. The I-site was mapped in both multi- and single domain DGC proteins and shown to be fully contained within the GGDEF domain itself. *In vivo* evolution experiments combined with kinetic analysis of the obtained I-site mutants led to the definition of an RXXD motif as the core allosteric binding site for c-di-GMP. Based on these results and based on the observation that the I-site is conserved in a majority of known and potential DGC proteins, we propose that product inhibition of DGC's is of fundamental importance for c-di-GMP signaling and cellular homeostasis. The definition of the I-site binding pocket provides an entry point into unraveling the molecular mechanisms of ligand-protein interactions involved in c-di-GMP signaling, makes DGC's a valuable target for drug design and offers new strategies against biofilm-related diseases.

In (Christen et al 2005, JBC) we show biochemically that CC3396, a GGDEF-EAL composite protein from *C. crescentus*, is a soluble PDE. The PDE activity, rapidly converts c-di-GMP into the linear dinucleotide pGpG is confined to the C-terminal EAL domain of CC3396, depends on the presence of Mg^{2+} ions and is strongly inhibited by Ca^{2+} ions. Remarkably, the associated GGDEF domain, which contains an altered active site motif (GEDEF), lacks detectable DGC activity. Instead, this domain is able to bind GTP and in response activates the PDE activity in the neighboring EAL domain. PDE activation is specific for GTP (K_D 4 μ M) and operates by lowering the K_M for c-di-GMP of the EAL domain to a physiologically significant level (420 nM). Mutational analysis suggested that the substrate-binding site (A-site) of the GGDEF domain is involved in the GTP-dependent regulatory function, arguing that a catalytically inactive GGDEF domain has retained the ability to bind GTP and in response can activate the neighboring EAL domain. Based on this we propose that the c-di-GMP-specific PDE activity is confined to the EAL domain, that GGDEF domains can either catalyze the formation of c-di-GMP or can serve as regulatory domains and that c-di-GMP-specific phosphodiesterase activity is coupled to the cellular GTP level in bacteria.

In addition to the contribution in understanding the c-di-GMP signaling circuitry we characterized in (Stephens et al 2007, JBac) the metabolic enzymes and regulators of D-xylose catabolism in *C. crescentus* by genetic and biochemical methods. A saturated transposon screen was used to define the *xyIXABCD* operon consisting of five genes, essential for xylose degradation. Subsequently biochemical and bioinformatical approaches were applied to provide enzymatic functions and predict possible conversion pathways for xylose catabolism. We demonstrated that the *xyIXABCD* operon is tightly control via a LacI like repressor and defined determinants of the xylose operator, critical for negative control of *xyIXABCD* transcription.

Index

1	Introduction.....	1
1.1	Signal transduction.....	2
1.2	Bacterial second messenger systems	2
1.3	Cellular function of GGDEF and EAL domain proteins.....	3
1.4	Involvement of c-di-GMP signaling in <i>C. crescentus</i> pole development	5
1.5	C-di-GMP signaling survey	7
2	Aim of the thesis	9
3	Results	10
3.1	DgrA is a member of a new family of cyclic di-GMP receptors and controls flagellar motor functions in <i>Caulobacter crescentus</i>	11
3.2	Allosteric Control of Cyclic di-GMP Signaling.....	42
3.3	Identification and Characterization of a Cyclic di-GMP-specific Phospho-diesterase and Its Allosteric Control by GTP	62
3.4	Genetic Analysis of a Novel Pathway for D-xylose Metabolism in <i>Caulobacter crescentus</i> 73	
4	Unpublished results	80
4.1	Isolation of <i>S. enterica</i> Transposon Mutants Impaired in c-di-GMP Dependent EPS Production.....	81
4.1.1	Introduction	82
4.1.2	Results and Discussion.....	83
4.1.3	Material and Methods.....	85
4.2	Genetic Identification of the Xylose Repressor <i>xyIR</i> and the Xylose Operator <i>xyIO</i> site .	87
4.2.1	Introduction	88
4.2.2	Results and Discussion.....	89
4.2.3	Material and Methods.....	96
5	Discussion.....	98

6 Outlooks 106

7 Appendix 107

List of Strains 108

References 116

List of figures 120

List of tables 121

Acknowledgments 122

Curriculum vitae 123

Abbreviations

AC	adenylate cyclase
c-di-GMP	cyclic diguanylic acid
CR	Congo Red
DGC	diguanylate cyclase
DgcA	diguanylate cyclase A (CC3285)
DGR	diguanylate receptor
DgrA	diguanylate receptor protein A (CC1599)
DgrB	diguanylate receptor protein B (CC3165)
EDTA	ethylenediaminetetraacetic acid
EGTA	ethylene glycol-bis(β -aminoethyl ether)-N,N,N',N'-tetra acetic acid
ESI-MS	electrospray ionization-mass spectrometry
EXSY	exchange spectroscopy
GC	guanylate cyclase
H6	hexa-histidine tag
HPLC	high performance liquid chromatography
HSQC	heteronuclear single quantum coherenc
IPTG	isopropyl 1-thio- β -D-galactopyranoside
LB	luria broth
MeOH	methanol
NMR	nuclear magnetic resonance
NOESY	nuclear overhauser effect spectroscopy
PAGE	polyacrylamide gel electrophoresis
PDE	phosphodiesterase
PYE	peptone yeast extract medium
PdeA	phosphodiesterase A (CC3396)
pGpG	linear diguanylic acid
rdar	red, dry, and rough phenotype

1 Introduction

1.1 Signal transduction

In a simple model, cells of living organisms can be interpreted as nondeterministic finite state automata (1). Various intra and extra cellular inputs are continuously perceived by specific receptors and transduced via complex signaling networks to affect and adapt the metabolic and developmental cell state. Convergent signaling pathways are often used to integrate multiple stimuli and control regulators by implementing logical operations. These regulators, in turn, frequently modulate divergent multiple output functions. For instance, signaling cascades affect gene expression by exercising transcriptional or translational control or modulate enzyme activities posttranslationally over covalent or noncovalent protein modifications. The majority of prokaryotic signal transduction systems consist of a receptor domain that is directly fused to an regulatory output domain (2). These so called one-component systems often link transcription of metabolic pathway genes to the availability of substrates (see chapter 4.2). The simple design of one-component signaling systems can be extended by physical separation of input and output domains to two different proteins interlinked via a phospho-relay. For instance, in two-component system a receptor coupled histidine kinase protein activates the output domain of a partner response regulator protein via phosphorylation (3). Often stimuli activated receptors do not directly interact with downstream regulators but instead affect the intracellular concentration of diffusible molecules that act as second messengers relaying the input information to the regulators. This signaling principle allows to couple different sensory inputs with synthesis and degradation of the second messenger and provides the opportunity of signal amplification and noise repression.

1.2 Bacterial second messenger systems

Small purine nucleotides are often used as second messengers in prokaryotic signaling systems (4,5). Whereas the cyclic mononucleotide cAMP is devoted to the regulation of alternative carbon sources catabolism and is synthesized by the action of adenylate cyclase (6), a derivative of GTP, the alarmone ppGpp is produced by a GTP pyrophosphokinase in response to nutritional deprivation and causes transcriptional repression of ribosomal RNA and tRNA or activates genes for amino acid synthesis and transport (7,8). Recently the cyclic dinucleotide c-di-GMP has been recognized as an important bacterial second messenger, widely used to orchestrate biofilm development (9).

1.3 Cellular function of GGDEF and EAL domain proteins

Cyclic diguanylate (c-di-GMP) was first isolated as an allosteric activator of cellulose synthase in *G. xylinum* (10-12). Two enzymes, diguanylate cyclase (DGC) and c-di-GMP specific phosphodiesterases (PDE) synthesize c-di-GMP out of two GTP molecules or hydrolyse c-di-GMP into the linear dinucleotide pGpG, respectively. Biochemical purification studies followed by a reverse genetic approach identified 6 isozymes composed of N-terminal PAS or GAF domains followed by a central GGDEF and a C-terminal EAL domain. The later two domains, which are named after a highly conserved signature sequence, are involved in enzymatic c-di-GMP turnover (13). Further genetic studies of cellulose synthesis in *R. leguminosarum* confirmed that expression of CelR2 (14), a regulator containing a putative response regulator with a C-terminal GGDEF domain, also causes activation of cellulose production, arguing that the GGDEF domain might possess DGC activity.

In *Pseudomonades*, several GGDEF and EAL domain proteins cause dramatic changes in colony morphology (15), autoaggregative behavior (16) or affect twitching motility (17). In particular, the ability to form small colony variants on low-osmolarity agar plates (18) was linked to the activity of WspR that constitutes a GGDEF-type response regulator. WspR regulates the production of an acetylated form of cellulose and controls expression of *cup* genes that encode a putative fimbrial adhesin (19,20). Interestingly, PvrP, an EAL domain protein with a N-terminal response regulator domain, was identified in a genetic screen as a regulatory protein that, unlike WspR, suppressed autoaggregation (21). In addition, transposon mutants inactivating the GGDEF-EAL composite protein FimX had defective type IV pili assembly and were impaired in twitching motility (17).

In *Vibrio* other GGDEF-EAL composite proteins were found to inversely regulate swarming and capsular polysaccharide production. Mutations in the *V. parahaemolyticus* gene *scrC* caused a rugose colony morphotype and blocked swarming motility (22), whereas *V. cholera* *rocS* mutants were unable to switch to the rugose phenotype under rugose inducing growth conditions (23). Similar to *scrC*, a *V. cholera* El Tor with a Tn10 insertion mutation in the *mbaA* gene results in the overproduction of exopolysaccharide and in dramatic differences in the mature biofilm architecture, but in contrast to *scrC* had no effect on the production of flagella or type IV pili (24). GGDEF and EAL domain proteins also affect expression of virulence factors such as cholera toxin. Interestingly, the *vieA* gene, coding for a response regulator protein with a central EAL domain, was discovered to affect transcription of the cholera toxin genes (*ctxAB*) during *V. cholera* host infection (25).





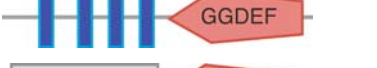








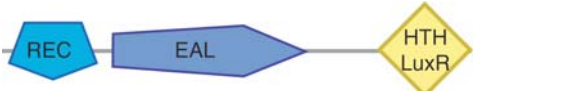
Domain organization	Name	Organism	Ref
	PleD	<i>C. crescentus</i>	(26)
	CelR2	<i>R. leguminosarum</i>	(14)
	ActA	<i>M. xanthus</i>	(27,28)
	WspR	<i>P. aeruginosa</i>	(19,20)
	HmsT	<i>Y. pestis</i>	(29)
	AdrA	<i>S. enterica</i>	(30,31)
	DgcA1	<i>G. xylinus</i>	(13)
	PdeA1	<i>G. xylinus</i>	(13)
	FimX	<i>P. aeruginosa</i>	(17)
	ScrC	<i>V. parahaemolyticus</i>	(22)
	MbaA	<i>V. cholera</i>	(24)
	RocS	<i>V. cholera</i>	(23)
	PvrR	<i>P. aeruginosa</i>	(21)
	VieA	<i>V. cholera</i>	(25)

Table 1: domain organization of different GGDEF and EAL proteins

The temperature dependent haemin storage (Hms) locus of *Yersinia pestis* has been shown to be involved in the blockage of fleas foregut and thereby causes increased transmission of *Y. pestis* from fleas to mammals (32). *hmsT*, coding for a GGDEF domain protein, and a four gene operon *hmsHFRS* are essential for induction of a haemin absorption system and auto aggregative behavior in the flea vector (29).

Concomitantly with curli fimbria expression, *Salmonella spp.* and *E. coli* cells develop a rough and dry colony morphology and bind the dye Congo Red (33-35). These characteristic phenotypic change become often manifested after prolonged incubation at temperatures below 37°C. In *S. enterica* serovar Typhimurium the transcriptional activator *agfD* has been demonstrated to control

this transition (30,31). AgfD not only regulates the *agfBA(C)* operon, encoding for fimbrial subunit proteins, but also activates expression of the putative transmembrane protein AdrA. Interestingly, mutants in the GGDEF domain protein AdrA lacked long-range intracellular adhesion and missed a unknown extracellular substance.

The *M. xanthus* GGDEF-type response regulator ActA regulates the maximum level of the morphogenetic C-signal, a cell surface associated protein that is required to pattern cell movement and shape the fruiting body. As a result, *actA* mutants are able to undergo starvation induced aggregation, but failed to sporulate (27,28).

1.4 Involvement of c-di-GMP signaling in *C. crescentus* pole development

Beside these examples, insights into the molecular function of the GGDEF domain was also provided by studies with the model organism *C. crescentus* contributing substantially to a better understanding of c-di-GMP signaling.

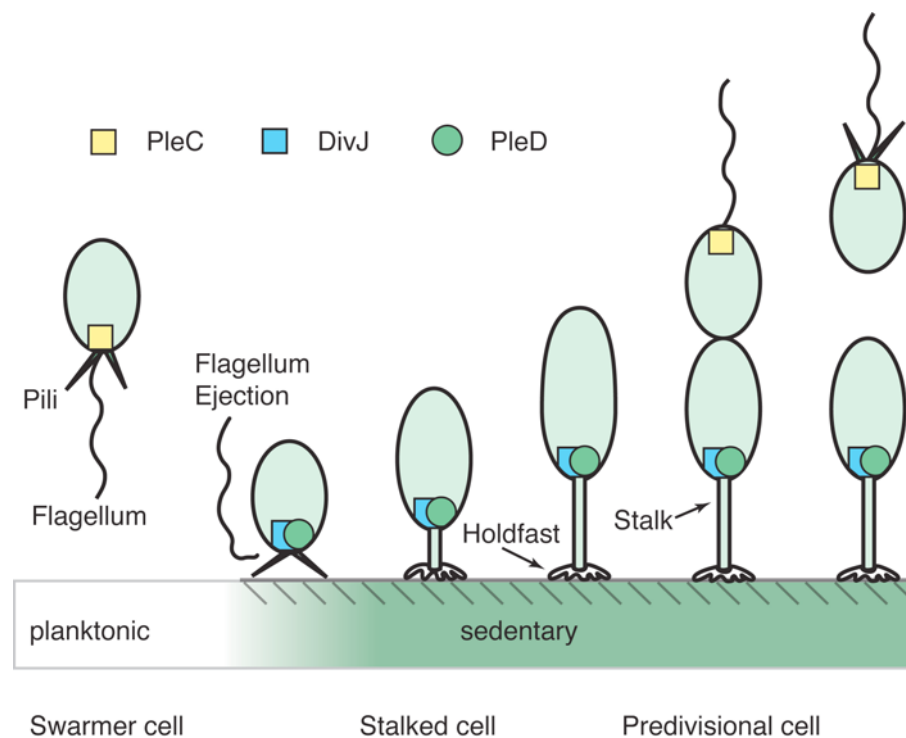


Figure 1: dynamic localization of PleD, PleC and DivJ over *C. crescentus* cell cycle

Dynamic localization of the histidine kinases PleC and DivJ and the response regulator PleD during the *Caulobacter crescentus* cell cycle. Cytoplasmic PleD (light green) localizes to the differentiating swarmer pole (green circle) upon transition into a stalked cell. Illustration according to (9,26,36).

C. crescentus has a biphasic life cycle and divides asymmetrically into two morphologically distinct daughter cells. A planktonic, motile swarmer cell type undergoes an obligate developmental transition into a surface attached stalked cell before it regain replication competence. This switch in life style requires continuous remodeling of polar cell organelles including correct assembly of a single flagellum, pili and their subsequent replacement by an adhesive holdfast at the tip of an cell wall protuberance called stalk (see Figure 1).

Genetic studies lead to the identification of a two component signaling cascade responsible for polar organelle development (37-41). Two sensor histidine kinases PleC, DivJ and the response regulators DivK and PleD are dynamically localized to the cell poles during cell cycle (26,36,42,43). Both histidine kinases integrate temporal and special signals and modulate the phosphorylation state of the unorthodox response regulator PleD during cell cycle progression (26). PleD harbors two N-terminal receiver domains and a C-terminal GGDEF domain. Genetic evidence suggested that the phosphorylated form of PleD is recruited to the differentiating stalk pole whereby it blocks flagellar motor function, activates flagellar ejection and initiates stalk formation (41,44). Further studies confirmed that an intact GGDEF motif is crucial for PleD activity. Remarkably, a chimeric PleD protein with the GGDEF domain replaced by the equivalent domain of the *P. aeruginosa* PleD ortholog WspR fully retained *in vivo* function (44). This was consistent with the idea that GGDEF domains are interchangeable and that their signal transduction mechanism relies probably not on specific protein-protein or protein-DNA interactions. However, the exact output function of the GGDEF domain remained elusive, until an exciting biochemical analysis demonstrated that PleD acts as a diguanylate cyclase (26). Interestingly, *in vitro* phosphorylation of PleD by the cognate histidine kinase DivJ stimulated the diguanylate cyclase output activity. Further, *in vivo* experiments suggested that only the phosphorylated form of PleD is sequestered to the differentiating stalk pole, arguing that spatially confined synthesis of c-di-GMP might contribute to polar organelle development in *C. crescentus* (26). Subsequently resolution of the PleD crystal structure in complex with the product c-di-GMP revealed a detailed molecular view on the structural folds, the catalytic center and possible activation mechanisms (see Figure 2) (45). The GGDEF domain was found to possess a fold similar to adenylate cyclase, whereby the highly conserved GGDEF motif constitutes part of the active site (A-site).

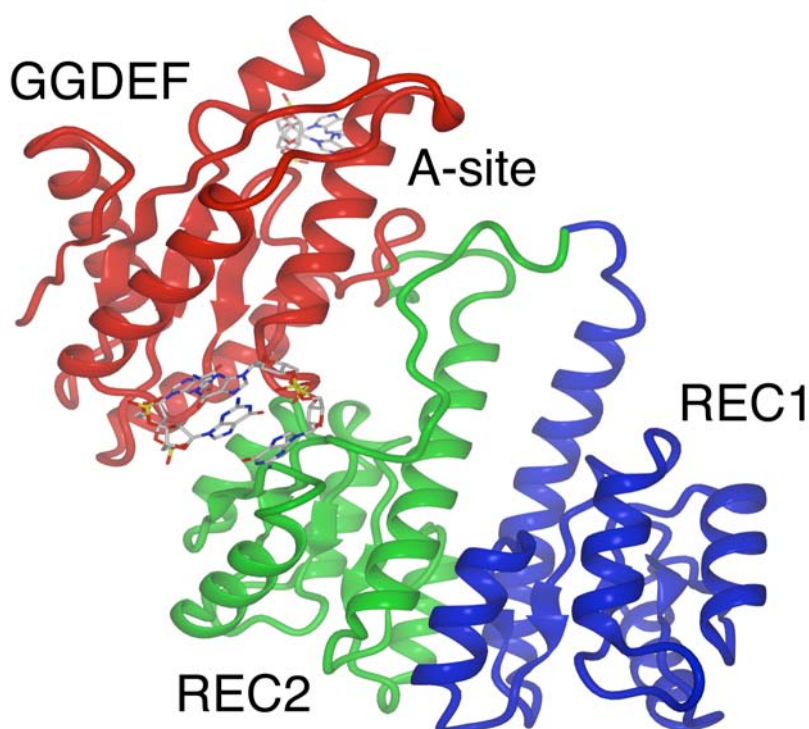


Figure 2: Crystal structure of PleD in complex with c-di-GMP:

Crystal structure of PleD with first response regulator domains REC1 (in blue) and REC2 (in green), and the C-terminal GGDEF domain (in red) which harbors diguanylate cyclase activity. GTP is modeled into the active site (A-site). Illustration according to (45).

The crystal structure of PleD exposed in addition to the catalytic site another nucleotide binding site. Surprisingly, an intercalating dimer of c-di-GMP was bound in the interface between the GGDEF and the central receiver like domain. While allosteric product inhibition was demonstrated (45) it remained unclear whether this second ligand site also exists in solution and contributes to the observed noncompetitive product inhibition of PleD.

1.5 C-di-GMP signaling survey

Interestingly, GGDEF and EAL proteins are found throughout the bacterial kingdom and, as a unifying theme, are implicated in diverse processes such as morphogenesis of cell appendages, production and secretion of extra-cellular carbohydrates or motility control (9,46). The GGDEF and EAL domains are frequently fused in a modular fashion to various N-terminal sensory domains arguing that these multi-domain proteins constitute a complex and widespread signaling system. Recent biochemical studies demonstrated that the diguanylate cyclase activity resides within the

GGDEF domains (26). The EAL domain, by virtue of its association with the GGDEF domain, was therefore predicted to be a good candidate for c-di-GMP specific phosphodiesterase activity (47). It could be hypothesized that composite proteins containing both GGDEF and EAL domains, upon stimulation, might switch between c-di-GMP synthesizing and hydrolyzing enzymatic activities and constitute an accurate signaling device to control intracellular c-di-GMP level. To add to the very preliminary knowledge about regulation and action of c-di-GMP, numerous questions regarding c-di-GMP signaling had to be answered. In particular the underlying signal transduction principles of the c-di-GMP circuitry and mechanisms of signal inactivation, signaling amplification, noise suppression and signal adaptation will be addressed.

2 Aim of the thesis

Cyclic diguanylic acid (c-di-GMP) has been recognized as a novel bacterial second messenger orchestrating surface colonization and biofilm formation in a wide variety of prokaryotes. While the diguanylate cyclase activity, has recently been assigned to the widespread GGDEF domain, many elements of the c-di-GMP signaling system remained elusive. The aim of this thesis was to characterize novel signaling components involved in c-di-GMP metabolism, describe regulatory principles and unravel the nature of c-di-GMP effectors. First, we will develop genetic and biochemical reporter assays to monitor diguanylate cyclase and c-di-GMP specific phosphodiesterase activity in vitro and in vivo. Second, we will apply these assays to identify c-di-GMP specific phosphodiesterases essential for signal inactivation, test the assumption that EAL domain proteins possess phosphodiesterase activity and investigate the function of GGDEF-EAL composite proteins. Third, we will address the hypothesis that diguanylate cyclases are subject to non-competitive product inhibition, design biochemical and genetic strategies to probe structural determinants required for allosteric control and analyze the impact of feedback regulation on the overall robustness of the c-di-GMP signaling network. Fourth, we will identify c-di-GMP effectors, characterize the corresponding c-di-GMP binding sites at the molecular level and investigate how the second messenger signal is transduced and causes a specific cellular response.

3 Results

3.1 DgrA is a member of a new family of cyclic di-GMP receptors and controls flagellar motor functions in *Caulobacter crescentus*

M. Christen, B. Christen, M. G. Allan, M. Folcher, S. Moes, P. Jenö, S. Grsziek, and U. Jenal
PNAS 280:30829-30837 (2007)

Summary

In this publication we enlightened the signal transduction mechanism of the bacterial second messenger c-di-GMP and demonstrate the existence of diguanylate receptor proteins. We report the biochemical purification of c-di-GMP effector proteins from *C. crescentus* crude extract and describe their physiological role in c-di-GMP dependent repression of cell motility. A multitude of biochemical, genetic and NMR experiments was used to characterize these effector proteins and homolog from *S. enterica* and *P. aeruginosa* down to molecular level. In particular, we used [³³P] c-di-GMP UV cross linking studies, to demonstrate that these receptors specifically bind c-di-GMP in the sub-micromolar range, and, in combination with NMR spectrometry, to elicit determinants for c-di-GMP binding. Further more, we performed genetic suppressor analysis and epistasis experiments with receptor deletion and point mutants, to corroborate that the identified diguanylate receptors from *C. crescentus* act in vivo downstream of the second messenger c-di-GMP.

DgrA is a member of a new family of cyclic di-GMP receptors and controls flagellar motor function in *Caulobacter crescentus*

Matthias Christen[¶], Beat Christen[¶], Martin G. Allan, Marc Folcher, Paul Jenö Stephan Grzesiek, and Urs Jenal[§]

Biozentrum, University of Basel, Klingelbergstrasse 70,

CH-4056 Basel, Switzerland

= These authors contributed equally to this work

[§] For correspondence:

Urs Jenal, Division of Molecular Microbiology, Biozentrum, University of Basel, Klingelbergstrasse 70, CH-4056 Basel, Switzerland, Telephone +41-61-267-2135, Fax +41-61-267-2118, E-mail urs.jenal@unibas.ch

Number of text pages: 16

Number of figures: 6

Number of tables: 1

Number of words in abstract: 185

Characters in text: 34.383

Total number of characters: 46983

Key words: c-di-GMP, PilZ, diguanylate receptor, *Caulobacter*, motility

Abstract

Bacteria are able to switch between two mutually exclusive lifestyles, motile single cells and sedentary multicellular communities that colonize surfaces. These behavioral changes contribute to an increased fitness in structured environments and are controlled by the ubiquitous bacterial second messenger cyclic di-GMP. In response to changing environments, fluctuating levels of c-di-GMP inversely regulate cell motility and cell surface adhesins. Whereas the synthesis and breakdown of c-di-GMP has been studied in detail, little is known about the downstream effector mechanisms. Using affinity chromatography we have isolated several c-di-GMP binding proteins from *Caulobacter crescentus*. One of these proteins, DgrA, is a PilZ homolog involved in mediating c-di-GMP-dependent control of *C. crescentus* cell motility. Biochemical and structural analysis of DgrA and homologs from *C. crescentus*, *Salmonella typhimurium* and *Pseudomonas aeruginosa* demonstrated that this protein family represents a class of specific diguanylate receptors and suggested a general mechanism for c-di-GMP binding and signal transduction. Increased concentrations of c-di-GMP or DgrA blocked motility in *C. crescentus* by interfering with motor function rather than flagellar assembly. We present preliminary evidence implicating the flagellar motor protein FliL in DgrA-dependent cell motility control.

Cyclic purine nucleotides are ubiquitous second messengers involved in cell signaling. They are produced through the action of growth factors, hormones or neurotransmitters and elicit their response by acting on a range of downstream effector proteins like protein kinases, transcription regulators, gated ion channels, or GTPase nucleotide exchange factors. Whereas cAMP is widespread through all kingdoms of life, cGMP seems to be restricted to signaling in eukaryotes. Recently, a third major cyclic nucleotide messenger, cyclic di-guanosine-monophosphate (c-di-GMP) has emerged as a ubiquitous signaling molecule in prokaryotes, where it antagonistically controls motility and virulence of planktonic cells on one hand and cell adhesion and persistence of multicellular communities on the other (1, 2) (supplemental Fig. 7). C-di-GMP is synthesized from two molecules of GTP and degraded into the linear dinucleotide pGpG by the opposing activities of diguanylate cyclases (DGC) and c-di-GMP-specific phosphodiesterases (PDE). DGC and PDE activities are comprised in GGDEF and EAL domains, respectively (3-8), which represent two large families of output domains found in bacterial one- and two-component signal transduction systems (9, 10).

The molecular principles of c-di-GMP signaling have been studied in the model organism *Caulobacter crescentus*, where c-di-GMP coordinates the developmental transition from a motile swarmer cell to a surface attached, replication competent stalked cell. Both acquisition of flagellar motility in the predivisional cell and its replacement by an adhesive organelle later in development are controlled by c-di-GMP. TipF, an EAL domain protein, is required for an early step of flagellum assembly in the predivisional cell (11), whereas the diguanylate cyclase PleD is involved in flagellum ejection and subsequent steps in pole remodeling (3, 12-15). Similarly, the second messenger c-di-GMP regulates motility, adhesion factors and biofilm formation in a wide variety of bacterial pathogens including *Yersinia*, *Pseudomonas*, *Vibrio* and *Salmonella* (1, 2). C-di-GMP influences flagellar motility as a function of growth (16) or adaptation to surfaces (17), affects pili assembly (18), and controls the production of surface structures like fimbriae and exopolysaccharide matrices (19). The wide variety of cellular functions that are affected by c-di-GMP calls for multiple receptors and signaling mechanisms. However, little information is available on specific targets of c-di-GMP action. With the exception of a component of the cellulose synthase complex from *Gluconacetobacter* (20, 21) and the recent prediction of a candidate c-di-GMP binding domain (22, 23), no c-di-GMP effector proteins have been reported. We have

designed a biochemical approach to purify and characterize c-di-GMP effector molecules from *Caulobacter crescentus* crude cell extracts.

Results:

Purification of c-di-GMP binding proteins from *C. crescentus*. Based on the assumption that c-di-GMP signal transduction depends on specific receptor proteins, we designed a biochemical purification strategy to identify such components. C-di-GMP binding proteins from *C. crescentus* were purified by two consecutive chromatography steps using BlueSepharose[®] CL-6B and affinity chromatography with GTP immobilized on Epoxy activated Sepharose 4B (Pharmacia). UV crosslinking with [³³P]c-di-GMP was used to identify proteins with specific binding activity for c-di-GMP (see Materials and Methods and supplemental Table II). Two binding proteins with apparent molecular weights of 47 kDa and 36 kDa were detected in the 0.4 – 0.7 M NaCl eluate of the BlueSepharose[®] column (Fig. 1A, B, lane 3) and the 0.7 – 0.9 M NaCl fraction contained several small c-di-GMP binding proteins with apparent molecular weights of 8-12 kDa (Fig. 1A, B, lanes 4-5; Fig. 1C). The latter fraction was dialyzed, concentrated and separated on a GTP Epoxy-Sepharose 4B affinity column (Fig. 1A,B lane 4 and Fig. C). One of these (labeled c in Fig. 1C) was identified by MS/MS as the product of gene CC1599, a conserved hypothetical 12.5 kDa protein that we consequently renamed as diguanylate receptor A (DgrA). Sequence comparison disclosed DgrA as a member of the PilZ protein family, members of which have recently been proposed by bioinformatics to be c-di-GMP effector proteins (22).

DgrA is a diguanylate receptor protein. In order to confirm that the identified protein is a c-di-GMP receptor, *dgrA* was subcloned into the expression vector pET-42b and the recombinant hexahistidine-tagged protein was purified by Ni-NTA-affinity chromatography. Like the semi-purified protein from *C. crescentus* (Fig. 1C), the recombinant protein showed strong labeling upon UV crosslinking with [³³P]c-di-GMP (Fig. 2A), confirming that DgrA is a c-di-GMP receptor protein. UV crosslinking experiments with DgrA in the presence of 60 nM ³³P labeled c-di-GMP and increasing concentrations of cold c-di-GMP, GTP (200 μM), or pGpG (200 μM) indicated that DgrA binds c-di-GMP with high affinity and specificity (Fig. 2B). Furthermore, c-di-GMP seems to bind to DgrA in a non-covalent manner since no radiolabeled c-di-GMP was incorporated without UV irradiation (Fig. 2B). The dissociation constant for c-di-GMP of the recombinant DgrA was determined using the UV

crosslinking assay (Table I). Saturated incorporation of radiolabeled c-di-GMP was already observed at 50 nM, indicating that the K_D of DgrA for c-di-GMP is below 50 nM.

To test if other members of the PilZ protein family also bind c-di-GMP we analyzed several ortho- or paralogs of DgrA, including CC3165 (renamed as DgrB), YcgR from *S. typhimurium* (24) and PA4608 from *P. aeruginosa* (Fig. 6). As shown in Fig. 2A all four proteins were efficiently labeled with ^{33}P c-di-GMP upon UV crosslinking, whereas the control protein BSA did not incorporate c-di-GMP. The c-di-GMP binding constants of DgrB, YcgR and PA4608 were determined by performing UV crosslinking experiments with 50 nM receptor protein in the presence of increasing concentrations of ^{33}P labeled c-di-GMP (50 - 1000 nM). All wild type diguanylate receptor proteins exhibit a binding affinity in the nanomolar range (Table I). Taken together, these data demonstrate that DgrA and its homologs containing a PilZ domain are members of a class of small diguanylate receptor proteins, which bind c-di-GMP, but not other guanine nucleotides, with high affinity. Thus, these proteins represent bona fide diguanylate receptor proteins and may be involved in the response of specific cell functions to fluctuating concentrations of c-di-GMP (2).

DgrA and DgrB mediate c-di-GMP-dependent motility control in *C. crescentus*. Low concentrations of c-di-GMP are generally associated with flagella or pili based motility of single planktonic cells, whereas increased concentrations of c-di-GMP promote multicellular traits and efficiently block cell motility (2). In agreement with this, *C. crescentus* cells are non-motile in the presence of a plasmid-borne copy of *dgcA*, which encodes a highly active, soluble diguanylate cyclase (15) (Fig. 3A). Electron micrographs and immunoblot experiments showed that these cells were flagellated and expressed similar level of flagellins (data not shown), arguing that increased c-di-GMP concentrations interfere with flagellar function rather than with the expression or assembly of flagellar components. To test if motility control by c-di-GMP involves *dgrA* or *dgrB*, single and double in frame deletion mutants were generated using a two-step homologous recombination procedure (see supplemental materials). In contrast to *C. crescentus* wild type, $\Delta dgrA$ and $\Delta dgrB$ mutants were motile even in the presence of the *dgcA* plasmid (Fig. 3A strains). This was not due to a reduction of the c-di-GMP concentration, as cellular levels of c-di-GMP in these mutants were indistinguishably high (data not shown). At low cellular concentrations of c-di-GMP, motility phenotypes were not significantly altered in the deletion mutants (data not shown), indicating that

DgrA and DgrB interact with cell motility primarily at conditions where the level of c-di-GMP is elevated. Together, these data suggested that the c-di-GMP binding proteins DgrA and DgrB are part of a signal transduction pathway that interferes with flagellar function in response to increasing concentrations of c-di-GMP. In agreement with this, overexpression of *dgrA* or *dgrB* from a plasmid efficiently blocked motility on swarmer plates (Fig. 3B) and in liquid media as observed microscopically (data not shown).

Analysis of c-di-GMP binding to the diguanylate receptor by NMR spectroscopy. The available NMR structure and resonance assignments of the DgrA homolog PA4608 from *P. aeruginosa* (25) (PDB 1YWU; BMRB 6514) provided an opportunity to characterize the ligand binding site on a molecular level and to investigate the structural consequences of ligand binding. PA4608 carrying an N-terminal hexahistidine tag was produced in uniformly ^{15}N - and ^{13}C -labeled form for NMR spectroscopy. The ^1H and ^{15}N chemical shifts observed for pure PA4608 were in good agreement with those reported in BMRB entry 6514. When c-di-GMP was added to the protein, ^1H - ^{15}N -HSQC spectra changed dramatically (supplemental Fig. 8). Free and ligand-bound PA4608 were in slow exchange on the NMR chemical shift time scale, and titration curves were in agreement with a K_D in the sub- μM range (data not shown). In order to assign resonances of the PA4608*c-di-GMP complex, exchange (EXSY) spectra were recorded on a roughly 3:1 mixture of free and c-di-GMP-bound PA4608; exchange within a mixing time of 800 ms was only observed after heating to 313 K. Standard triple-resonance NMR spectra recorded on PA4608 saturated with c-di-GMP were used to complete the backbone resonance assignments. No resonances were observed for residues M3-H12 (hexahistidine tag), H22, F33-I36, G73, I91, E125, L128, and D130-L138¹. Probably, these residues are flexible on a μs to ms time scale, and peaks are broadened beyond detection due to intermediate chemical exchange. Secondary $^{13}\text{C}^\alpha$ and $^{13}\text{C}^\beta$ shifts (26) showed that the secondary structure of PA4608 remained essentially unchanged after ligand binding (supplemental Fig. 9).

In order to localize the ligand binding site on the protein surface, backbone amide ^1H and ^{15}N chemical shifts of the PA4608*c-di-GMP complex were compared to those of the free protein, and the differences were mapped

¹ Residue numbering for PA4608 as in BMRB entry 6514, which differs from that in PDB structure 1YWU by +22, is used throughout this text.

on the structure of the free protein (Figs. 5, 8). Large shift differences are found on one face of the β barrel (around V58, I63), in the C-terminus (V142, A144), and in the N-terminus (R30-D39). We conclude that c-di-GMP binds to the outside of the β barrel close to V58, and that the termini, which are partially flexible in the apo form, fold around the bound ligand. Presumably the side chain N-H group of W99 forms a hydrogen bond with the ligand, since the $^{15}\text{N}^{\epsilon 1}$ and $^1\text{H}^{\epsilon 1}$ resonances strongly shift towards higher chemical shifts by 8.24 and 1.66 ppm, respectively.

Due to their distinct chemical shifts (>10.7 ppm), the H1 imino hydrogens of guanine in c-di-GMP could be identified once the assignment of protein backbone $^1\text{H}^{\text{N}}$ and tryptophan $^1\text{H}^{\epsilon 1}$ resonances had been completed. Since four separate H1 resonances of about equal intensity are observed for c-di-GMP in complex with PA4608, and each molecule of c-di-GMP contains two guanine bases, c-di-GMP binds to PA4608 as a dimer. Consistent with the ligand-binding site outlined above, two of these H1 imino resonances show intermolecular NOEs to L64 and W99 (supplemental Fig. 10).

Amide ^{15}N T_1 and T_2 relaxation times and heteronuclear $\{^1\text{H}\}$ - ^{15}N NOEs were measured at 20°C for free and c-di-GMP-bound PA4608 (data not shown). Isotropic rotational correlation times (τ_c) were determined from these data with the program TENSOR (27) as 11.3 and 12.3 ns for free and ligand-bound protein, respectively. These τ_c are in reasonable agreement with values expected for monomeric apo-PA4608 (16.7 kDa, 9.8 ns) and c-di-GMP-bound PA4608 (18.1 kDa, 10.6 ns). Thus, PA4608 is a monomer before and after ligand binding.

C-di-GMP binding mutants of DgrA are unable to control motility. Alignments of the amino acid sequences of PA4608, DgrA, DgrB, and YcgR revealed that the key residues that, based on NMR data, were postulated to be involved in c-di-GMP binding to PA4608, are conserved among other diguanylate receptor proteins (Fig. 6). To probe the c-di-GMP binding site of DgrA and to define the minimal requirements for c-di-GMP binding, residues R11, R12, D38, and W75 were replaced with Ala and the mutant proteins were analyzed for c-di-GMP binding. Mutants R11AR12A and W75A strongly reduce c-di-GMP binding, whereas mutant D38A is still able to bind c-di-GMP (Fig. 5A). In agreement with this, the binding constant for the D38A mutant was marginally increased to 740 nM, whereas the K_D for the W75A mutant (6.4 μM) was increased 100-1000 fold as compared to wild type (Table I). Binding of c-di-GMP was completely abolished in the R11AR12A mutant. To analyze the

importance of c-di-GMP binding for DgrA mediated signaling, the *dgrA* mutant alleles were tested for functionality *in vivo*. As indicated above, overexpression of wild type *dgrA* renders cells non-motile (Figs. 4B, 6B). In contrast, overexpression of *dgrAD38A*, *dgrAR11AR12A*, or *dgrAW75A* only partially affected motility (Fig. 5B). In particular, changing W75 to Ala almost completely abolished the ability of DgrA to block motility under these conditions (Fig. 5B). Similarly, when the *dgrAW75A* mutant allele was expressed in single copy from its original chromosomal locus, cells were fully motile even in the presence of the *dgcA* plasmid, arguing that DgrAW75A can no longer control motility in response to increased c-di-GMP levels (Fig. 3). We isolated suppressors that alleviated the *dgrA*-mediated motility block (see Materials and Methods). One of the intragenic *dms* (diguanylate receptor motility suppressors) mutations mapped to V74, in the immediate vicinity of the Trp residue critical for c-di-GMP binding (Fig. 5B, Fig. 6). Other intragenic *dms* mutations (D62, G82) mapped to conserved residues of DgrA, emphasizing the functional importance of these residues (Fig. 6). In conclusion, these results support the view that ligand binding is essential for the regulatory function of the diguanylate receptor and suggest that DgrA blocks motility in its c-di-GMP bound state.

Motility control by DgrA correlates with cellular levels of the FliL motor protein. Immunoblot analysis revealed that overexpression of *dgrA* or *dgrB* blocks motility without interfering with the expression of known class II, class III or class IV components of the flagellar hierarchy (Fig. 3C). Because the expression of each class of genes depends on the successful expression and assembly of components of the preceding class of the hierarchy (28), this result suggested that flagella are assembled normally in cells overexpressing *dgrA* or *dgrB*. In agreement with this, flagella were readily observed by electron microscopy in these non-motile cells (data not shown). The only flagellar protein whose concentration was severely affected in cells overexpressing *dgrA* was FliL (Fig. 3C). The *C. crescentus fliL* gene is not part of the flagellar hierarchy and its product is not assembled into the flagellar structure (29). However, *fliL* is required for flagellar rotation (29). To examine if reduced FliL levels are linked to motility we screened the pool of *dms* mutants (see above) for extragenic suppressors (see Materials and Methods). From a total of 120 independently isolated motile suppressors, only one mapped to the chromosome. This suppressor mutation (*dms0541*), which mapped to gene CC3587 coding for the ribosomal protein S1, not only restored motility but also re-established normal levels of FliL (Fig. 3C).

Discussion:

Motility control by c-di-GMP is implemented through gene expression, organelle assembly, or motor function (2). In *C. crescentus*, increased cellular concentrations of c-di-GMP block motility by interfering with motor function rather than by altering expression or assembly of structural components of the flagellum (13). How are increased levels of c-di-GMP sensed and how is this information transmitted to the flagellar motor? The data presented here suggest that DgrA and DgrB are high affinity receptors for c-di-GMP that, in a ligand-bound form, interfere with the flagellar motor either directly or indirectly. Motor control by DgrA-like proteins is not unique to *Caulobacter*. *E. coli* H-NS mutants lack flagella because the expression of the flagellar master control operon *flhCD* is reduced. Ectopic expression of *flhCD* restores flagellation but leaves the motors partially paralyzed (24). Under these conditions flagellar function can be restored either by a mutation in *ycgR*, coding for the *E. coli* DgrA homolog, or by providing multiple copies of *yhjH*, which encodes a presumable c-di-GMP specific phosphodiesterase (24). Together with our data demonstrating that the *Salmonella* YcgR protein specifically binds c-di-GMP, this suggests that in *C. crescentus* and in enteric bacteria flagellar motor function might be controlled by c-di-GMP via similar mechanisms.

But how would DgrA or YcgR interfere with the function of the flagellum? Our data propose the FliL protein as a candidate for such a role. FliL was the only flagellar protein that showed significantly reduced levels in non-motile cells overexpressing *dgrA*. In *C. crescentus* the FliL protein is not part of the flagellar structure but is required for flagellar rotation (29). Intriguingly, *fliL* mutant strains exhibit an identical motility phenotype like cells that have high levels of c-di-GMP or overexpress *dgrA* (29). Because the expression of *fliM*, the gene located immediately downstream of *fliL* in the same operon (30), was not affected by DgrA, FliL changes must be the result of altered translation or protein stability. An extragenic suppressor mutation that restored motility under these conditions also re-established normal FliL concentrations, indicating that the two phenotypes are linked. The simplest model that is in agreement with these results predicts that DgrA, upon binding of c-di-GMP, represses FliL by a so far unknown mechanism and through this blocks motor function. The extragenic suppressor mutation restoring FliL levels was mapped to the coding region of *rpsA* (*ribosomal protein S1*). RpsA enhances translation initiation by binding to mRNA regions upstream of the Shine-Dalgarno sequence and by

tethering the mRNAs on the 30S subunit of the ribosome (31-33). We are currently investigating how DgrA and its ligand c-di-GMP modulate FliL levels. Recently, FliL was reported to be involved in surface sensing and virulence gene expression in the urinary tract pathogen *Proteus mirabilis* (34). Thus, it is possible that FliL has a more general role in controlling the switch between a planktonic and a surface-associated lifestyle.

A bioinformatics study originally proposed that the PilZ domain is a specific c-di-GMP binding module (22). This was recently substantiated by the demonstration that YcgR, a PilZ protein from *E. coli*, is able to bind c-di-GMP (23). Here we presented genetic, biochemical, and structural evidence that further validate this hypothesis and propose a model for ligand binding and activation of proteins containing a PilZ domain. NMR studies with the DgrA homolog PA4608 showed that a dimer of c-di-GMP binds to a well-defined binding site on the surface of the β -barrel (Fig. 4). Large chemical shift differences between free and ligand-bound PA4608, which indicate changes in the local environment, were also observed in both termini of the protein, with the largest differences observed for residues R30-R32, V142, and A144. These regions are structurally ill defined in the absence of ligand (25) and are probably flexible. The observed chemical shift differences indicate that these regions come in direct contact with the ligand after complex formation. The N-terminal part of PA4608 contains three consecutive Arg residues, which are conserved in most PilZ domains (22) (Fig. 6). Arg side chains are likely to be involved in hydrogen bonds or in electrostatic or π stacking interactions with c-di-GMP, as has been shown for the allosteric binding site of the diguanylate cyclases PleD and DgcA (15, 35). Furthermore, it is conceivable that the positively charged head groups of Arg are sufficient for transient binding to the phosphate groups of c-di-GMP and that their position on the flexible N-terminus increases the ligand capture radius of the protein, as in the “fly-casting mechanism” proposed in (36). Alternatively, the observed folding of previously flexible parts of the protein may be responsible for communication of the c-di-GMP signal to downstream elements, either by forming new interaction surfaces or by determining the relative position of neighboring domains. Similarly, the chemical shift differences of the C-terminal part of PA4608 could be explained by a specific role in ligand binding. However, the fact that residues V142 and A144, which showed the largest chemical shift differences are not conserved, argues against this possibility. Several of the motile *dgrA* loss of function suppressors that were isolated had frameshift mutations in the very C-terminus of DgrA (Fig. 6), suggesting that this part of the protein is critical for its *in vivo* function. One possibility is that the C-terminus

contributes to the specific readout mechanism of this protein family. Upon c-di-GMP binding to the β -barrel surface, the C-terminus could be untied to interact with downstream components. In accordance with such a view, the very C-terminus of the *P. aeruginosa* PilZ protein has recently been proposed to interact with the PilF protein required for type 4-pilus assembly (37). To complement our picture of the c-di-GMP circuitry, future studies will have to focus on interaction partners of DgrA and related PilZ domain proteins.

It is intriguing that genetic and biochemical studies of the *C. crescentus* DgrA protein and structural analysis of PA4608 from *P. aeruginosa* identified the same set of key amino acids involved in c-di-GMP binding (Fig. 6). This finding is a strong indication that these proteins bind c-di-GMP in a similar way and suggests that they may share a common signaling mechanism. Based on these results we postulate that most or all PilZ domain proteins function as diguanylate receptor proteins.

Materials and Methods:

Strains, plasmids and media. *E. coli* strains were grown in Luria Broth (LB). *C. crescentus* strains were grown in complex peptone yeast extract (PYE) (38) supplemented with antibiotics, where necessary. For the exact procedure of strain and plasmid construction see supplemental material.

UV cross-linking with [³³P]c-di-GMP, and isolation of DgrA. Procedures for enzymatic production of [³³P]c-di-GMP and, UV cross-linking with [³³P]c-di-GMP were published earlier (6, 39). For a detailed protocol used for the isolation of DgrA see supplemental material.

Preparation of isotope-labeled protein, NMR samples and NMR spectroscopy. The detailed procedures for overexpression and ¹³C, ¹⁵N- double-labeling of PA4608 are described in supplemental material. NMR samples (Shigemi microtubes) were prepared as 0.8 mM U-¹³C/¹⁵N-labeled protein in 300 μl 95 % H₂O/5% D₂O, 250 mM NaCl, 10 mM DTT, 1 mM sodium azide, 10 mM Tris at pH 7.1. C-di-GMP was added at suitable molar ratios from a 7.7 mM stock solution. NMR spectra were recorded on Bruker DRX 600 and 800 MHz spectrometers at 293 K (20°C) with the exception of EXSY spectra that were recorded at 313 K for faster exchange. Standard 1D, 2D and 3D spectra were recorded and processed as described elsewhere (40).

Isolation and mapping of motile *dgrA* suppressors. A plasmid carrying *dgrA* (pBBR::*dgrA*) was conjugated into a *C. crescentus recA* mutant strain and 150 individual transconjugants were patched onto PYE swarmer plates. Motile *dms* (diguanylate receptor motility suppressors) mutants were isolated and analyzed by immunoblot using an α-DgrA antibody. Mutants with reduced DgrA levels were discarded. The rest was analyzed by retransforming plasmids into the *recA* mutant strain in order to distinguish between intra- and extragenic suppressors. Intragenic mutations were identified by sequencing. The extragenic suppressor (*dms0541*) was mapped by *Tn5* linkage (41) and co-transduction with phage ΦCR30, and identified by sequencing.

Acknowledgments

We would like to thank Suzette Moes for handling of MS samples, Martha Gerber and Flora Mauch for help with the suppressor screen, Jacob Malone for a gift of *P. aeruginosa* DNA, and Colin Manoil for providing plasmid pIT2. This work was supported by Swiss National Science Foundation Fellowships 3100A0-108186 to U.J. and 31-109712 to S.G.

References:

1. Kolter, R. & Greenberg, E. P. (2006) *Nature* **441**, 300-302.
2. Jenal, U. & Malone, J. (2006) *Annual Review of Genetics* **40**, 385-407.
3. Paul, R., Weiser, S., Amiot, N. C., Chan, C., Schirmer, T., Giese, B. & Jenal, U. (2004) *Genes Dev* **18**, 715-727.
4. Ryjenkov, D. A., Tarutina, M., Moskvina, O. V. & Gomelsky, M. (2005) *J Bacteriol* **187**, 1792-8.
5. Schmidt, A. J., Ryjenkov, D. A. & Gomelsky, M. (2005) *J Bacteriol* **187**, 4774-81.
6. Christen, M., Christen, B., Folcher, M., Schauerte, A. & Jenal, U. (2005) *J Biol Chem* **280**, 30829-37.
7. Bobrov, A. G., Kirillina, O. & Perry, R. D. (2005) *FEMS Microbiol Lett* **247**, 123-30.
8. Tamayo, R., Tischler, A. D. & Camilli, A. (2005) *J Biol Chem* **280**, 33324-3.
9. Galperin, M. Y., Nikolskaya, A. N. & Koonin, E. V. (2001) *FEMS Microbiol Lett* **203**, 11-21.
10. Ulrich, L. E., Koonin, E. V. & Zhulin, I. B. (2005) *Trends Microbiol* **13**, 52-6.
11. Huitema, E., Pritchard, S., Matteson, D., Radhakrishnan, S. K. & Viollier, P. H. (2006) *Cell* **124**, 1025-37.
12. Aldridge, P. & Jenal, U. (1999) *Mol Microbiol* **32**, 379-91.
13. Aldridge, P., Paul, R., Goymer, P., Rainey, P. & Jenal, U. (2003) *Mol Microbiol* **47**, 1695-708.
14. Levi, A. & Jenal, U. (2006) *J Bacteriol* **188**, 5315-8.
15. Christen, B., Christen, M., Paul, R., Schmid, F., Folcher, M., Jenoe, P., Meuwly, M. & Jenal, U. (2006) *Journal of Biological Chemistry*.
16. Choy, W. K., Zhou, L., Syn, C. K., Zhang, L. H. & Swarup, S. (2004) *J Bacteriol* **186**, 7221-8.
17. Boles, B. R. & McCarter, L. L. (2002) *J Bacteriol* **184**, 5946-54.
18. Kazmierczak, B. I., Lebron, M. B. & Murray, T. S. (2006) *Mol Microbiol* **60**, 1026-43.
19. Kader, A., Simm, R., Gerstel, U., Morr, M. & Romling, U. (2006) *Mol Microbiol* **60**, 602-16.
20. Ross, P., Mayer, R., Weinhouse, H., Amikam, D., Huggirat, Y., Benziman, M., de Vroom, E., Fidder, A., de Paus, P., Sliedregt, L. A. & et al. (1990) *J Biol Chem* **265**, 18933-43.
21. Weinhouse, H., Sapir, S., Amikam, D., Shilo, Y., Volman, G., Ohana, P. & Benziman, M. (1997) *FEBS Lett* **416**, 207-11.
22. Amikam, D. & Galperin, M. Y. (2006) *Bioinformatics* **22**, 3-6.
23. Ryjenkov, D. A., Simm, R., Romling, U. & Gomelsky, M. (2006) *J Biol Chem* **281**, 30310-4.
24. Ko, M. & Park, C. (2000) *J Mol Biol* **303**, 371-82.
25. Ramelot, T. A., Yee, A., Cort, J. R., Semesi, A., Arrowsmith, C. H. & Kennedy, M. A. (2006) *Proteins*.
26. Spera, S. & Bax, A. (1991) *Journal of the American Chemical Society* **113**, 5490-5492.
27. Dosset, P., Hus, J.-C., Blackledge, M. & Marion, D. (2000) *J. Biomol. NMR* **16**, 23-28.
28. Gober, J. W. a. E., J.C. (2000) in *Prokaryotic development*, ed. Shimkets, Y. V. B. a. L. J. (ASM Press, Washington, DC), pp. 319-339.
29. Jenal, U., White, J. & Shapiro, L. (1994) *J Mol Biol* **243**, 227-44.
30. Yu, J. & Shapiro, L. (1992) *J Bacteriol* **174**, 3327-38.
31. Sengupta, J., Agrawal, R. K. & Frank, J. (2001) *Proc Natl Acad Sci U S A* **98**, 11991-6.
32. Komarova, A. V., Tchufistova, L. S., Supina, E. V. & Boni, I. V. (2002) *Rna* **8**, 1137-47.
33. Sorensen, M. A., Fricke, J. & Pedersen, S. (1998) *J Mol Biol* **280**, 561-9.
34. Belas, R. & Suvanasuthi, R. (2005) *J Bacteriol* **187**, 6789-803.
35. Chan, C., Paul, R., Samoray, D., Amiot, N. C., Giese, B., Jenal, U. & Schirmer, T. (2004) *Proc Natl Acad Sci U S A* **101**, 17084-9.
36. Shoemaker, B. A., Portman, J. J. & Wolynes, P. G. (2000) *Proceedings of the National Academy of Sciences of the United States of America* **97**, 8868-+.
37. Kim, K., Oh, J., Han, D., Kim, E. E., Lee, B. & Kim, Y. (2006) *Biochemical and Biophysical Research Communications* **340**, 1028-1038.
38. Ely, B. (1991) *Methods Enzymol* **204**, 372-84.
39. Christen, B., Christen, M., Paul, R., Schmid, F., Folcher, M., Jenoe, P., Meuwly, M. & Jenal, U. (2006) *J Biol Chem* **281**, 32015-24.
40. Grzesiek, S., Bax, A., Hu, J. S., Kaufman, J., Palmer, I., Stahl, S. J., Tjandra, N. & Wingfield, P. T. (1997) *Protein Science* **6**, 1248-1263.

41. Jacobs, M. A., Alwood, A., Thaipisuttikul, I., Spencer, D., Haugen, E., Ernst, S., Will, O., Kaul, R., Raymond, C., Levy, R., Chun-Rong, L., Guenther, D., Bovee, D., Olson, M. V. & Manoil, C. (2003) *PNAS* **100**, 14339-14344.

Fig. 1. Isolation of c-di-GMP binding proteins from *C. crescentus*. A) Coomassie stained SDS-PAGE gel with protein fractions used for UV-crosslinking with [³³P]c-di-GMP. Lane 1: 100.000 × g supernatant, lane 2: 60% ammonium sulfate precipitation, lane 3: 0.4 - 0.7 M NaCl eluate from Blue Sepharose[®], lane 4: 0.7 - 0.9 M NaCl eluate from Blue Sepharose[®] and lane 5: 125 mM NaCl eluate from GTP-sepharose column. B) Autoradiograph of SDS-PAGE gel shown in A. C-di-GMP binding proteins a, b, and c were identified by MS/MS and their role in c-di-GMP signaling is under investigation. Protein c was identified by MS/MS as hypothetical protein CC1599 and was renamed DgrA (Diguanylate receptor protein A).

Fig. 2. DgrA is a member of a novel family of c-di-GMP binding proteins. A) UV crosslinking of purified hexahistidine-tagged diguanylate receptor proteins with [³³P]c-di-GMP. The following proteins were used: DgrA (CC1599; *C. crescentus*), DgrB (CC3165; *C. crescentus*), PA4608 (*P. aeruginosa*), YcgR (*S. typhimurium*), and BSA (control). The Coomassie-stained gel (left) and the autoradiograph (right) are shown. B) UV crosslinking of 10 μM DgrA in the presence of 60 nM of ³³P labeled c-di-GMP. Samples were supplemented with increasing concentrations of non-labeled nucleotides as indicated. Controls carried out in the absence of UV irradiation or with BSA are shown on the right.

Fig. 3. DgrA and DgrB are involved in motility control by c-di-GMP. Motility behavior of *C. crescentus* wild type strain CB15 and mutants are shown on semisolid agar plates. Three different colonies from independent conjugation experiment are shown. A) The following strains containing plasmid pUJ142::dgcA or control plasmid pUJ142 were analyzed: CB15/pUJ142::dgcA (a), CB15ΔdgrA/pUJ142::dgcA (b), CB15dgrAW75A/pUJ142::dgcA (c), CB15ΔdgrB/pUJ142::dgcA (d), CB15ΔdgrAΔdgrB/pUJ142::dgcA (e), CB15/pUJ142 (f). B) Overexpression of dgrA or dgrB from the lactose promoter (Plac) repressed *C. crescentus* motility. CB15/pBBR (vector control) (a), CB15/pBBR::dgrA (b), CB15/pBBR::dgrB (c). C) Levels of class II, class III, and class IV structural components of the *C. crescentus* flagellum were determined by immunoblot analysis for the following strains: CB15/pBBR (wild-type), CB15/pBBR::dgrA (DgrA), CB15/pBBR::dgrB (DgrB) and the extragenic diguanylate receptor motility suppressors CB15dms0541 pBBR::dgrA (dms0541). The motility behavior of each strain is shown on top of the graph.

Fig. 4. Combined amide ^1H and ^{15}N shift differences ($\Delta\delta$) between PA4608 in its free and ligand-bound form. Shift differences are color-coded on the structure of free PA4608 (PDB 1YWU, model 12). Combined chemical shift differences were calculated as $\Delta\delta = \text{sqrt}([(\Delta\delta_{\text{H}})^2 + (\Delta\delta_{\text{N}}/5)^2]/2)$. These data are also shown in supplemental Fig. 8. Residue W99 is shown as sticks, and N^{e1} and H^{e1} are shown in red to highlight the large $\Delta\delta$ value (1.67 ppm) for these atoms.

Fig. 5. C-di-GMP binding and motility control of DgrA mutants. A) UV crosslinking of different DgrA mutant proteins with [^{33}P]c-di-GMP. Coomassie stained SDS-PAGE (top) and autoradiograph (bottom) with purified wild-type and mutant DgrA proteins (10 μM). B) Motility behavior of *C. crescentus* wild type CB15 overexpressing different *dgrA* alleles. CB15/pBBR::*dgrA* (a), CB15/pBBR::*dgrAR11AR12A* (b), CB15/pBBR::*dgrAD38A* (c), CB15/pBBR::*dgrAV74A* (d), CB15/pBBR::*dgrAR11AR12AV74A* (e), CB15/pBBR::*dgrAW75A* (f), CB15/pBBR (vector control) (g). Three different colonies from independent conjugation experiment are shown.

Fig. 6. Sequence alignment of the c-di-GMP binding proteins DgrA, DgrB, YcgR and PA4608 according to the PilZ PFAM entry PF07238. The PilZ domain is highlighted in green. DgrA residues shown to be important for c-di-GMP binding and *in vivo* function (red) and the positions of intragenic *dms* suppressor mutations (black) are highlighted above the alignment. Residues of PA4608 with large chemical shift differences upon c-di-GMP binding (blue) are indicated below the alignment.

Table I:
Binding constants of diguanylate receptor proteins determined by UV crosslinking with ³³P c-di-GMP

Organism	Protein	K _D in nM	ΔK _D	
<i>C. crescentus</i>	DgrB	132	36	
	DgrA	wt [*]	< 50	14
		RR11AA	N. D. ^{**}	-
		D38A	761	149
		W75A	6200	496
<i>S. typhimurium</i>	YcgR	182	29	
<i>P. aeruginosa</i>	PA4608	< 50	27	

protein concentrations used for binding assay: 50 nM

^{*} wt, wild type

^{**} N.D. not detectable

Table II:
Purification of c-di-GMP binding proteins from *C. crescentus* CB15 crude extracts

Sample	Total yield of protein		Total yield of binding activity	Purification
	μg	%	%	fold
100.000 x g supernatant	680.000	100	100	1
60 % (NH ₄) ₂ SO ₄ precipitation	323,000	47.5	95	2
BlueSepharose 0.4 - 0.7 M NaCl	10.800	1.59	40	26
BlueSepharose 0.7 - 0.9 M NaCl	7.800	1.15	41	35
GTP Sepharose 125 mM NaCl	24	0.0035	11	3200

Figure 1

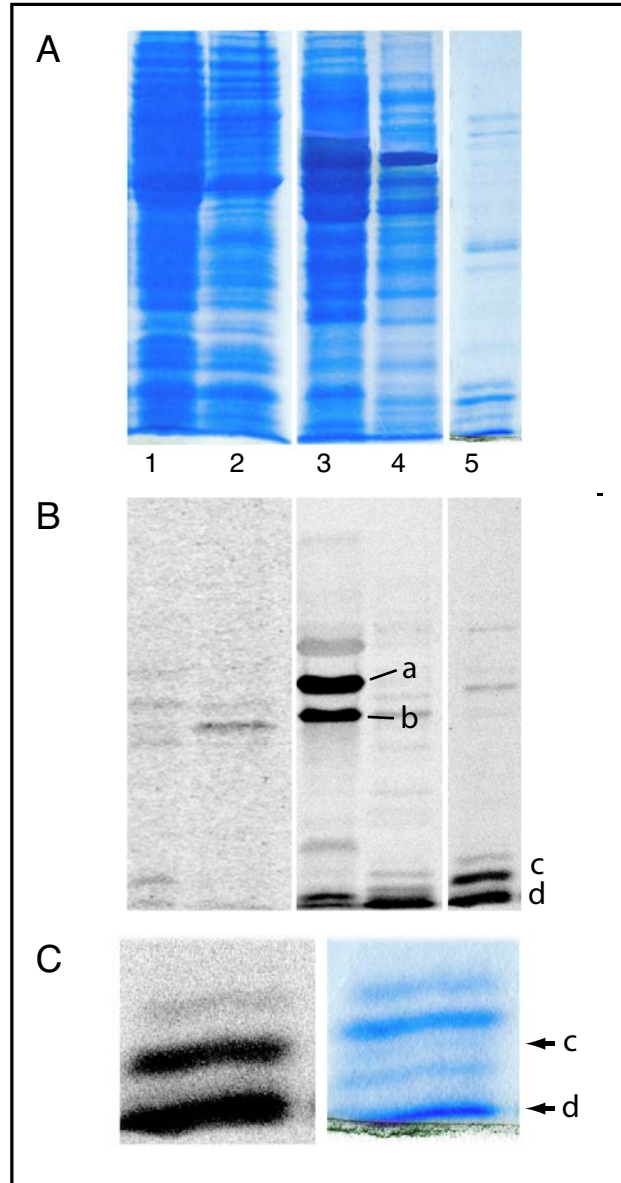


Figure 2

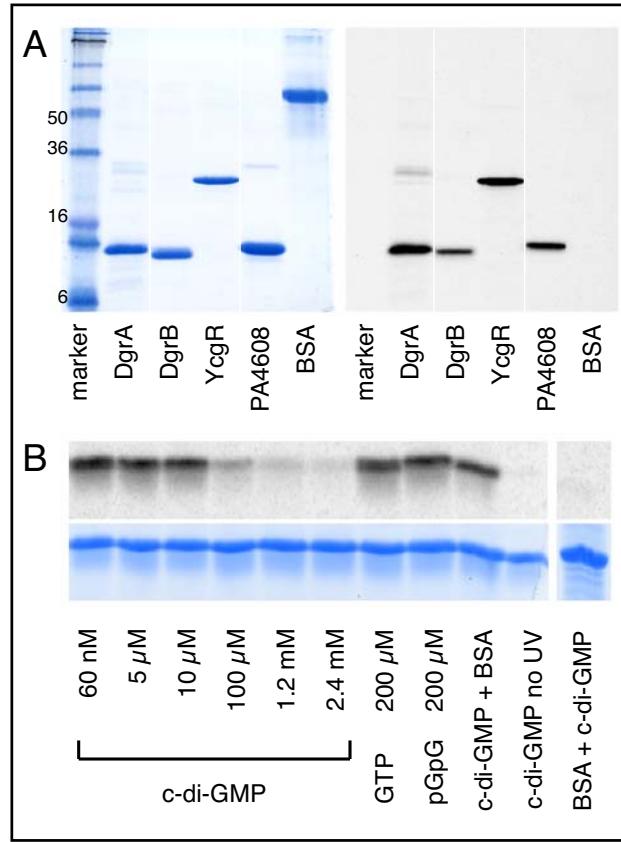


Figure 3

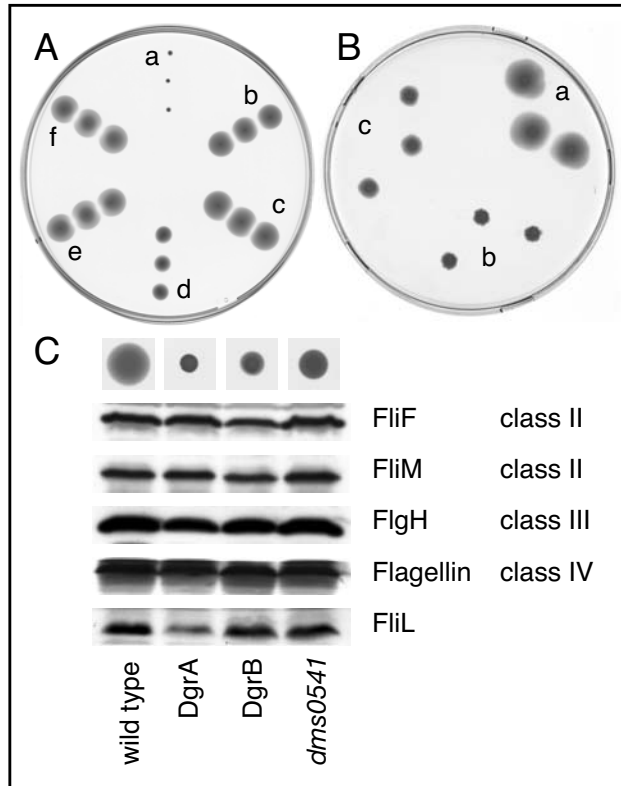


Figure 4

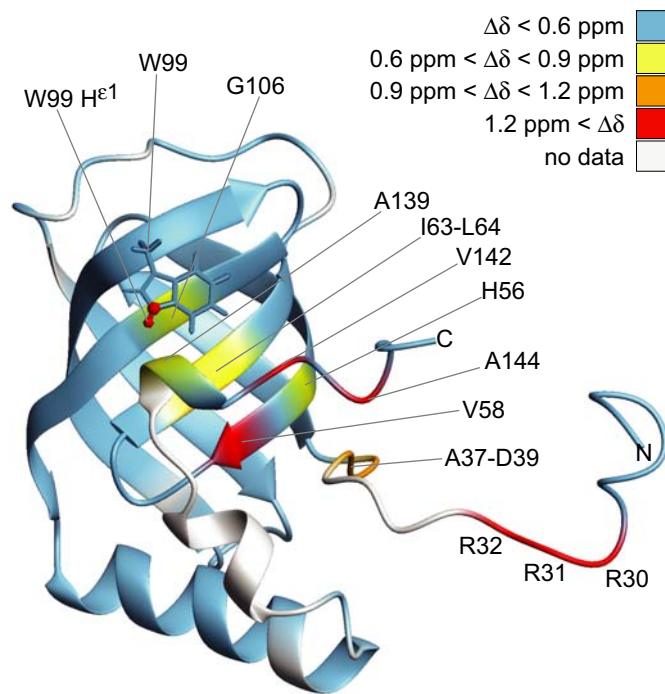


Figure 5

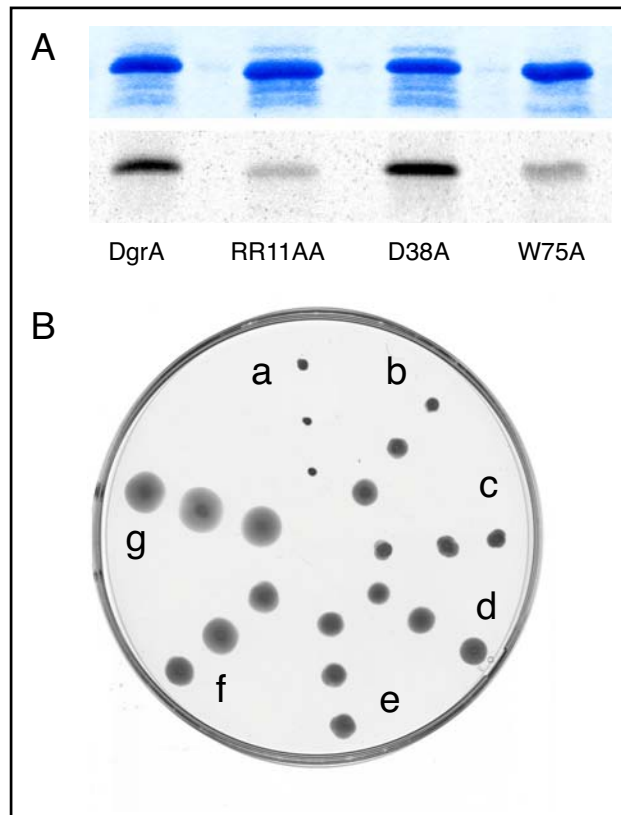


Figure 6

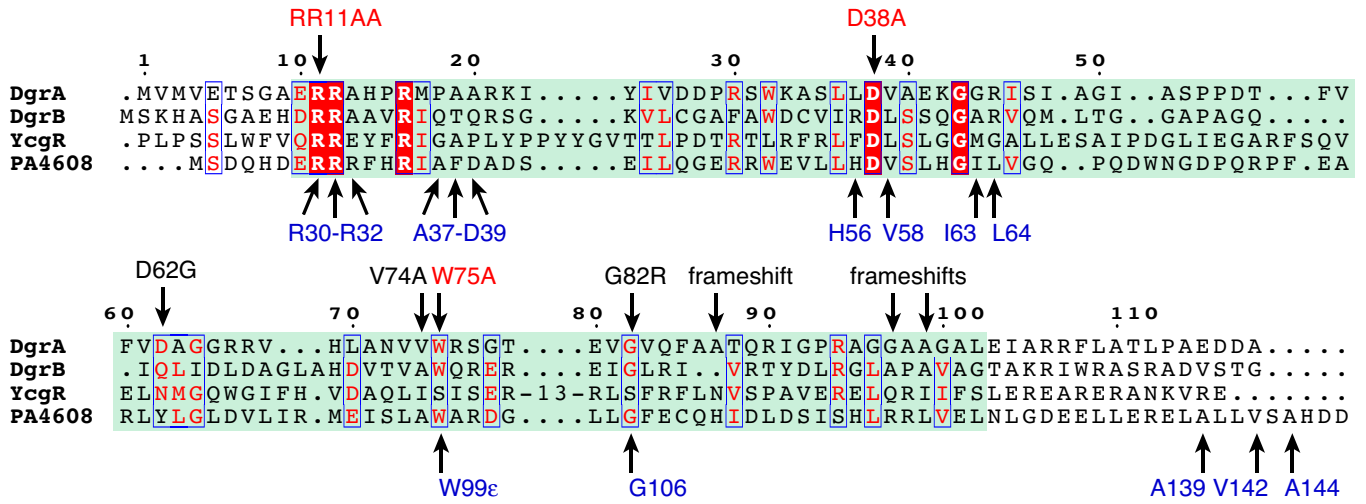


Figure 7

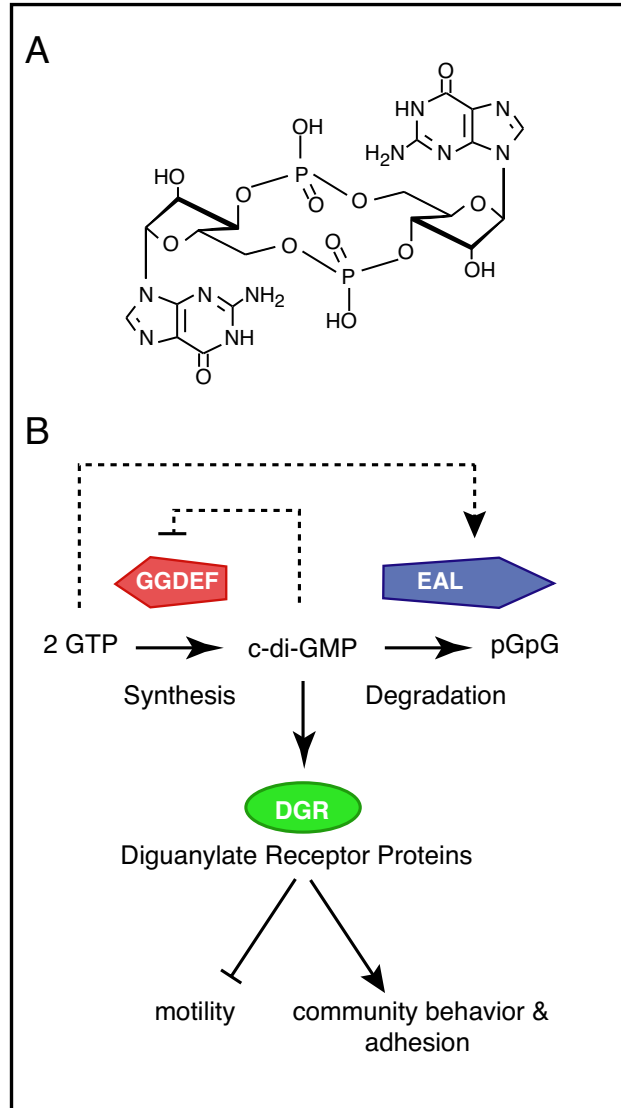


Figure 8

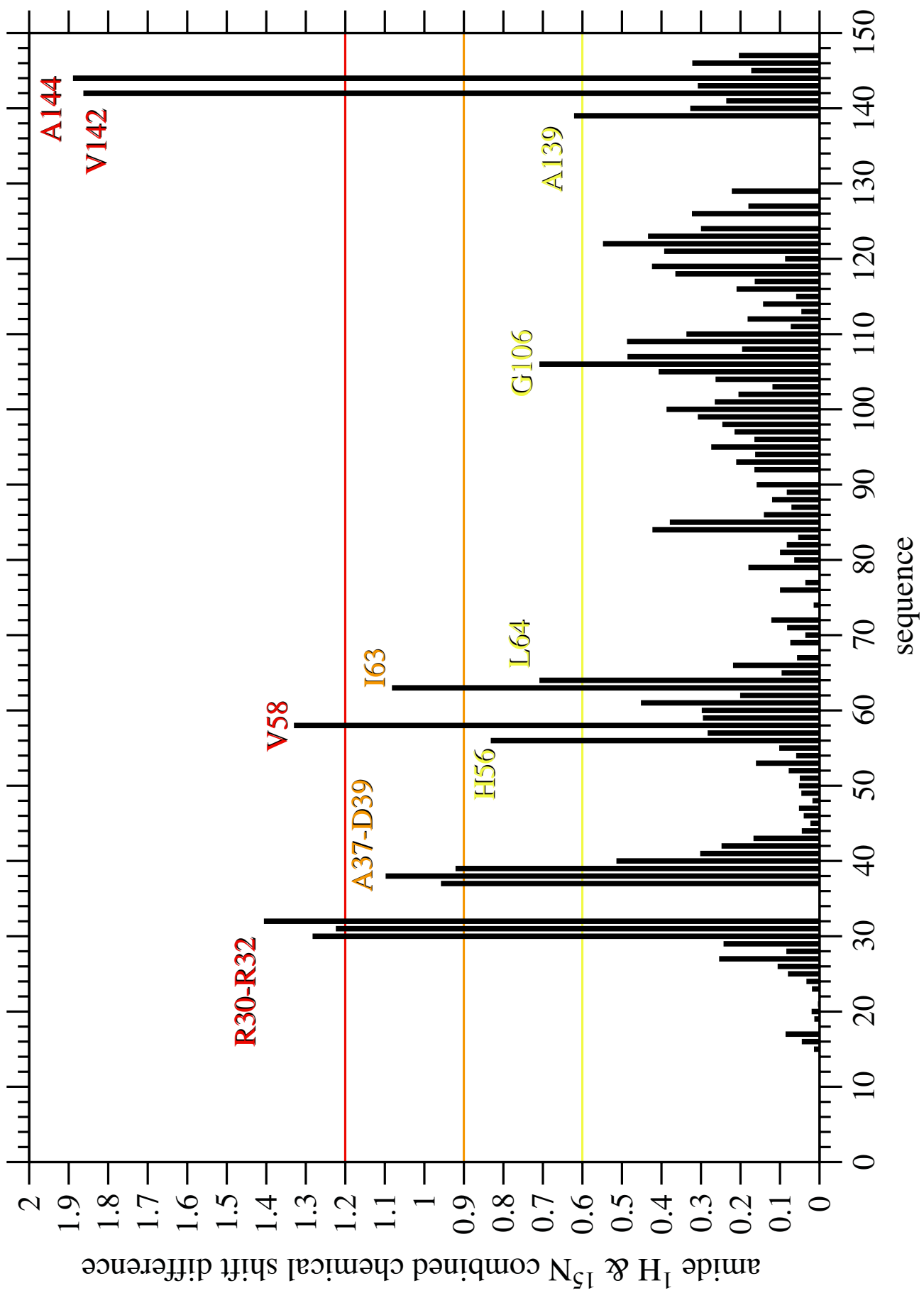


Figure 9

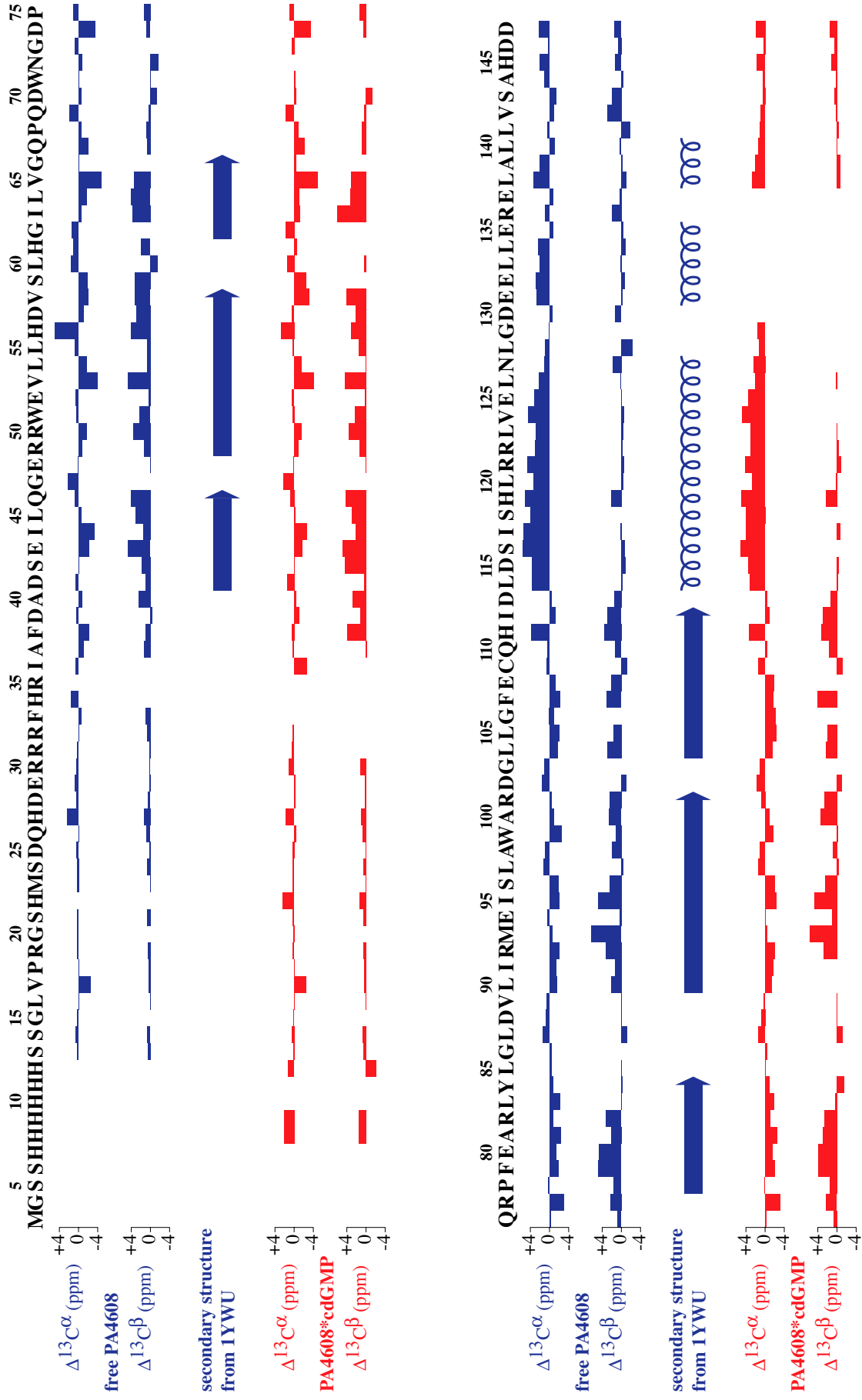
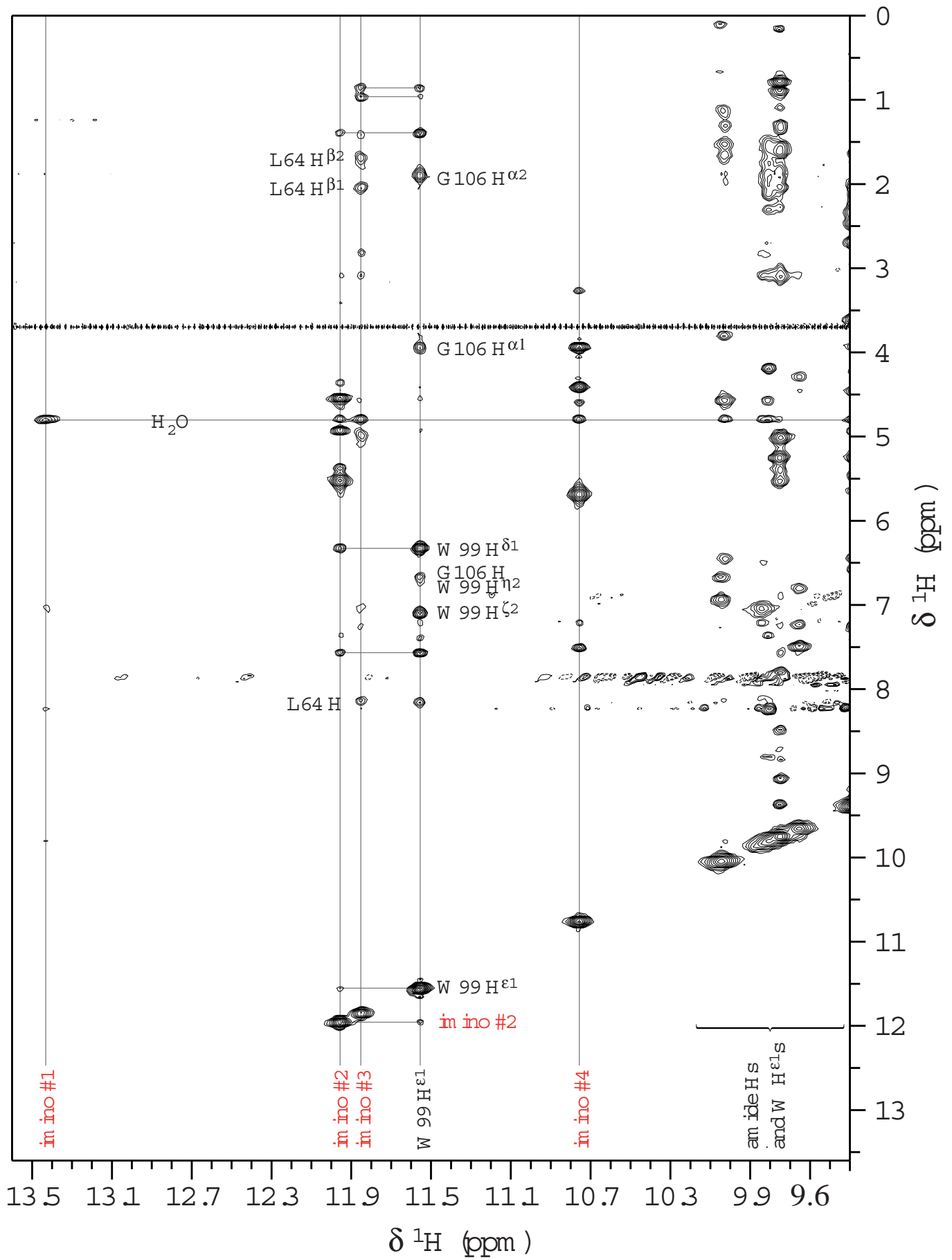


Figure 10



3.2 Allosteric Control of Cyclic di-GMP Signaling

B. Christen, M. Christen, R. Paul, F. Schmid, M. Folcher, P. Jenö, M. Meuwly and U. Jenal
JBC 281:32015-32024 (2006)

Summary

In this publication we describe an important novel feature of GGDEF proteins, which produce the ubiquitous bacterial signaling molecule cyclic-di-GMP. This paper reports the results of in depth structure-function analysis of an allosteric feedback inhibition mechanism that generally acts to regulate diguanylate cyclase activities in bacteria. The mechanism involves binding of the second messenger product, c-di-GMP at an inhibition site (I-site) that is coupled via a conserved beta-strand to the active site (A-site) of the enzyme. The study involves an array of biochemical and genetic techniques applied on various diguanylate cyclases to establish the sequence determinants of the I-site as well as the in vivo physiological relevance of I-site function. To assist the interpretation of the present data and to provide information on binding induced mobility, atomistically detailed simulations were carried out. Normal mode calculations on ligated and unligated PleD were used to analyze the structural transitions that occur during I-site binding of c-di-GMP. Allosteric product inhibition of diguanylate cyclases turns out to have fundamental functional and physiological implications, including threshold setting for cyclic-di-GMP production by particular GGDEF proteins, which can contribute to precision, robustness, noise reduction and accelerated kinetics of cyclic-di-GMP signaling.

Allosteric Control of Cyclic di-GMP Signaling*[§]

Received for publication, April 13, 2006, and in revised form, June 21, 2006. Published, JBC Papers in Press, August 21, 2006, DOI 10.1074/jbc.M603589200

Beat Christen^{†1}, Matthias Christen^{†1}, Ralf Paul[‡], Franziska Schmid[§], Marc Folcher[‡], Paul Jenoe[‡], Markus Meuwly[§], and Urs Jenal^{†2}

From the [†]Biozentrum and the [§]Department of Chemistry, University of Basel, Klingelbergstrasse 70, 4056 Basel, Switzerland

Cyclic di-guanosine monophosphate is a bacterial second messenger that has been implicated in biofilm formation, antibiotic resistance, and persistence of pathogenic bacteria in their animal host. Although the enzymes responsible for the regulation of cellular levels of *c*-di-GMP, diguanylate cyclases (DGC) and phosphodiesterases, have been identified recently, little information is available on the molecular mechanisms involved in controlling the activity of these key enzymes or on the specific interactions of *c*-di-GMP with effector proteins. By using a combination of genetic, biochemical, and modeling techniques we demonstrate that an allosteric binding site for *c*-di-GMP (I-site) is responsible for non-competitive product inhibition of DGCs. The I-site was mapped in both multi- and single domain DGC proteins and is fully contained within the GGDEF domain itself. *In vivo* selection experiments and kinetic analysis of the evolved I-site mutants led to the definition of an RXXD motif as the core *c*-di-GMP binding site. Based on these results and based on the observation that the I-site is conserved in a majority of known and potential DGC proteins, we propose that product inhibition of DGCs is of fundamental importance for *c*-di-GMP signaling and cellular homeostasis. The definition of the I-site binding pocket provides an entry point into unraveling the molecular mechanisms of ligand-protein interactions involved in *c*-di-GMP signaling and makes DGCs a valuable target for drug design to develop new strategies against biofilm-related diseases.

A global signaling network that relies on the production of the second messenger cyclic diguanylic acid has recently been discovered in bacteria (1, 2). The *c*-di-GMP³ system emerges as a regulatory mastermind orchestrating multicellular behavior and biofilm formation in a wide variety of bacteria (2). In addition, *c*-di-GMP signaling also plays a role in bacterial virulence

and persistence (3–7). The broad importance of this novel signaling molecule in pathogenic and non-pathogenic bacteria calls for careful analysis of the molecular mechanisms that control cellular levels of *c*-di-GMP and regulate its downstream targets. *c*-di-GMP is formed by the condensation of two GTP molecules (8–10) and is hydrolyzed to GMP via the linear intermediate pGpG (11–14). Two widespread and highly conserved bacterial protein domains have been implicated in the synthesis and hydrolysis of *c*-di-GMP, respectively (15). The breakdown of *c*-di-GMP is catalyzed by the EAL domain (12–14), and the diguanylate cyclase (8) activity resides in the GGDEF domain (10, 16). The highly conserved amino acid sequence GG(D/E)EF forms part of the catalytically active site (A-site) of the DGC enzyme (8). In agreement with this, mutations that change the GG(D/E)EF motif generally abolish the activity of the respective proteins (14, 16–18).

GGDEF domains are often found associated with sensor domains, arguing that DGC activity is controlled by direct signal input through these domains (1). The best understood example for controlled activation of a DGC is the response regulator PleD, which constitutes a timing device for *Caulobacter crescentus* pole development (17, 19, 20). PleD is activated during *C. crescentus* development by phosphorylation of an N-terminal receiver domain and, as a result, sequesters to the differentiating cell pole (17, 19). An additional layer of control was suggested by the crystal structure of PleD solved recently in complex with *c*-di-GMP (8) (Fig. 1). A *c*-di-GMP binding site was identified in the crystal, spatially separated from the catalytically active site (A-site). Two mutually intercalating *c*-di-GMP molecules were found tightly bound to this site, at the interface between the GGDEF and the central receiver-like domain of PleD (Fig. 1). Based on the observation that PleD activity shows a strong non-competitive product inhibition, it was proposed that this site might constitute an allosteric binding site (I-site) (8). Based on the observation that functionally important residues of the PleD I-site are highly conserved in a majority of GGDEF proteins listed in the data base, we tested the hypothesis that allosteric product inhibition is a general regulatory principle of bacterial diguanylate cyclases.

MATERIALS AND METHODS

Strains, Plasmids, and Media—*Escherichia coli* and *Salmonella enterica* serovar Typhimurium strains were grown in Luria broth (LB). *C. crescentus* strains were grown in complex peptone yeast extract (21). For DGC activity assays *in vivo*, *E. coli* was plated onto LB Congo Red plates (Sigma, 50 µg/ml). To determine the IPTG induction phenotype, 3 µl of a liquid log phase culture was spotted onto LB Congo Red plates with-

* This work was supported by Swiss National Science Foundation Fellowship 3100A0-108186 (to U. J.) and by a Swiss National Science Foundation Förderprofessur (to M. M.). The costs of publication of this article were defrayed in part by the payment of page charges. This article must therefore be hereby marked "advertisement" in accordance with 18 U.S.C. Section 1734 solely to indicate this fact.

[§] The on-line version of this article (available at <http://www.jbc.org>) contains supplemental text and Figs. S1–S4.

[†] These authors contributed equally to this work.

[‡] To whom correspondence should be addressed: Tel.: 41-61-267-2135; Fax: 41-61-267-2118; E-mail: urs.jenal@unibas.ch.

³ The abbreviations used are: *c*-di-GMP, cyclic diguanylic acid; pGpG, linear diguanylic acid; LB, Luria broth; DGC, diguanylate cyclase; PDE, phosphodiesterase; H6, hexa-histidine tag; rdar, red, dry, and rough; IPTG, isopropyl 1-thio-β-D-galactopyranoside; DgcA, diguanylate cyclase A; PdeA, phosphodiesterase A; CR, Congo Red; AC, adenylate cyclase; GC, guanylate cyclase.

Diguanylate Cyclase Feedback Control

out and with 1 mM IPTG. Biofilm formation was quantified after overnight growth by staining with 1% Crystal Violet as described (22). Motility phenotypes were determined using LB or peptone yeast extract motility plates containing 0.3% Difco-Agar. The exact procedure of strain and plasmid construction is available on request.

Random I-site Tetrapeptide Library—The *dgcA* gene (CC3285) was amplified by PCR using primers #1006 and #1007 (for primer list see supplemental text). The PCR product was digested with NdeI and XhoI and cloned into pET21a (Novagen). In a next step a *dgcA*ΔRESΔ allele with a silent PstI restriction site was generated by splicing with overlapping extension PCR using primers #1129, #670, and #1132. The resulting PCR product was digested with NdeI and XhoI and cloned into pET42b (Novagen) to produce pET42b::*dgcA*ΔRESΔ. The PstI/XhoI fragment of pET42b::*dgcA*ΔRESΔ was replaced by 20 independent PCR products, which had been generated using pET42b::*dgcA*ΔRESΔ as a template and primers #1131 and #670. The resulting 20 independent random libraries were individually transformed into *E. coli* BL21 and screened on Congo Red plates (LB plates supplemented with 50 μg/ml Congo Red). As a control reaction, the deleted I-site was reverted back to the wild-type RESΔ motif by cloning the PCR product generated with primers #1130 and #670 into the PstI and XhoI site of pET42b::*dgcA*ΔRESΔ.

Diguanylate Cyclase and Phosphodiesterase Activity Assays—DGC reactions were performed at 30 °C with 0.5 μM purified hexahistidine-tagged DgcA or 5 μM PleD in DGC reaction buffer containing 250 mM NaCl, 25 mM Tris-Cl, pH 8.0, 5 mM β-mercaptoethanol, and 20 mM MgCl₂. For inhibition assays the protein was preincubated with different concentrations of c-di-GMP (1–100 μM) for 2 min at 30 °C before 100 μM [³³P]GTP (Amersham Biosciences) was added. The reaction was stopped at regular time intervals by adding an equal volume of 0.5 M EDTA, pH 8.0. DGC/PDE tandem assays were carried out using 1 μM hexahistidine-tagged DgcA, which was preincubated for 2 min in the presence or absence of 4.5 μM hexahistidine-tagged phosphodiesterase PdeA. The reaction was started by adding 100 μM [³³P]GTP. The reactions were stopped at regular time intervals of 15 s by adding equal volumes of 0.5 M EDTA, pH 8.0, and their nucleotide composition was analyzed as described below.

Initial velocity (V_o) and inhibition constants were determined by plotting the corresponding nucleotide concentration *versus* time and by fitting the curve according to allosteric product inhibited Michaelis-Menten kinetics with the program ProFit 5.6.7 (with fit function $[c\text{-di-GMP}]_t = a(1)^*t/(a(2) + t)$, where the initial velocity V_o is defined as $a(1)/a(2)$) using the Levenberg-Marquardt algorithm. K_i values were determined by plotting V_o *versus* c-di-GMP concentration and using the following fit function, $V_{o[c\text{-di-GMP}]} = V_{o[c\text{-di-GMP}] = 0} * (1 - ([c\text{-di-GMP}]/(K_i + [c\text{-di-GMP}])))$.

Polyethyleneimine Cellulose Chromatography—Samples were dissolved in 5 μl of running buffer containing 1:1.5 (v/v) saturated NH₄SO₄ and 1.5 M KH₂PO₄, pH 3.60, and blotted on Polygram® CEL 300 polyethyleneimine cellulose TLC plates (Macherey-Nagel). Plates were developed in 1:1.5 (v/v) saturated NH₄SO₄ and 1.5 M KH₂PO₄, pH 3.60 ($R_f(c\text{-di-GMP})$ 0.2,

$R_f(pGpG)$ 0.4), dried, and exposed on a storage phosphor imaging screen (Amersham Biosciences). The intensity of the various radioactive species was calculated by quantifying the intensities of the relevant spots using ImageJ software version 1.33. V_o and K_i were determined with the Software ProFit 5.6.7.

UV Cross-linking with [³³P]c-di-GMP—The ³³P-labeled c-di-GMP was produced enzymatically using [³³P]GTP (3000 Ci/mmol) and purified according to a previous study (14). Protein samples were incubated for 10 min on ice in DGC reaction buffer (25 mM Tris-HCl, pH 8.0, 250 mM NaCl, 10 mM MgCl₂, 5 mM β-mercaptoethanol) together with 1 μM c-di-GMP and ³³P-radiolabeled c-di-GMP (0.75 μCi, 6000 Ci/mmol). Samples were then irradiated at 254 nm for 20 min in an ice-cooled, parafilm-wrapped 96-well aluminum block in an RPR-100 photochemical reactor with a UV lamp RPR-3500 (Southern New England Ultraviolet Co.). After irradiation, samples were mixed with 2× SDS-PAGE sample buffer (250 mM Tris-HCl at pH 6.8, 40% glycerol, 8% SDS, 2.4 M β-mercaptoethanol, 0.06% bromophenol blue, 40 mM EDTA) and heated for 5 min at 95 °C. Labeled proteins were separated by SDS-PAGE and quantified by autoradiography.

Nucleotide Extraction and Analysis—2.0 ml of *E. coli* cell cultures (A_{600} 0.4) were harvested by centrifugation, and supernatant was discarded. The cell pellet was dissolved in 200 μl of 0.5 M formic acid, and nucleotides were extracted for 10 min at 4 °C. Insoluble cell components were then pelleted, and the supernatant was directly analyzed by chromatography. Nucleotides were extracted and separated according to a previous study (23) on a 125/4 Nucleosil 4000-1 polyethyleneimine column (Macherey-Nagel) using the SMART-System (Amersham Biosciences). The nucleotide peak corresponding to c-di-GMP was verified by co-elution with a chemically synthesized c-di-GMP standard.

DgcA Protein Expression Levels—DgcA protein expression levels in *E. coli* BL21 were determined by Western blot analysis using Anti-His(C-Term) antibody (Invitrogen) and horseradish peroxidase conjugate of goat anti-mouse IgG (Invitrogen) as secondary antibody. The protein concentration was determined by measuring the intensities of the relevant spots using ImageJ software version 1.33. Signals were calibrated to defined concentrations of purified wild-type DgcA.

Molecular Modeling of PleD—All-atom simulations were carried out using the CHARMM (24) program and the CHARMM22/27 force field (25). For additional information see the supplemental material.

RESULTS

Feedback Inhibition of the PleD Diguanylate Cyclase Requires Binding of c-di-GMP to the I-site—The PleD crystal structure indicated the existence of an allosteric binding pocket (I-site) at the interface of the GGDEF and REC2 domains (8). Binding of a c-di-GMP dimer in the I-site is mediated by specific electrostatic interactions with charged residues of the GGDEF and REC2 domain (Fig. 1). To provide evidence for c-di-GMP binding to the I-site pocket in solution, trypsin digests were performed with purified PleD protein (5 μM) in the presence or absence of c-di-GMP (25 μM). The resulting peptide fragments were separated on a C18 column and analyzed by matrix-as-

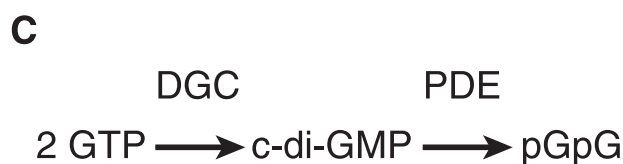
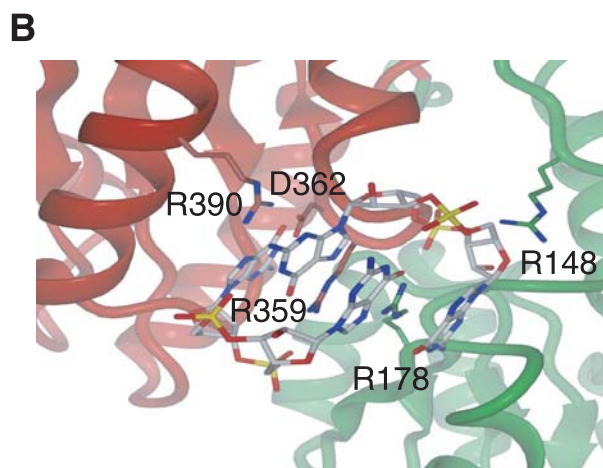
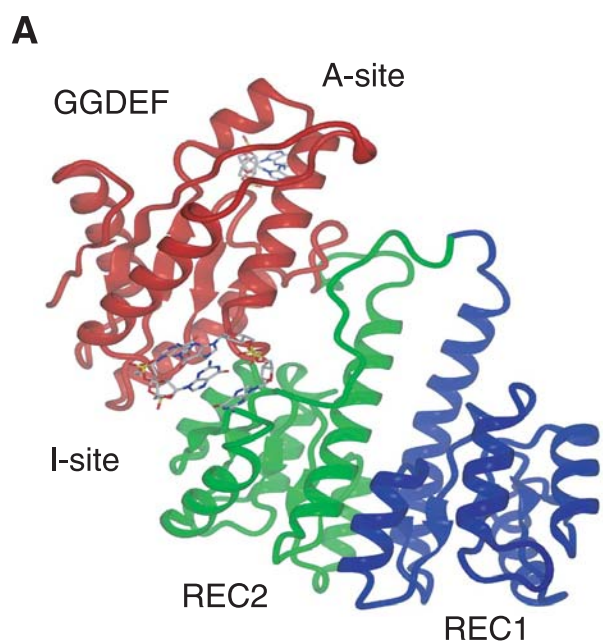


FIGURE 1. Crystal structure of the response regulator PleD. *A*, domain architecture of PleD with receiver domain REC1 (blue), receiver domain REC2 (green), and GGDEF domain harboring diguanylate cyclase activity (red). The active site (A-site) loop and the allosteric binding site (I-site) are indicated. *B*, zoom in view of the I-site pocket with a bound dimer of c-di-GMP with intercalated purine bases. Residues Arg-148 and Arg-178 (green) from the REC2 domain and residues Arg-359, Asp-362, and Arg-390 (red) from the GGDEF domain make specific contacts to the ligand in the crystal structure. *C*, schematic of c-di-GMP synthesis and degradation reactions.

sisted laser desorption ionization time-of-flight. Both chromatograms were identical, with the exception of two peaks that were only detected in the absence of ligand but were protected when c-di-GMP present during tryptic digest (supplemental Fig. S1). One of the two peptides (T47, retention time 25.6 min) was identified by mass spectrometry and corresponds to the amino acids 354–359 (supplemental Fig. S1), arguing that c-di-GMP specifically protects from trypsin cleavage at Arg-359. To

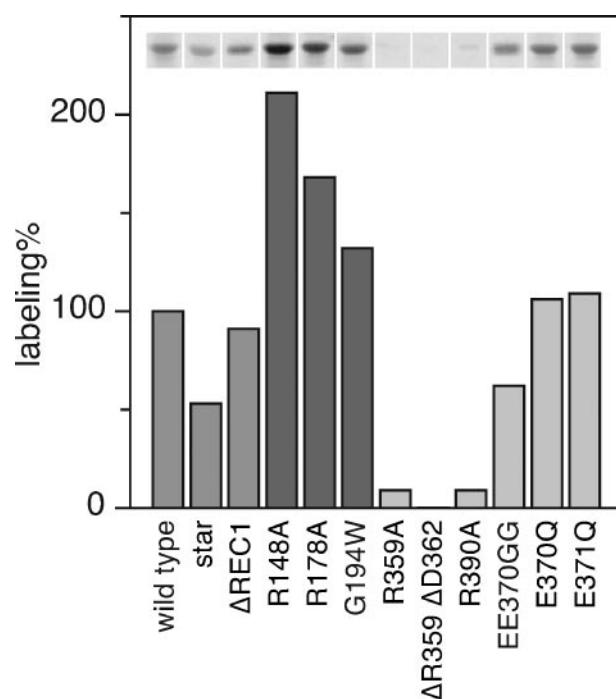


FIGURE 2. c-di-GMP labeling efficiency of different PleD mutants. The upper lane shows autoradiographs of [33 P]c-di-GMP UV cross-linked hexahistidine-tagged PleD mutant proteins separated by SDS-PAGE. Relative labeling efficiency with c-di-GMP is shown below with wild-type PleD corresponding to 100%. Specific mutants in different domains are colored in gray (REC1), dark gray (REC2) and light gray (GGDEF).

provide additional evidence for ligand binding in solution, we performed UV cross-linking assays using 33 P-labeled c-di-GMP (14). Residues Arg-148 and Arg-178 of the REC2 domain and Arg-359, Asp-362, and Arg-390 of the GGDEF domain were replaced with alanine, and the resulting protein variants were analyzed. As shown in Fig. 2, mutating I-site residues of the GGDEF domain abolished (Δ R359 Δ D362) or strongly reduced (R359A and R390A) c-di-GMP binding. In contrast, mutations in the A-site (E370Q, E371Q, and EE370GG), which completely abolished enzymatic activity (Table 1), had no effect on c-di-GMP binding (Fig. 2), indicating that labeling with radioactive c-di-GMP results from ligand binding at the I-site. Although mutations R359A, R359V, Δ R359 Δ D362, and D362A all showed a dramatically reduced or complete loss of enzymatic activity, mutant R390A showed wild-type-like DGC activity (Table 1). In agreement with the reduced binding of c-di-GMP (Fig. 2), the K_i of mutant R390A was increased \sim 20-fold (Table 1). PleD proteins harboring mutations in the REC2 portion of the I-site (R148A and R178A) showed an increased binding of c-di-GMP (Fig. 2) and slightly lower K_i values than wild type (Table 1). Surprisingly, R148A/R178A single and double mutants displayed a 5- to 20-fold higher DGC activity compared with wild-type PleD (Table 1). Finally, c-di-GMP binding was normal in mutant proteins that either lacked the REC1 receiver domain or had a bulky tryptophan residue introduced at the REC2-GGDEF interface (G194W, Fig. 2). Together these results implied that the structural requirements for c-di-GMP binding are contained within the GGDEF domain of PleD and that residues Arg-359, Asp-362, and Arg-390 form the core of an allosteric binding pocket for c-di-GMP.

Diguanylate Cyclase Feedback Control

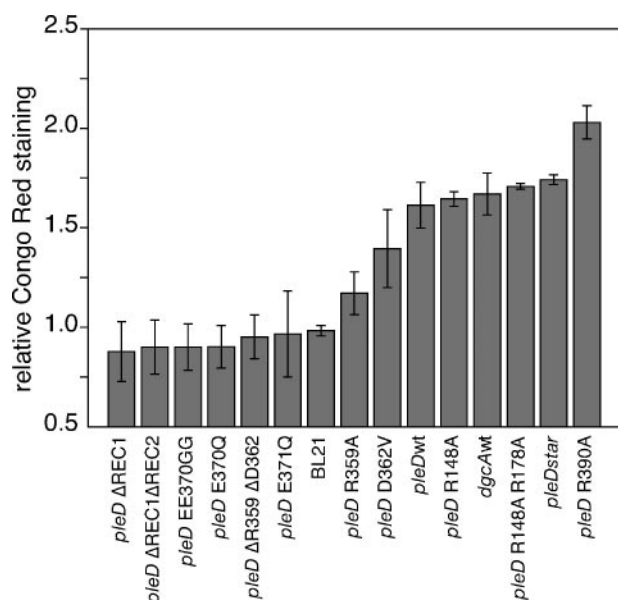


FIGURE 3. *In vivo* activity of different PleD and DgcA mutant proteins. *E. coli* BL21 strains expressing different *pleD* alleles and *dgcA* wild type were spotted onto Congo Red plates. Relative Congo Red binding was determined using imageJ software with BL21 corresponding to 100%.

Evidence for an in Vivo Role of I-site-mediated Feedback Control—To test a possible role for feedback inhibition of diguanylate cyclases *in vivo*, we developed a simple assay based on the observation that in *E. coli* and other *Enterobacteriaceae* increased cellular levels of *c*-di-GMP correlate with Congo Red (CR) staining of colonies on plates (28). Low level expression (in the absence of the inducer IPTG) of active *pleD* alleles caused a red colony phenotype in the *E. coli* B strain BL21, whereas cells expressing inactive *pleD* alleles under the same conditions stained white (Fig. 3). Interestingly, PleD mutants with dramatically different diguanylate cyclase activities *in vitro* showed only minor differences of CR staining *in vivo*. For instance, PleDR148A/R178A, which showed a 20-fold increased activity (Table 1), or PleD*, a constitutively active mutant of PleD several 100-fold more active than wild-type (9), caused virtually identical CR values like PleD wild type (Fig. 3). In contrast, expression of the feedback inhibition mutant PleDR390A resulted in a significantly higher CR staining even though its *in vitro* DGC activity was lower than wild-type PleD (Table 1). This argued that *in vivo* steady-state concentrations of *c*-di-GMP were determined mainly by the PleD inhibition constant (as opposed to the overall activity of the enzyme) and that a functional I-site is critical for DGC control *in vivo*.

DgcA, a Single Domain Diguanylate Cyclase, Is Subject to Allosteric Product Inhibition—Sequence alignments of >1000 annotated GGDEF domain proteins revealed that that I-site residues Arg-359 and Asp-362 of PleD are highly conserved. 57% of the proteins containing a GGDEF domain and 27% of GGDEF/EAL composite proteins possess this motif. This suggested that *c*-di-GMP product inhibition could be a general regulatory mechanism of bacterial diguanylate cyclases. To test this, hexahistidine-tagged derivatives of two *C. crescentus* GGDEF domain proteins were analyzed biochemically with respect to their DGC activities and *c*-di-GMP binding proper-

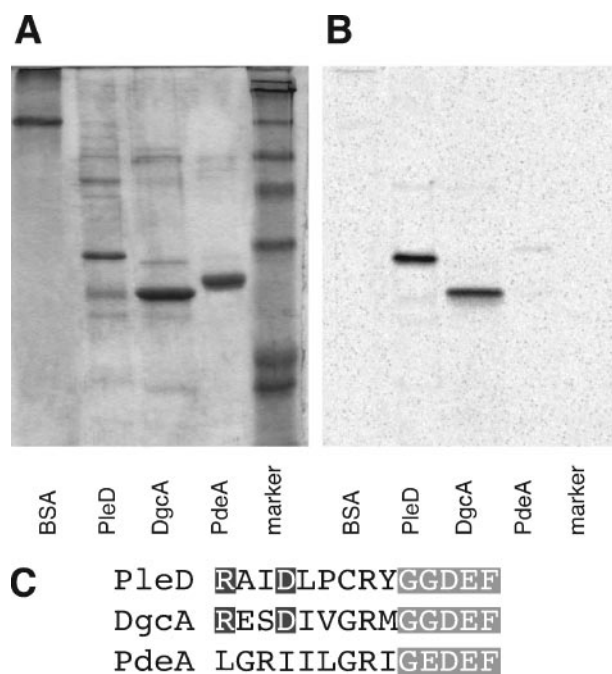


FIGURE 4. UV cross-linking of different GGDEF domains with ³³P-labeled *c*-di-GMP. **A**, Coomassie-stained SDS-PAGE and **B**, autoradiograph of BSA (control), PleDΔREC1, DgcA, and the isolated GGDEF domain of the *c*-di-GMP-specific phosphodiesterase PdeA (CC3396) after UV cross-linking with [³³P]*c*-di-GMP. **C**, alignment of I- and A-site sequence of PleD, DgcA, and PdeA. I-site (RXXD) and A-site residues (GGDEF) are marked in *black* and *gray*, respectively.

ties. Purified DgcA (diguanylate cyclase A, CC3285), a soluble, single domain GGDEF protein that lacks an obvious N-terminal input domain, showed strong diguanylate cyclase activity (Fig. 5A). DgcA has an RESD motive five amino acids upstream of the conserved GGDEF active site and was readily labeled with [³³P]*c*-di-GMP in a cross-linking experiment (Fig. 4). Consistent with this, DgcA showed strong feedback inhibition (Fig. 5A) with its K_i (1 μ M) being in the same range as the inhibition constant determined for PleD (8). In contrast, the GGDEF domain of PdeA (phosphodiesterase A, CC3396), which lacks catalytic activity (14), had no conserved I-site residues and did not bind radiolabeled *c*-di-GMP (Fig. 4). Thus, specific binding of *c*-di-GMP correlated with the presence of a conserved I-site motif RXXD (Fig. 4).

Diguanylate cyclase activity assays revealed strong and rapid product inhibition of DgcA. DgcA alone was able to convert only a small fraction of the available GTP substrate pool into the product *c*-di-GMP ($V_o = 2.8 \mu$ mol of *c*-di-GMP μ mol protein⁻¹ min⁻¹) (Fig. 5B). In contrast, GTP consumption and conversion into *c*-di-GMP and pGpG was rapid ($V_o = 43.0 \mu$ mol of *c*-di-GMP μ mol protein⁻¹ min⁻¹) and almost complete when the PDE CC3396 was added in excess to the enzymatic reaction (Fig. 5B). This argued that *c*-di-GMP feedback inhibition is abolished in a sequential DGC-PDE reaction, because the steady-state concentration of the inhibitor *c*-di-GMP is kept low by continuous degradation of *c*-di-GMP into the linear dinucleotide pGpG. As a consequence of rapid feedback inhibition, the experimentally determined V_o values of the DGC reaction are generally underestimated. In conclusion, these results strengthen the view that allosteric product inhibi-

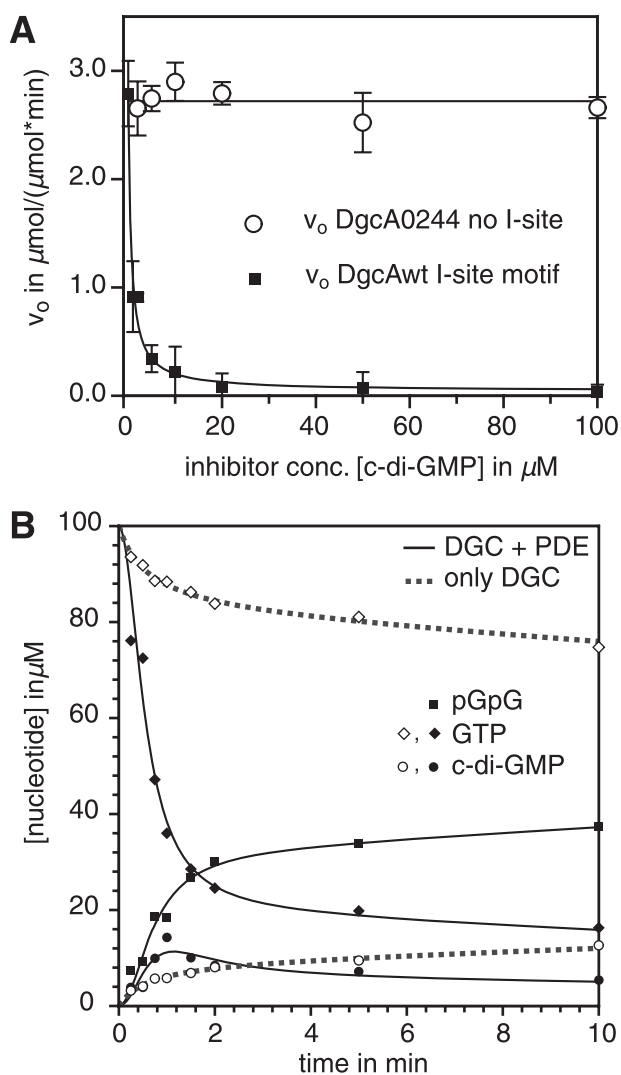


FIGURE 5. *c*-di-GMP product inhibition of DgcA. *A*, initial velocities of the wild-type diguanylate cyclase DgcA (*squares*) and the non-feedback-inhibited I-site mutant DgcA0244 (*circles*) in the presence of increasing concentrations of *c*-di-GMP. *B*, conversion of GTP into *c*-di-GMP by DgcA (*dashed lines*) and accelerated GTP consumption, *c*-di-GMP synthesis, and cleavage into pGpG by a diguanylate cyclase-phosphodiesterase tandem reaction (*plain lines*).

tion is a general principle of diguanylate cyclases and that high affinity binding of *c*-di-GMP requires an RXXD I-site motif positioned in close proximity to the active site.

Development of an *in Vivo* Assay to Genetically Probe Allosteric Control of DgcA—DGCs from different bacterial species have been shown to be functionally interchangeable (17, 26, 27). To determine if DgcA is active *in vivo* we expressed a plasmid-based copy of the *dgcA* gene in *C. crescentus*, *S. enterica*, and *Escherichia coli* B and tested the respective strains for the phenotypes known to result from increased cellular levels of *c*-di-GMP (17, 26, 27). Consistent with these earlier findings, expression of *dgcA* strongly inhibited flagellar-based motility in all three organisms, dramatically increased the ability of *S. enterica* and *E. coli* for surface colonization, and produced the characteristic red, dry, and rough (rdar) colony morphotype when plated on CR plates (Fig. 6, *A–F*) (29). The red phenotype provided the basis for a visual genetic screen on CR plates. Under these conditions, cells producing active DgcA variants would

produce dark red single colonies, whereas cells producing inactive DgcA mutants would remain white. This prompted us to use the CR screen to isolate *dgcA* mutants, which had a specific defect in feedback regulation, and to define the minimal requirements for product inhibition of this class of enzymes.

Randomization of *c*-di-GMP Binding Pocket Reveals Three Mutant Classes—To probe the minimal requirements of the I-site for *c*-di-GMP binding and product inhibition, a *dgcA* mutant library was constructed with the RESD signature replaced by a randomized tetrapeptide sequence (see “Materials and Methods”). In short, a *dgcA* gene, which carried a deletion of the four I-site codons, was used as template for a PCR reaction. For the amplification step a primer complementary to the 3'-end of *dgcA* was used in combination with a mixture of oligonucleotides that spanned the deletion site and contained 12 randomized base pairs at the position coding for the deleted amino acids. The resulting PCR fragments were fused in-frame with the 5'-end of *dgcA* in the expression plasmid pET42b and were transformed into *E. coli* BL21. The resulting gene library contains a theoretical number of 1.67×10^7 (4^{12}) different *dgcA* alleles, coding for DgcA variants with different combinations of I-site residues.

When plated on CR plates, colonies transformed with a wild-type *dgcA* allele showed the typical rdar colony morphology (Fig. 6*G*). Transformation of *E. coli* BL21 with a plasmid expressing a mutant DgcA, which lacked the four amino acids of the I-site (DgcA Δ RESD), produced white colonies on CR plates (Fig. 6*H*), indicating that this mutant form had lost DGC activity. About 10% of the clones with random tetrapeptide insertions stained red on CR plates and thus had retained DGC activity (Fig. 6*I*). This result is consistent with the observation that alanine scanning of the PleD I-site almost exclusively produced non-active enzyme variants (Table 1) and argues that the majority of amino acid substitutions introduced at the I-site are detrimental for the catalytic activity of the DGC. To further characterize active DgcA I-site variants, a total of 800 red colonies was isolated and patched onto CR plates without (Fig. 6, *J* and *K*) or with the inducer IPTG (Fig. 6, *L* and *M*). This secondary screen was based on the observation that IPTG-induced expression of the *pleDR390A* allele (Table 1), but not of the *pleD* wild-type allele, abolished growth of *E. coli* BL21 (data not shown). This suggested that at elevated protein levels, DGCs that lack feedback control are toxic *in vivo* (see below). The majority of the I-site library clones tested failed to grow on plates containing IPTG, indicating that their activity is no longer controlled by product inhibition (Fig. 6, *L* and *M*). Only 7 mutants (out of 9000 colonies screened) showed a wild-type-like behavior in that they stained dark red on CR plates and tolerated the presence of the inducer IPTG (Fig. 6, *L* and *M*).

This genetic screen led to the isolation of three different I-site mutant classes with the following characteristics: 1) catalytically inactive mutants (A^- , frequency $\sim 90\%$); 2) feedback control negative mutants (I^-A^+ , frequency $\sim 10\%$); and wild-type-like mutants (I^+A^+ , frequency $\sim 0.1\%$). A subset of class 1 and 2 mutants and all seven class 3 mutants were selected, and hexahistidine-tagged forms of the respective proteins were purified for biochemical characterization. Kinetic parameters of activity (V_0) and feedback inhibition (K_i) were determined

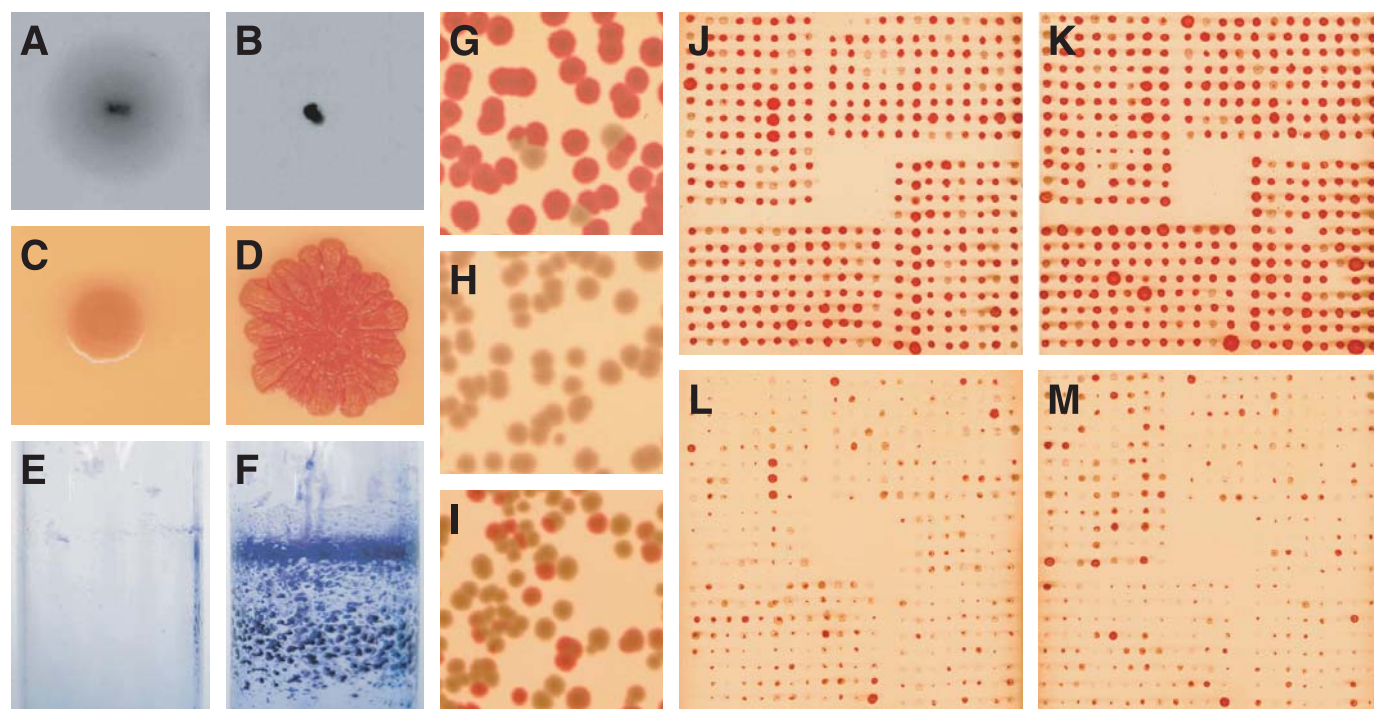


FIGURE 6. Phenotypic characterization of ectopically expressed diguanylate cyclase *dgca* in *E. coli* and *S. enterica*. Behavior of *E. coli* strain BL21 with empty pET42b plasmid (A) and pET42b::*dgca* (B) on motility plates. Colony morphology of *E. coli* strain BL21 with empty pET42b plasmid (C) and with pET42b::*dgca* (D) on Congo Red plates. Biofilm formation of *S. enterica* serovar Typhimurium *trp::T7RNAP* with empty pET42b (E) and pET42b::*dgca* (F) grown in liquid culture and stained with crystal violet. *E. coli* BL21 transformed with PCR-restored *dgca* wild type on pET42b::*dgca* (G), with the inactive allele *dgca*ΔRESΔ (pET42b::*dgca*ΔRESΔ) (H), and with a library of random tetrapeptide insertions in the I-site (pET42b::*dgca*AXXX) (I) and plated on Congo Red plates. *E. coli* BL21 expressing different I-site mutant alleles were spotted onto Congo Red plates without (J and K) and with 1 mM IPTG (L and M) to screen for feedback inhibition *dgca* alleles.

TABLE 1
Kinetic analysis of PleD mutants

Protein	V_o	ΔV_o	K_i	ΔK_i
	$\mu\text{mol } c\text{-di-GMP}/$ $(\mu\text{mol protein} \cdot \text{min})$		μM	
PleD wild type	0.202	± 0.023	5.8	± 1.0
PleDR359A	0.005	ND ^a	>100	ND
PleDR359V	0.0	ND		
PleDΔ359Δ362	0.0	ND		
PleDD362A	0.0	ND		
PleDR390A	0.076	± 0.007	115.0	± 18.1
PleDR148A	0.822	± 0.020	2.8	± 1.2
PleDR178A	0.918	± 0.292	3.6	± 0.1
PleDR148AR178A	3.75	± 0.43	2.9	± 0.6
PleDG194W	0.161	± 0.005	6.3	± 1.9
PleDEE370GG	0.0	ND		
PleDE370Q	0.0	ND		
PleDE371Q	0.0	ND		

^a ND, not determined.

individually using an *in vitro* diguanylate cyclase activity assay (16). Consistent with their rdar-like *in vivo* phenotype, only class 2 and class 3 mutants showed detectable diguanylate cyclase activity with an initial velocity between 1.93 and 14.21 μmol of *c*-di-GMP $\mu\text{mol protein}^{-1} \text{min}^{-1}$ (Table 2). Only mutant proteins from the IPTG tolerant class 3 showed product inhibition with K_i values close to 1 μM (Table 2). In contrast, all proteins from class 2 mutants showed no feedback inhibition *in vitro*, arguing that their *in vivo* toxicity is the result of uncontrolled run-off DGC activity (Fig. 5A and Table 2). Support for this hypothesis comes from experiments determining the cellular concentration of *c*-di-GMP and DgcA protein expression levels in *E. coli* BL21 carrying selected *dgca* alleles on plasmid pET42b (see "Materials and Methods"). Alleles *dgcaA0244*,

dgcaA1229, and *dgcaA1250* were chosen, because the DGC activity of these enzymes is similar to wild type DgcA (Table 2). Basal level expression (no IPTG) of *dgcaA0244*, the allele coding for a DGC that completely lacks feedback inhibition, resulted in a more than 100-fold increased cellular level of *c*-di-GMP as compared with cells expressing wild-type *dgca* (Table 3). This was due to an almost 100-fold higher overall turnover of the mutant enzyme as compared with wild type (Table 3). In contrast, enzymatic turnover and cellular concentration of *c*-di-GMP was increased only marginally in *E. coli* cells expressing alleles *dgcaA1229*, and *dgcaA1250* with restored feedback inhibition control (Table 3).

Sequence analysis of the tetrapeptide insertions of class 2 and class 3 mutants revealed several important characteristics of a functional allosteric I-site binding pocket. All catalytically active and feedback inhibition competent mutants restored the wild-type Arg and Asp residues at positions one and four of the RXXD motive (Table 2). Whereas most of the mutants that had lost feedback inhibition had altered either one or both of these charged residues (Table 2) only two feedback inhibition mutants had retained both charges with changes in the intervening residues (Table 2). Obviously, Arg and Asp, while being strictly required for feedback inhibition, need to be placed in the appropriate sequence context of the I-site loop. These experiments define the minimal requirements of the I-site core region and demonstrate that the Arg and Asp residues that make direct contacts to the *c*-di-GMP ligand in the crystal structure are of critical functional importance for DGC feedback inhibition *in vivo* and *in vitro*. This provides a plausible

TABLE 2
Diguanylate cyclase activity and inhibition constant of DgcA I-site mutant proteins

Protein	Motif	V_o $\mu\text{mol c-di-GMP}/$ $(\mu\text{mol protein}\cdot\text{min})$	ΔV_o	K_i μM	ΔK_i
DgcA wt	RES D	2.79	± 0.01	0.96	± 0.09
DgcA1406	RQGD	5.35	± 0.05	7.02	± 2.92
DgcA1040	RLVD	4.92	± 0.19	4.52	± 1.81
DgcA1229	RGAD	2.03	± 0.01	1.84	± 0.26
DgcA1524	RSAD	3.70	± 0.13	7.36	± 2.69
DgcA1529	RLAD	2.79	± 0.04	1.01	± 0.23
DgcA0751	RCAD	3.65	± 0.10	3.51	± 0.52
DgcA1250	RGGD	2.07	± 0.02	2.24	± 0.49
DgcA Δ RES D		0.14	± 0.06		ND ^a
DgcA0207	GMGG	14.21	± 0.54	No inhibition	
DgcA0244	VMGG	2.57	± 0.05	No inhibition	
DgcA0613	GGVA	4.29	± 0.06	No inhibition	
DgcA0646	GRDC	8.90	± 0.10	No inhibition	
DgcA0913	GVDG	3.81	± 0.04	No inhibition	
DgcA1300	MEGD	0.87	± 0.02	No inhibition	
DgcA1733	GGNH	11.47	± 0.17	No inhibition	
DgcA3018	RESE	11.1	± 0.11	No inhibition	
DgcA0230	RNRD	3.02	± 0.06	No inhibition	
DgcA0642	RVDS	4.17	± 0.08	No inhibition	
DgcA1007	RAGG	6.06	± 0.05	No inhibition	
DgcA2006	RGQD	1.93	± 0.01	No inhibition	

^a ND, not determined.

TABLE 3
DgcA protein levels and cellular c-di-GMP concentrations in the absence or presence of IPTG induction at 1 mM

	Protein conc. ^a		c-di-GMP conc.		Turnover ^b	
	No induction	1 mM IPTG	No induction	1 mM IPTG	No induction	1 mM IPTG
	<i>pmol protein/mg dry weight</i>		<i>pmol c-di-GMP/mg dry weight</i>		<i>pmol c-di-GMP per pmol protein</i>	
DgcA0244	4.1	22	1466.3	1570.7	357.6	71.4
DgcA1229	3.5	31	87.6	139.5	25.0	4.5
DgcA1250	2.7	43	24.2	305.4	9.0	7.1
DgcA wt	2.9	33	13.75	189.4	4.7	5.7
DgcA Δ RES D	3.5	23	ND ^c	ND	NA ^d	NA

^a See "Materials and Methods."

^b As derived from the cellular c-di-GMP concentration divided by the cellular protein concentration.

^c ND, not detectable.

^d NA, not applicable.

explanation for the strong conservation of the RXXD motif in GGDEF domains.

The molecular mechanism of product inhibition through I-site binding remains unclear. To assist the interpretation of the present data and provide information on binding induced mobility, atomistically detailed simulations were carried out. Normal mode calculations on ligated and unligated PleD were used to analyze the structural transitions that occur during I-site binding of c-di-GMP. Normal mode calculations on the optimized structures yielded no imaginary frequencies, and translational and rotational frequencies were close to zero ($|\omega| \leq 0.02 \text{ cm}^{-1}$). This indicated that the minimized structures correspond to real minima on the potential energy surface. The displacements calculated for the ligated and the unligated protein showed a significant decrease in mobility for both I- and A-site residues upon complexation (supplemental Figs. S2 and S3). Whereas motion in the I-site is suppressed due to steric interactions upon ligand insertion, quenching of the A-site residues suggested that the two sites might be dynamically coupled via the short connecting β -strand (β_2). Backbone C α -atoms and side chains of the I-site and A-site loops were displaced by an average of 1–4 Å in opposite directions, arguing that a balance-like movement centered around β_2 could be responsible for direct information transfer between the two sites (Fig. 7). The cumulated displacements per residue over all 147 modes

(supplemental Fig. S3) showed different mobilities in additional regions of the protein. The C α atoms of residues exhibiting large changes in flexibility upon ligand binding are depicted as *spheres* in supplemental Fig. S3. Reduced flexibility (*yellow spheres*) is found at the I-site, A-site, phosphorylation site, and the dimer interface, whereas the flexibility is enhanced (*black spheres*) at the REC1/REC2 interface. In summary, these simulations show that I-site binding of c-di-GMP not only reduced the mobility around the RXXD motif but also of the residues of the A-site loop.

DISCUSSION

Feedback Inhibition Is a General Control Mechanism of Diguanylate Cyclases—The data presented here propose a general mechanism to regulate the activity of diguanylate cyclases (DGCs), key enzymes of c-di-GMP-based signal transduction in bacteria. High affinity binding of c-di-GMP to a site distant from the catalytic pocket (I-site) efficiently blocks enzymatic activity in a non-competitive manner. Mutational analysis of multi- and single-domain DGC proteins has provided convincing evidence for the role of several charged amino acids in c-di-GMP binding and allosteric regulation. Furthermore, these experiments indicated that the allosteric binding site is functionally contained within the GGDEF domain. An *in vivo* selection experiment using a random tetrapeptide library, and

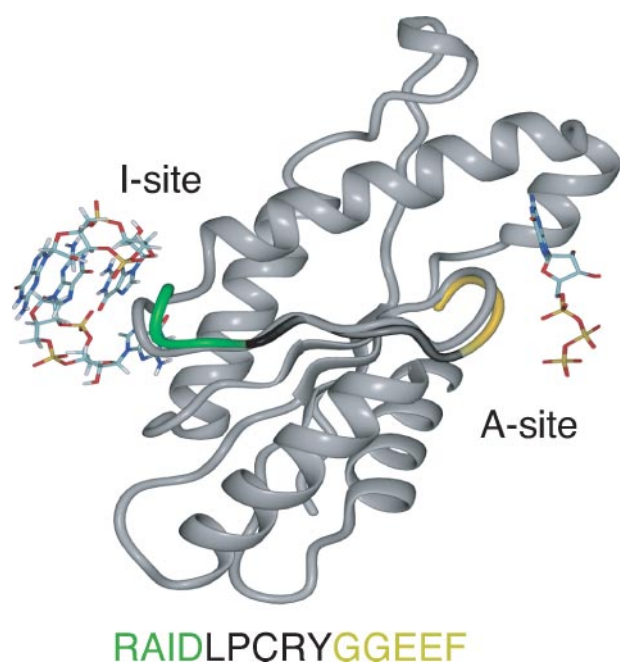


FIGURE 7. Comparison of the energy-minimized structures of the PleD GGDEF domain with and without ligand bound to the I-site. For improved clarity, the domain is sliced through the I-site loop/ β 2/A-site loop plane. The unligated protein is shown in gray and the I-site loop (green), β 2 (black), and A-site loop (gold) of the bound structure are shown as an overlay. GTP bound to the active site is modeled according to the orientation of c-di-GMP bound to the A-site in the crystal structure. The PleD amino acid sequence of I-site, β 2, and A-site is indicated below.

designed to re-engineer the I-site has led to the definition of a highly conserved RXXD core motif of the c-di-GMP binding pocket. The RXXD motif forms a turn at the end of a short five-amino acid β -sheet that directly connects the I-site with the conserved catalytic A-site motif, GG(D/E)EF (Fig. 7). This raised the question of how I-site ligand binding modulates DGC enzyme activity. In the multidomain protein PleD, c-di-GMP bound to the I-site physically connects the GGDEF domain with the REC1-REC2 dimerization stem. It was speculated that product inhibition occurs by domain immobilization, which would prevent the encounter of the two DGC substrate binding sites (8). Several observations argue in favor of a more direct communication between I- and A-sites. First, with a large variety of domains found to be associated with GGDEF domains, it seems unlikely that functional I-sites are generally formed by the interface of a GGDEF with its neighboring domain (2). In agreement with this, residues of the PleD REC2 domain are not required for c-di-GMP binding and feedback inhibition. Second, the single domain DGC protein, DgcA, shows I-site-dependent allosteric control with a K_i of $1 \mu\text{M}$. Third, the introduction of a bulky tryptophan residue (G194W) at the GGDEF-REC2 interface did not affect activity, I-site binding, or feedback inhibition of PleD (Fig. 2 and Table 1). Fourth, atomistic simulations of ligated and unligated PleD predicted a marked drop in flexibility of C α -atoms both in the I- and A-site upon ligand binding. Simultaneous with motion quenching, β 2 and its flanking I- and A-loops undergo a balance-like movement that repositions A-site residues in the catalytic active site (Fig. 7). This is consistent with the idea that structural changes within the GGDEF domain upon binding of c-di-GMP at the

I-site lead to repositioning of active site residues and possibly altered kinetic parameters. Thus, we propose that c-di-GMP binding and allosteric control represents an intrinsic regulatory property of DGCs that contain an RXXD motif.

Like guanylate and adenylate cyclases (GCs and ACs) and DNA polymerases, DGCs catalyze the nucleophilic attack of the 3'-hydroxyl group on the α -phosphate of a nucleoside triphosphate. Despite the lack of obvious sequence similarities, the PleD x-ray structure revealed that DGCs possess a similar domain architecture like ACs and GCs (8, 30). Based on mutational analysis (8, 14, 16) and on structural comparisons between DGC, AC, GC, and DNA polymerases (31–34), a model for DGC catalysis can be proposed. In contrast to the heterodimeric ACs and GCs, DGCs form homodimers, with a GTP molecule bound within the catalytic core of each DGC monomer (8). Two Mg^{2+} ions are coordinated by the highly conserved glutamic acid residue Glu-371, which is part of the GGDEF motif, and possibly by Asp-327 on the opposing β -sheet. The divalent Mg^{2+} carboxyl complex coordinates the triphosphate moiety of GTP and activates the 3'-hydroxyl group for intermolecular nucleophilic attack. Substrate specificity of AC and GC can be interchanged by converting a few key residues involved in purine recognition (31, 34, 35). This includes an arginine residue, which in PleD corresponds to the highly conserved Arg-366 located in the β -sheet connecting the I- and A-sites. Based on the active site model, two alternative inhibition mechanisms can be envisaged. In a first scenario, binding of c-di-GMP to the I-site would change the orientation of Arg-366 and would thereby disturb the guanine binding pocket resulting in an increased K_m for GTP. Alternatively, inhibitor binding could rearrange the Mg^{2+} carboxyl complex and thus destabilize the active state.

In Silico Analysis of the GGDEF Protein Family Indicates That Product Inhibition Is a General Regulatory Mechanism—DGC activity of GGDEF domain proteins seems to strictly depend on conserved GGDEF or GGEEF motifs in the active site (10, 16, 18, 36–38). Consistent with this, ~90% of the GGDEF and 62% of the GGDEF/EAL composite proteins show a conserved GG(D/E)EF A-site motif. Of the GGDEF proteins with a highly conserved A-site motif, >60% have conserved RXXD I-site residues and a conserved spacer length between I- and A-site, arguing that the three-dimensional arrangement of catalytic and allosteric pocket is likely to be similar in all DGCs. From a total of 19 GGDEF proteins, for which convincing evidence for a DGC activity exists, 14 have a conserved I-site (supplemental Fig. S4). Ryjenkov and coworkers (10) reported severe toxicity problems when expressing diguanylate cyclases lacking I-site residues in *E. coli* BL21. This is consistent with the growth defect observed upon expression of *dgcA* feedback inhibition mutants in *E. coli* BL21 and argues that these proteins are not feedback-controlled. The molecular basis of growth interference under these conditions is unclear. It is possible that depletion of the GTP pool or adverse effects of unphysiologically high levels of c-di-GMP are responsible for this effect. Although the experiments presented here define a role for the I-site in DGC feedback inhibition, the c-di-GMP binding pocket could also be exploited for other roles in c-di-GMP signaling. It has been proposed recently that non-catalytic GGDEF

domains with variant A-site motifs can fulfill regulatory functions (14). It is attractive to speculate that a subgroup of GGDEF proteins that has degenerate catalytic A-sites but conserved c-di-GMP binding pockets, represents a novel class of c-di-GMP effector proteins that regulate cellular functions in response to c-di-GMP binding.

Regulatory Significance of DGC Feedback Control—GGDEF domains are often associated with sensory domains in one- or two-component signaling systems (39, 40). Thus it is reasonable to assume that in most cases DGC activity is controlled by direct signal input through these domains. But why then would a substantial portion of these enzymes also be subject to feedback inhibition? There are several possibilities, which among themselves are not mutually exclusive. Given the anticipated regulatory complexity of the c-di-GMP signaling network (2, 39) and the potentially dramatic changes in cellular physiology and behavior caused by fluctuating levels of c-di-GMP, it is in the cell's best interest to rigorously control the production of the second messenger. Product inhibition of DGCs allows the establishment of precise threshold concentrations of the second messenger, or, in combination with counteracting PDEs, could produce short spikes or even generate oscillations of c-di-GMP. In addition, negative feedback loops have been implicated in neutralizing noise and providing robustness in genetic networks by limiting the range over which the concentrations of the network components fluctuate (41, 42). Similarly, product inhibition of DGCs could contribute to the reduction of stochastic perturbations and increase the stability of the c-di-GMP circuitry by keeping c-di-GMP levels in defined concentration windows. Alternatively, DGC autoregulation may influence the kinetics of c-di-GMP signaling. Mathematical modeling and experimental evidence suggested that negative autoregulation in combination with strong promoters substantially shortens the rise-time of transcription responses (43–45). In analogy, a desired steady-state concentration of c-di-GMP can in principle be achieved by two regulatory designs: (a) a low activity DGC with no product inhibition, and (b) a high activity DGC with built-in negative autoregulation. In cases where circuits have been optimized for fast up-kinetics, design B will be superior. It is plausible that DGCs with or without I-site motifs can be divided into these two kinetically different classes.

This study contributes to the emerging understanding of the c-di-GMP regulatory network in bacteria. The current emphasis lies on the identification of effector molecules, regulatory mechanisms, and processes controlled by c-di-GMP. With the long term goal in mind of approaching a detailed systems-level understanding of c-di-GMP signaling, kinetic parameters of signaling mechanisms will require our particular attention. Our experiments provide an entry point into the kinetic analysis of individual DGCs and the quantitative assessment of the c-di-GMP circuitry.

Acknowledgments—We thank Tilman Schirmer for helpful discussions and students of the Microbiology and Immunology Course (Biozentrum of the University of Basel, 2005) and of the Advanced Bacterial Genetics Course (Cold Spring Harbor, 2005) for their help in mutant screening.

REFERENCES

- Jenal, U. (2004) *Curr. Opin. Microbiol.* **7**, 185–191
- Romling, U., Gomelsky, M., and Galperin, M. Y. (2005) *Mol. Microbiol.* **57**, 629–639
- Brouillette, E., Hyodo, M., Hayakawa, Y., Karaolis, D. K. R., and Malouin, F. (2005) *Antimicrob. Agents Chemother.* **49**, 3109–3113
- Hisert, K. B., MacCoss, M., Shiloh, M. U., Darwin, K. H., Singh, S., Jones, R. A., Ehrt, S., Zhang, Z. Y., Gaffney, B. L., Gandotra, S., Holden, D. W., Murray, D., and Nathan, C. (2005) *Mol. Microbiol.* **56**, 1234–1245
- Kuleskara, H., Lee, V., Brencic, A., Liberati, N., Urbach, J., Miyata, S., Lee, D. G., Neely, A. N., Hyodo, M., Hayakawa, Y., Ausubel, F. M., and Lory, S. (2006) *Proc. Natl. Acad. Sci. U. S. A.* **103**, 2839–2844
- Lestrade, P., Dricot, A., Delrue, R. M., Lambert, C., Martinelli, V., De Bolle, X., Letesson, J. J., and Tibor, A. (2003) *Infect. Immun.* **71**, 7053–7060
- Tischler, A. D., Lee, S. H., and Camilli, A. (2002) *J. Bacteriol.* **184**, 4104–4113
- Chan, C., Paul, R., Samoray, D., Amiot, N. C., Giese, B., Jenal, U., and Schirmer, T. (2004) *Proc. Natl. Acad. Sci. U. S. A.* **101**, 17084–17089
- Ross, P., Weinhouse, H., Aloni, Y., Michaeli, D., Weinbergerohana, P., Mayer, R., Braun, S., Devroom, E., Vandermarel, G. A., Vanboom, J. H., and Benziman, M. (1987) *Nature* **325**, 279–281
- Ryjenkov, D. A., Tarutina, M., Moskvina, O. V., and Gomelsky, M. (2005) *J. Bacteriol.* **187**, 1792–1798
- Ross, P., Mayer, R., and Benziman, M. (1991) *Microbiol. Rev.* **55**, 35–58
- Schmidt, A. J., Ryjenkov, D. A., and Gomelsky, M. (2005) *J. Bacteriol.* **187**, 4774–4781
- Tamayo, R., Tischler, A. D., and Camilli, A. (2005) *J. Biol. Chem.* **280**, 33324–33330
- Christen, M., Christen, B., Folcher, M., Schauerte, A., and Jenal, U. (2005) *J. Biol. Chem.* **280**, 30829–30837
- Tal, R., Wong, H. C., Calhoon, R., Gelfand, D., Fear, A. L., Volman, G., Mayer, R., Ross, P., Amikam, D., Weinhouse, H., Cohen, A., Sapir, S., Ohana, P., and Benziman, M. (1998) *J. Bacteriol.* **180**, 4416–4425
- Paul, R., Weiser, S., Amiot, N. C., Chan, C., Schirmer, T., Giese, B., and Jenal, U. (2004) *Genes Dev.* **18**, 715–727
- Aldridge, P., Paul, R., Goymer, P., Rainey, P., and Jenal, U. (2003) *Mol. Microbiol.* **47**, 1695–1708
- Kirillina, O., Fetherston, J. D., Bobrov, A. G., Abney, J., and Perry, R. D. (2004) *Mol. Microbiol.* **54**, 75–88
- Aldridge, P., and Jenal, U. (1999) *Mol. Microbiol.* **32**, 379–391
- Hecht, G. B., and Newton, A. (1995) *J. Bacteriol.* **177**, 6223–6229
- Ely, B. (1991) *Methods Enzymol.* **204**, 372–384
- O'Toole, G. A., Pratt, L. A., Watnick, P. I., Newman, D. K., Weaver, V. B., and Kolter, R. (1999) *Methods Enzymol.* **34**, 586–595
- Ochi, Y., Hosoda, S., Hachiya, T., Yoshimura, M., Miyazaki, T., and Kajita, Y. (1981) *Acta Endocrinol.* **98**, 62–67
- Brooks, B. R., Bruccoleri, R. E., Olafson, B. D., States, D. J., Swaminathan, S., and Karplus, M. (1983) *J. Comput. Chem.* **4**, 187–217
- MacKerell, A. D., Bashford, D., Bellott, M., Dunbrack, R. L., Evanseck, J. D., Field, M. J., Fischer, S., Gao, J., Guo, H., Ha, S., Joseph-McCarthy, D., Kuchnir, L., Kuczera, K., Lau, F. T. K., Mattos, C., Michnick, S., Ngo, T., Nguyen, D. T., Prodhom, B., Reiher, W. E., Roux, B., Schlenkerich, M., Smith, J. C., Stote, R., Straub, J., Watanabe, M., Wiorkiewicz-Kuczera, J., Yin, D., and Karplus, M. (1998) *J. Phys. Chem. B* **102**, 3586–3616
- Ausmees, N., Mayer, R., Weinhouse, H., Volman, G., Amikam, D., Benziman, M., and Lindberg, M. (2001) *FEMS Microbiol. Lett.* **204**, 163–167
- Simm, R., Fetherston, J. D., Kader, A., Romling, U., and Perry, R. D. (2005) *J. Bacteriol.* **187**, 6816–6823
- Garcia, B., Latasa, C., Solano, C., Portillo, F. G., Gamazo, C., and Lasa, I. (2004) *Mol. Microbiol.* **54**, 264–277
- Zogaj, X., Nimtz, M., Rohde, M., Bokranz, W., and Romling, U. (2001) *Mol. Microbiol.* **39**, 1452–1463
- Pei, J., and Grishin, N. V. (2001) *Proteins* **42**, 210–216
- Tucker, C. L., Hurley, J. H., Miller, T. R., and Hurley, J. B. (1998) *Proc. Natl. Acad. Sci. U. S. A.* **95**, 5993–5997
- Zhang, G. Y., Liu, Y., Ruoho, A. E., and Hurley, J. H. (1997) *Nature* **388**, 204 (Erratum)

Diguanylate Cyclase Feedback Control

33. Tesmer, J. J., Sunahara, R. K., Johnson, R. A., Gosselin, G., Gilman, A. G., and Sprang, S. R. (1999) *Science* **285**, 756–760
34. Sunahara, R. K., Beuve, A., Tesmer, J. J. G., Sprang, S. R., Garbers, D. L., and Gilman, A. G. (1998) *J. Biol. Chem.* **273**, 16332–16338
35. Baker, D. A., and Kelly, J. M. (2004) *Mol. Microbiol.* **52**, 1229–1242
36. Hickman, J. W., Tifrea, D. F., and Harwood, C. S. (2005) *Proc. Natl. Acad. Sci. U. S. A.* **102**, 14422–14427
37. Mendez-Ortiz, M. M., Hyodo, M., Hayakawa, Y., and Membrillo-Hernandez, J. (2006) *J. Biol. Chem.* **281**, 8090–8099
38. Simm, R., Morr, M., Kader, A., Nimtz, M., and Romling, U. (2004) *Mol. Microbiol.* **53**, 1123–1134
39. Galperin, M. Y., Nikolskaya, A. N., and Koonin, E. V. (2001) *FEMS Microbiol. Lett.* **204**, 213–214
40. Ulrich, L. E., Koonin, E. V., and Zhulin, I. B. (2005) *Trends Microbiol.* **13**, 52–56
41. Becskei, A., and Serrano, L. (2000) *Nature* **405**, 590–593
42. Gardner, T. S., Cantor, C. R., and Collins, J. J. (2000) *Nature* **403**, 339–342
43. McAdams, H. H., and Arkin, A. (1997) *Proc. Natl. Acad. Sci. U. S. A.* **94**, 814–819
44. Rosenfeld, N., Elowitz, M. B., and Alon, U. (2002) *J. Mol. Biol.* **323**, 785–793



SUPPLEMENTAL MATERIAL:

MATERIALS AND METHODS:

Purification of His-tagged proteins - *E. coli* BL21 cells carrying the respective expression plasmid were grown in LB medium with ampicillin (100 μ g/ml) or kanamycin (30 μ g/ml) and expression was induced by adding IPTG at OD₆₀₀ 0.4 to a final concentration of 0.4 mM. After harvesting by centrifugation, cells were resuspended in buffer containing 50 mM Tris-HCl, pH 8.0, 250 mM NaCl, 5 mM β -mercaptoethanol, lysed by passage through a French pressure cell, and the suspension was clarified by centrifugation for 10 min at 5,000 x g. Soluble and insoluble protein fractions were separated by a high-spin centrifugation step (100,000 x g, 1 h). The supernatant was loaded onto Ni-NTA affinity resin (Qiagen), washed with buffer, and eluted with an imidazol-gradient as recommended by the manufacturer. Protein preparations were examined for purity by SDS-PAGE and fractions containing pure protein were pooled and dialyzed for 12 h at 4°C.

Molecular modeling of PleD

All-atom simulations were carried out using the CHARMM (25) program and the CHARMM22/27 force field (26). The A chain of the X-ray dimer structure (PDB entry: 1W25 (17)) was used. All titratable side chains were generated in their standard protonation state at pH 7. Parameters and partial charges for the non-standard residue c-di-GMP were adopted from the extended CHARMM parameter sets for nucleic acids. The structure of the ligated (intercalated c-di-GMP bound to the I-site) and the unligated protein, to which hydrogen atoms were added, were minimized using a distance-dependent dielectric with $\epsilon=4$ and a cutoff of 12 Å for non-bonded interactions. 5000 steps of steepest descent minimization were followed by adopted Newton Raphson minimization until a RMS gradient of 10⁻⁷ kcal/mol·Å was reached. Such a threshold is found to be sufficient for normal mode calculations (49). Normal modes were calculated with the diagonalization in a mixed basis (DIMB) method, as implemented in CHARMM. The DIMB method is an approximate scheme retaining the full atomistic description of the protein, where the Hessian is approximated iteratively. The total number of basis functions was 153 and cumulated displacements were calculated for $T = 300$ K.

For ligated PleD motion is suppressed at L(β 1, α 1) (res.10-12), L(β 3, α 3) domain REC1, the C-terminal end of α 3 (res. 220-224) of domain REC2, the unstructured linker between REC2 and GGDEF domain (res. 282-284), the residues forming the A-site (res. 352), L(α 2, β 2) (res. 357-

360, I-site), L(β 2, β 3) (res. 367-373, A-site) and at the C-terminal end of α 3 (res. 396-398) of the GGDEF domain. By contrast upon ligand binding mobility increases for α 1 (res. 24), α 4 (res. 96-99) of domain REC1, residues (res. 149, 175), L(β 2, α 2) (res. 205-207), L(β 5, α 5) (res. 254-257) of domain REC2 and residues L(β 3', β 3'') (res. 404-407) and L(β 4, α 4) (res. 422-424) of the GGDEF domain.

Primer list

The following primers were used: #1006, ACA CGC TAC ATA TGA AAA TCT CAG GCG CCC GGA C; #1007, ACT CTC GAG AGC GCT CCT GCG CTT; #1129, CAA GCG GCT GCA GGC CAA TGT GAT CGT CGG CCG CAT GGG TGG TGA; #670, TGC TAG TTA TTG CTC AGC GG; #1006 ACA CGC TAC ATA TGA AAA TCT CAG GCG CCC GGA C; #1130, CAA GCG GCT GCA GGC CAA TGT GCG CGA AAG CGA CAT CGT CGG CCG CAT GGG TGG TGA; #1132, CAC ATT GGC CTG CAG CCG CTT GGC GAC; #1131, CAA GCG GCT GCA GGC CAA TGT GNN NNN NNN NNN NAT CGT CGG CCG CAT GGG TGG TGA.

FIGURE LEGENDS:

Figure S1: Separation of peptides yielded from tryptic digest of PleD in the presence (red chromatogram) or absence of c-di-GMP (black chromatogram) on a C18 column. Peaks identified by ESI-MS: c-di-GMP m/z 691, t_R 7.70 min, T47 (amino acids 354-359) m/z 659.3 t_R 25.64 min. T49 (amino acids 367-386) m/z 2167.7 t_R 47.73 min.

Figure S2: Normal modes of PleD I-site and A-site residues. The displacements for each mode of the ligated and unligated structures are shown in Å for the residues of the REC2 domain (green) and the GGDEF domain (red). Insertion of intercalated c-di-GMP in the I-site quenches motion in both the I-site (R359-D362, R390) and the A-site (G368-E371), suggesting that the two sites are dynamically coupled.

Figure S3: Representation of the PleD protein (blue: REC1, green: REC2, red: DGC) with c-di-GMP bound to the I-site. C α -atoms at positions of considerable changes in flexibility upon ligand binding are shown as spheres; reduced flexibility (yellow) and enhanced flexibility (black). Note that binding of c-di-GMP at the I-site (I) affects mobility not only in the I-site, but also in other regions of the protein, e.g. A-site (A), phosphorylation site (P) and dimer interface.

Figure S4: Alignment of I- and A-site sequence of biochemically characterized diguanylate cyclases. I-site residues (RXXD) are underlined in green and A-site residues (GGDEF) are underlined in yellow.

FIGURE LEGENDS:

Figure S1: Separation of peptides yielded from tryptic digest of PleD in the presence (red chromatogram) or absence of c-di-GMP (black chromatogram) on a C18 column. Peaks identified by ESI-MS: c-di-GMP m/z 691, t_R 7.70 min, T47 (amino acids 354-359) m/z 659.3 t_R 25.64 min. T49 (amino acids 367-386) m/z 2167.7 t_R 47.73 min.

Figure S2: Normal modes of PleD I-site and A-site residues. The displacements for each mode of the ligated and unligated structures are shown in Å for the residues of the REC2 domain (green) and the GGDEF domain (red). Insertion of intercalated c-di-GMP in the I-site quenches motion in both the I-site (R359-D362, R390) and the A-site (G368-E371), suggesting that the two sites are dynamically coupled.

Figure S3: Representation of the PleD protein (blue: REC1, green: REC2, red: DGC) with c-di-GMP bound to the I-site. $C\alpha$ -atoms at positions of considerable changes in flexibility upon ligand binding are shown as spheres; reduced flexibility (yellow) and enhanced flexibility (black). Note that binding of c-di-GMP at the I-site (I) affects mobility not only in the I-site, but also in other regions of the protein, e.g. A-site (A), phosphorylation site (P) and dimer interface.

Figure S4: Alignment of I- and A-site sequence of biochemically characterized diguanylate cyclases. I-site residues (RXXD) are underlined in green and A-site residues (GGDEF) are underlined in yellow.

Figure S1

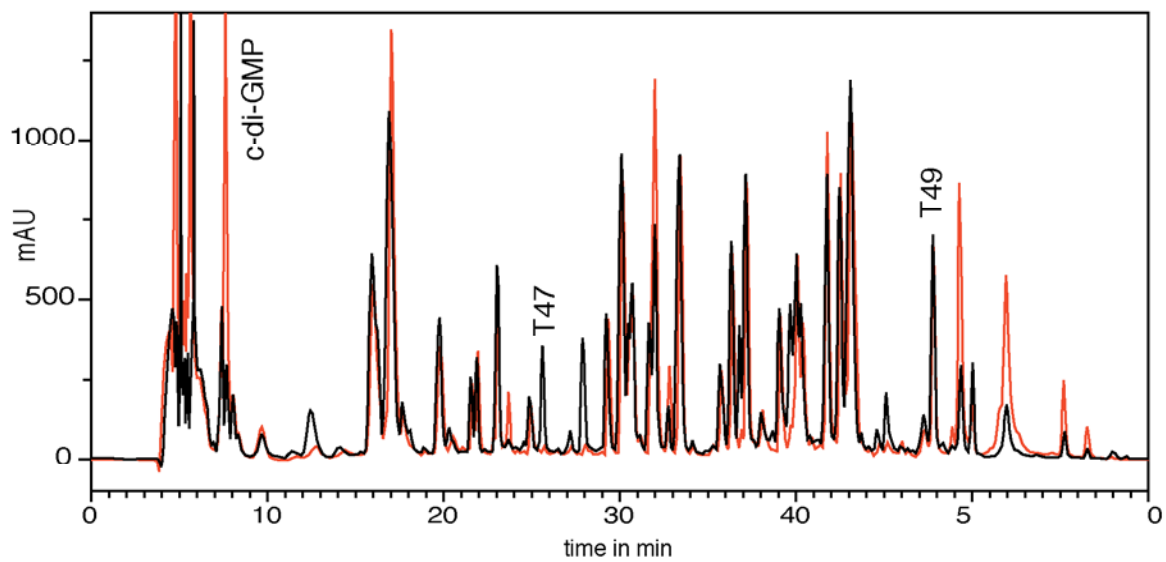


Figure S2

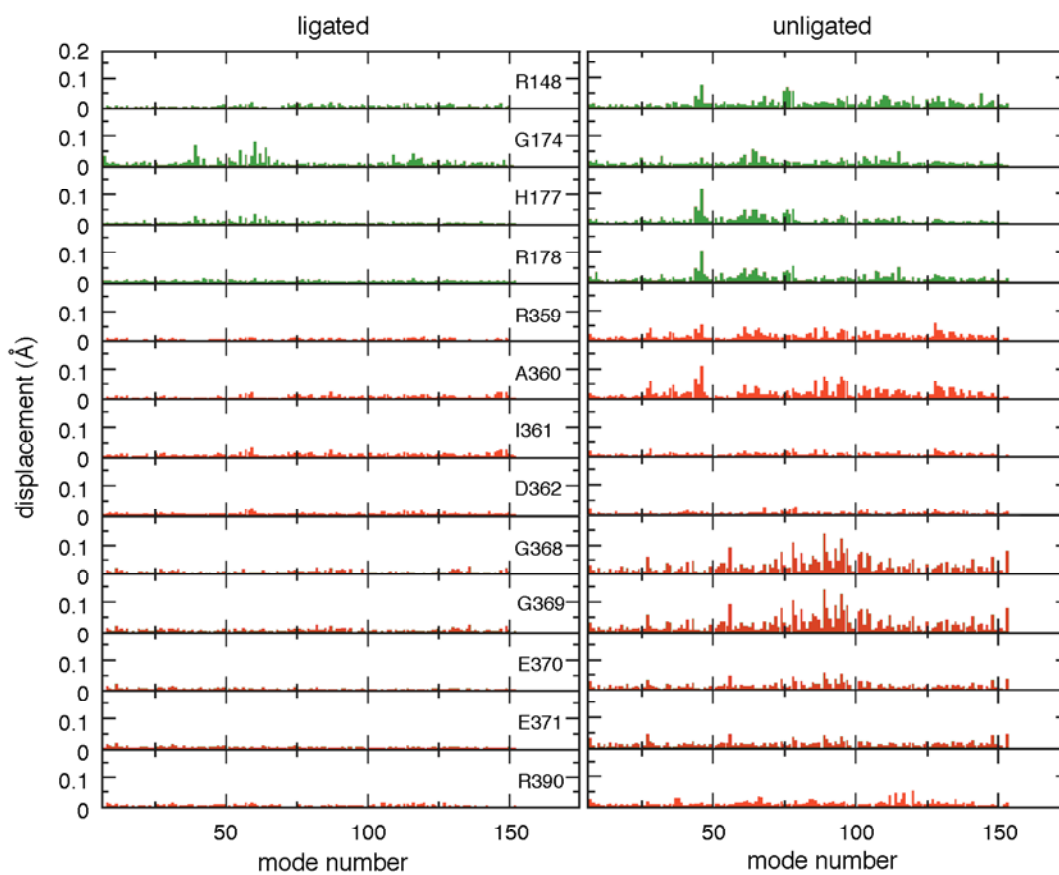


Figure S3

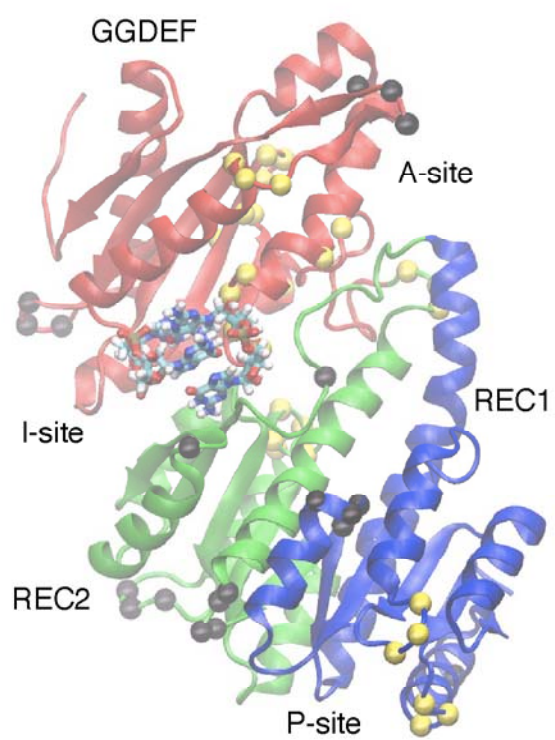


Figure S4

Gene	Sequence	Reference
BORBU_BB0419	LKYKIDVARYGGEEFI	(Ryjenkov et al, 2005)
CAUCR_DgcA	VRESDIVGRMGDEFA	- this study
CAUCR_PleD	VRAIDLPCRYGGEEFV	(Paul et al, 2004)
DEIRA_DRB0044	LPGGASLYRVGGDEFV	(Ryjenkov et al, 2005)
ECOLI_YddV	VRSSDYVFRYGGDEFI	(Mendez-Ortiz, 2006)
ECOLI_YeaP	QQNGEVIGRLGGDEFL	(Ryjenkov et al, 2005)
PSEAE_PA1107	TRSSDSVARLGGEEFL	(Kulesekara et al, 2006)
PSEAE_PA1120	LRESDLVARLGGDEFA	(Kulesekara et al, 2006)
PSEAE_PA1727	VRAQDTIARLGGDEFV	(Kulesekara et al, 2006)
PSEAE_PA2870	LREVDLLGRLGGEEFA	(Kulesekara et al, 2006)
PSEAE_PA3343	RRPLDMAVRLGGEEFA	(Kulesekara et al, 2006)
PSEAE_WspR	SRSSDLAARYGGEEFA	(Hickman et al, 2005)
PSEPA_PA0847	LRQPKAYRLGGDEFA	(Kulesekara et al, 2006)
RHOSP_Rsp3513	LGPADALGRIGGEEFA	(Ryjenkov et al, 2005)
SALTY_AdrA	LRGSDIIGRFGGDEFA	(Simm et al, 2005)
SYNY3_Slr1143	LRSYDILGRWGGDEFM	(Ryjenkov et al, 2005)
THEMA_TM1163	VRESDLVFRYGGDEFL	(Ryjenkov et al, 2005)
VIBCH_VCA096	CRDGVTAYRYGGEEFA	(Ryjenkov et al, 2005)
YERPS_HmsT	VRSRDIVVRYGGEEFL	(Simm et al, 2005)
Consensus	r d R GG#EF	

3.3 Identification and Characterization of a Cyclic di-GMP-specific Phosphodiesterase and Its Allosteric Control by GTP

M. Christen, B. Christen, M. Folcher, A. Schauerte, and U. Jenal

JBC 280:30829-30837 (2005)

Summary

This paper adds a striking new twist to the story of the signaling molecule cyclic-di-GMP (c-di-GMP), which controls motility and biofilm formation in bacteria and is produced by GGDEF domain proteins. We report the finding that the c-di-GMP specific phosphodiesterase activity resides in the widespread EAL domain. By analyzing the enzymatic reaction products and investigating the substrate specificity of wild type and various mutant enzymes, we demonstrate that a single EAL domain itself catalyzes in Mg^{2+} dependent manner the cleavage of the second messenger c-di-GMP into the linear dinucleotide pGpG. Furthermore we report the discovery that in a GGDEF-EAL protein a catalytic inactive GGDEF domain can bind GTP and in response allosterically activates the EAL domain. Thus we conclude that the GGDEF domain can have either catalytic or regulatory function and suggest, that the cellular GTP pool may serve as an input signal into c-di-GMP-mediated signal transduction.

Statement of my work

Beside my substantial contribution to the biochemical analysis of the c-di-GMP specific phosphodiesterase CC3396, I constructed a multitude of constructs, analysed deletion and over expression phenotypes and performed as well site directed mutagenesis to define crucial residues for in vitro PDE function.

Identification and Characterization of a Cyclic di-GMP-specific Phosphodiesterase and Its Allosteric Control by GTP*

Received for publication, April 22, 2005, and in revised form, June 23, 2005
Published, JBC Papers in Press, July 1, 2005, DOI 10.1074/jbc.M504429200

Matthias Christen, Beat Christen, Marc Folcher, Alexandra Schauerte, and Urs Jenal‡

From the Division of Molecular Microbiology, Biozentrum, University of Basel, Klingelbergstrasse 70,
4056 Basel, Switzerland

Cyclic diguanylic acid (c-di-GMP) is a global second messenger controlling motility and adhesion in bacterial cells. Synthesis and degradation of c-di-GMP is catalyzed by diguanylate cyclases (DGC) and c-di-GMP-specific phosphodiesterases (PDE), respectively. Whereas the DGC activity has recently been assigned to the widespread GGDEF domain, the enzymatic activity responsible for c-di-GMP cleavage has been associated with proteins containing an EAL domain. Here we show biochemically that CC3396, a GGDEF-EAL composite protein from *Caulobacter crescentus* is a soluble PDE. The PDE activity, which rapidly converts c-di-GMP into the linear dinucleotide pGpG, is confined to the C-terminal EAL domain of CC3396, depends on the presence of Mg²⁺ ions, and is strongly inhibited by Ca²⁺ ions. Remarkably, the associated GGDEF domain, which contains an altered active site motif (GEDEF), lacks detectable DGC activity. Instead, this domain is able to bind GTP and in response activates the PDE activity in the neighboring EAL domain. PDE activation is specific for GTP (K_D 4 μ M) and operates by lowering the K_m for c-di-GMP of the EAL domain to a physiologically significant level (420 nM). Mutational analysis suggested that the substrate-binding site (A-site) of the GGDEF domain is involved in the GTP-dependent regulatory function, arguing that a catalytically inactive GGDEF domain has retained the ability to bind GTP and in response can activate the neighboring EAL domain. Based on this we propose that the c-di-GMP-specific PDE activity is confined to the EAL domain, that GGDEF domains can either catalyze the formation of c-di-GMP or can serve as regulatory domains, and that c-di-GMP-specific phosphodiesterase activity is coupled to the cellular GTP level in bacteria.

The cyclic nucleotides cAMP and cGMP are universally used as second messengers in intracellular signal transduction pathways. They mediate cellular processes such as vision, electrolyte homeostasis, or smooth muscle relaxation by modulating the activity of protein kinases, GTPases, or ion channels (1, 2). The intracellular levels of cAMP and cGMP are tightly controlled by their rate of synthesis (catalyzed by adenylyl or guanylyl cyclases) and hydrolysis (catalyzed by phosphodies-

terases). Phosphodiesterases (PDE)¹ play a mayor role in the cellular response mediated by cyclic nucleotides and are used as primary therapeutic targets for several diseases (3). They act as effectors of signal transduction, function as homeostatic regulators of cyclic nucleotide levels, have been implicated in desensitization and termination of stimulation, and may also play an important role in controlling the diffusion of cyclic nucleotides and in channeling cyclic nucleotide signals (4, 5) (e.g. photoreception in human rod cells is mediated by rhodopsin and light signal transduction results from a dramatic reduction in cGMP concentrations, catalyzed by cGMP-specific PDE (1)).

Whereas cAMP signaling is common to both prokaryotes and eukaryotes, cGMP does not seem to be used by bacterial cells. However, there is accumulating evidence that the cyclic dimer of GMP, c-di-GMP, plays a critical role in bacterial signaling (6, 7). c-di-GMP is synthesized from two GTP molecules by diguanylate cyclases (DGCs), and hydrolyzed by PDEs via the linear intermediate pGpG to GMP (Fig. 1A). Even though c-di-GMP was discovered almost two decades ago (8), its global role in bacterial signaling has become apparent only recently in the view of the growing bacterial genome sequence information available. In recent years, a rapidly increasing number of genetic studies has linked proteins involved in c-di-GMP synthesis or turnover to the ability of different bacteria to switch between a motile, single-cell state and a multicellular behavior associated with the production of extracellular matrix components and surface adhesion (9–21). Biochemical studies have associated the DGC activity with the readout domain of the *Caulobacter crescentus* PleD response regulator protein (22). This domain, termed GGDEF (after its signature amino acid motif Gly-Gly-Asp-Glu-Phe), is widespread in bacteria but is not found outside the bacterial kingdom (23). The observation that GGDEF domains are often associated with domains involved in signal perception or signal transduction, argued for the existence of a dedicated regulatory network that converts a variety of different signals into the production of the second messenger c-di-GMP (6, 23). The resolution of the three-dimensional structure of the PleD response regulator in complex with c-di-GMP has not only revealed that the overall fold of the GGDEF domain is virtually identical to the adenylyl cyclase, but has also proposed a catalytic mechanism for the condensation of two GTP molecules into c-di-GMP (24). In contrast to the molecular nature of the DGC, the c-di-GMP-specific PDE activity has remained somewhat of a mystery. Initial genetic and biochemical studies have linked PDE activity to proteins that contain both GGDEF and EAL domains (18, 19, 25, 26). Like

* This work was supported by Swiss National Science Foundation Fellowships 31–59050.99 and 3100A0–108186/1 (to U. J.). The costs of publication of this article were defrayed in part by the payment of page charges. This article must therefore be hereby marked “advertisement” in accordance with 18 U.S.C. Section 1734 solely to indicate this fact.

‡ To whom correspondence should be addressed: Division of Molecular Microbiology, Biozentrum, University of Basel, Klingelbergstrasse 70, 4056 Basel, Switzerland. Tel.: 41-61-267-2135; Fax: 41-61-267-2118; E-mail: urs.jenal@unibas.ch.

¹ The abbreviations used are: PDE, phosphodiesterase; c-di-GMP, cyclic diguanylic acid; pGpG, linear diguanylic acid; MeOH, methanol; DGC, diguanylate cyclase; H6, hexahistidine tag; HPLC, high performance liquid chromatography; ESI-MS, electrospray ionization-mass spectrometry.

GGDEF, the EAL (after its signature amino acid motif Glu-Ala-Leu) domain is found only in bacteria and its distribution more or less mirrors that of the GGDEF domains (23, 27). Together, this has led to the proposal that the c-di-GMP-specific PDE activity might reside in the EAL domain (23).

The PleD response regulator is required for pole development during the *C. crescentus* cell cycle (11). During *Caulobacter* cell differentiation PleD specifically sequesters to one pole of the cell, where the morphological changes take place (22). Polar sequestration of PleD is coupled to the activation of the C-terminal GGDEF output domain via phosphorylation of the N-terminal receiver domain (22). This observation was lending support for the idea that synthesis of c-di-GMP by PleD might be limited to one cell pole may be to locally activate downstream targets or to restrict c-di-GMP production to one compartment during *Caulobacter* asymmetric cell division (22). One would imagine that in both cases, a potent cellular PDE activity is required to rapidly counteract the DGC activity over time and to maintain spatial gradients established by PleD. To monitor and characterize the c-di-GMP-specific PDE activity in *C. crescentus*, we first developed an assay based on the hydrolysis of ³³P-radiolabeled c-di-GMP. We then showed that the soluble fraction of *C. crescentus* cell extracts indeed contains a strong PDE activity. To characterize this activity more closely, we concentrated on EAL proteins encoded in the *C. crescentus* chromosome. A mutant lacking gene CC3396, which codes for a GGDEF-EAL composite protein, showed a more than 80% reduction of the soluble PDE activity (Table I). Enzymatic assays and UV cross-link experiments with purified full-length protein and single domain fragments confirmed that the PDE activity is contained within the EAL domain of CC3396. Remarkably, EAL-based PDE activity of CC3396 is allosterically controlled by GTP. Consistent with this, the GGDEF domain of CC3396, which contains an unorthodox active site motif (GEDEF), lacks DGC activity, but has retained the ability to bind GTP at the active site. Based on this and on the finding that the GGDEF domain is strictly required for the GTP-specific activation of the EAL phosphodiesterase, we postulate that in CC3396 and possibly in other GGDEF-EAL protein homologues, the GGDEF domain acts as an allosteric regulatory domain for the EAL-borne PDE activity (Fig. 1B).

MATERIALS AND METHODS

Strains, Plasmids, and Media—*C. crescentus* strains were grown in complex peptone yeast extract or in minimal glucose media (28). *Escherichia coli* strains were grown in Luria broth (LB) supplemented with antibiotics for selection, where necessary. The exact procedure of strain and plasmid construction is available on request.

Purification of CC3396 and Preparation of *C. crescentus* Cell Extracts—*E. coli* BL21 cells carrying the respective expression plasmid were grown in LB medium with ampicillin (100 µg/ml), and expression was induced by adding isopropyl 1-thio-β-D-galactopyranoside at A₆₀₀ 0.4 to a final concentration of 0.4 mM. After harvesting by centrifugation, cells were resuspended in buffer containing 50 mM Tris-HCl, pH 8.0, 250 mM NaCl, 5 mM β-mercaptoethanol, lysed by passage through a French pressure cell, and the suspension was clarified by centrifugation for 10 min at 5,000 × g. Soluble and insoluble protein fractions were separated by a high-spin centrifugation step (100,000 × g, 1 h). The supernatant was loaded onto nickel-nitrilotriacetic acid affinity resin (Qiagen), washed with buffer, and eluted with an imidazole gradient. Protein preparations were examined for purity by SDS-PAGE, and fractions containing pure protein were pooled and dialyzed for 12 h at 4 °C.

C. crescentus CB15 cells were grown in peptone yeast extract and harvested by centrifugation at an A₆₆₀ of 0.4. Cells were resuspended in buffer containing 50 mM Tris-HCl, pH 8.0, 250 mM NaCl, 5 mM mercaptoethanol, and 5 mM EDTA. Soluble and insoluble protein fractions were separated by a high-spin centrifugation step (100,000 × g, 1 h). The supernatant was dialyzed for 4 h in buffer containing EDTA and then for 8 h in the same buffer without EDTA. Protein concentrations were measured by UV absorption.

Synthesis and Purification of [³³P]c-di-GMP—³³P-Labeled c-di-GMP was produced enzymatically using α-labeled [³³P]GTP (3000 Ci/mmol, Amersham Bioscience) and purified hexahistidine-tagged PleD*, a phosphorylation independent constitutive active form of the PleD diguanylate cyclase (22). To a mixture of 87.5 µl of reaction buffer (250 mM NaCl, 25 mM Tris-HCl, pH 8.0, 10 mM MgCl₂, 5 mM β-mercaptoethanol, and 10.5 µM PleD*-H6), 12.5 µl of α-labeled [³³P]GTP (125 µCi, 41.66 pmol, 3000 Ci/mmol) was added. After 5 min at 25 °C, the reaction was stopped by adding an equal volume of 0.5 M EDTA, pH 8.0. The protein was precipitated by heating for 5 min at 95 °C followed by centrifugation for 2 min at 10,000 × g. The supernatant was loaded on a batch RP-18 column, salt was removed by washing 5 times with 200 µl of 25 mM triethylenammonium carbonate buffer, pH 7.0, containing 1% (v/v) MeOH. c-di-GMP was eluted with 2 × 200 µl of triethylenammonium carbonate containing 5% (v/v) MeOH. The buffer was subsequently removed in the SpeedVac and the purity of the compound was tested by separation on polyethyleneimine-cellulose plates (1:1.5 (v/v) saturated NH₄SO₄ and 1.5 M KH₂PO₄, pH 3.6).

Phosphodiesterase Assay—c-di-GMP-specific phosphodiesterase activity was measured by monitoring the decrease of [³³P]c-di-GMP and the increase of [³³P]pGpG by thin-layer chromatography. The PDE reaction buffer for the 100,000 × g supernatant of *C. crescentus* cell extracts or purified preparations of hexahistidine-tagged protein contained 250 mM NaCl, 25 mM Tris, pH 8.0, 10 mM MgCl₂, and 5 mM β-mercaptoethanol. The GTP/protein mixtures were preincubated for 2 min prior to the addition of c-di-GMP. The reactions were carried out at 30 °C, aliquots were removed at different time points, and the reaction was stopped by adding an equal volume of 0.5 M EDTA, pH 8.0.

Diguanylate Cyclase Assay—The reaction mixtures with purified hexahistidine-tagged protein contained 25 mM Tris-HCl, pH 8.0, 250 mM NaCl, 10 mM MgCl₂ and were started by the addition of 100 µM [³³P]GTP (Amersham Biosciences; 3000 Ci/mmol). At regular time intervals the reaction was stopped with an equal volume of 0.5 M EDTA, pH 8.0.

Polyethyleneimine-cellulose Chromatography—Samples were dissolved in 5 µl of running buffer containing 1:1.5 (v/v) saturated NH₄SO₄ and 1.5 M KH₂PO₄, pH 3.60, and blotted on Polygram® CEL 300 polyethyleneimine-cellulose thin-layer chromatography plates (Macherey-Nagel). Plates were developed in 1:1.5 (v/v) saturated NH₄SO₄ and 1.5 M KH₂PO₄, pH 3.60 (*R*_c(c-di-GMP) 0.2, *R*_r(pGpG) 0.4), dried, and exposed on a Storage PhosphorScreen (Amersham Biosciences). The intensity of the various radioactive species was calculated by quantifying the intensities of the relevant spots using ImageJ software, version 1.33.

Limited Tryptic Proteolysis—To 90 µl of purified hexahistidine-tagged protein samples (0.5–11 mg/ml) dissolved in PDE Reaction Buffer (see above), 10 µl of trypsin solution (2 µg/ml trypsin in 1 mM HCl and 250 mM NaCl) was added. After incubation for 5 min at 37 °C, 2 µl of freshly prepared phenylmethylsulfonyl fluoride (AppliChem) solution (0.1% in ethanol) was added, and the reaction was filtered through a 0.45-µm syringe filter (Whatman) before the digest products were separated by gel filtration. Gel filtration experiments were performed on a SMART System using a Superdex 75 column (Amersham Biosciences) at a flow rate of 80 µl/min. The buffer contained 250 mM NaCl, 25 mM Tris, pH 8.0, 10 mM MgCl₂, and 5 mM β-mercaptoethanol. Fractions of 80 µl were collected for the phosphodiesterase activity assay and for UV cross-linking experiments.

UV Cross-linking with [³³P]GTP and [³³P]c-di-GMP—Protein samples were incubated for 10 min on ice in PDE reaction buffer containing 10 µM c-di-GMP, 100 µM GTP, and [³³P]c-di-GMP (0.75 µCi, 6000 Ci/mmol) or [³³P]GTP (0.75 µCi, 3000 Ci/mmol). Samples were irradiated at 254 nm for 20 min on an ice-cooled, parafilm-wrapped 96-well aluminum block in an RPR-100 photochemical reactor with a RPR-3500 UV lamp (The Southern New England Ultraviolet Co.). After irradiation, samples were mixed with 2× SDS-PAGE sample buffer (250 mM Tris-HCl, pH 6.8, 40% glycerol, 8% SDS, 2.4 M β-mercaptoethanol, 0.06% bromophenol blue, 40 mM EDTA) and heated for 5 min at 95 °C. Labeled proteins were separated by SDS-PAGE and quantified by autoradiography.

HPLC Analysis and ESI-MS Mass Spectrometry—Reaction products were analyzed on an Agilent 1100 analytical reverse phase high performance liquid chromatography system with a diode array detector at 254 nm. Macherey-Nagel CC125/3 LiChrospher 100 RP-18, 5-µm particle size, was used at 30 °C with 25 mM triethylammonium carbonate buffer, pH 7.0, containing 5% (v/v) methanol as mobile phase and a flow rate of 0.3 ml/min. ESI-MS mass spectra were measured on an Esquire 3000plus (Bruker Daltonics) and on a TSQ7000 (Finnigan) mass spectrometer. Matrix-assisted laser desorption ionization spectra were measured on a Reflex III spectrometer (Bruker Daltonics).

TABLE I
Comparison of specific PDE activities in *C. crescentus* crude extracts and purified CC3396

Strain/protein	PDE activity		DGC activity ^a
	c-di-GMP-specific	pGpG-specific	
<i>C. crescentus</i> CB15 ^b	0.12 ± 0.02 μmol/(mg min)	0.054 ± 0.004 μmol/(mg min)	ND ^c
UJ2812 (ΔCC3396) ^b	0.02 ± 0.01 μmol/(mg min)	ND	ND
CC3396-His ₆ ^d	2.42 ± 0.28 μmol/(μmol min)	0.12 ± 0.06 μmol/(μmol min)	10 ± 5 pmol/(μmol min)

^a Diguanylate cyclase activity of purified CC3396-His₆ was determined as indicated in Ref. 22.

^b c-di-GMP and pGpG-specific activity of 100,000 × g supernatant as measured by TLC.

^c ND, not determined.

^d c-di-GMP and pGpG-specific activity of purified CC3396-His₆ as measured by thin layer chromatography.

RESULTS

PDE Activity in the Soluble Fraction of *C. crescentus* Cell Extracts—To analyze the *C. crescentus* protein fractions for c-di-GMP-specific PDE activity, we developed an enzymatic assay, which is based on the hydrolysis of radiolabeled c-di-GMP and separation of the products on thin layer chromatography plates (see “Materials and Methods”). The constitutive active PleD mutant form, PleD*-H6 (22), was purified to homogeneity and used to enzymatically convert [³³P]GTP to [³³P]-c-di-GMP. When purified [³³P]-c-di-GMP was added to aliquots of the dialyzed 100,000 × g supernatant of cell extracts of *C. crescentus* wild-type strain CB15, the dicyclic nucleotide was rapidly hydrolyzed (Table I), arguing for the presence of a potent PDE activity in the soluble fraction of these cells.

A total of five genes encoding soluble EAL proteins were found on the *C. crescentus* chromosome. To identify a candidate PDE protein and to verify that it contributes to the enzymatic activity found in cell extracts, we selected CC3396 for further analysis. This decision was mainly based on the relatively small size and simple domain architecture of CC3396 (Fig. 1B). An in-frame deletion mutation of gene CC3396 was generated, and extracts of the resulting mutant strain UJ2812 were assayed for PDE activity *in vitro*. As shown in Table I, PDE activity of strain UJ2812 was reduced by about 80% as compared with wild-type, arguing that under the conditions tested, CC3396 is responsible for a major fraction of the PDE activity of the cell.

Purified CC3396 Is a c-di-GMP-specific PDE, Which Converts c-di-GMP into the Linear Form pGpG—The above experiments suggested that CC3396 is a prime candidate for a soluble PDE in *C. crescentus*. A hexahistidine-tagged version of the CC3396 protein was expressed in *E. coli* and purified to homogeneity on a nickel affinity column. When used in the PDE assay described above, purified fractions of the CC3396 protein could readily hydrolyze radiolabeled c-di-GMP (Table I). Separation of the reaction mixture on TLC plates revealed that the labeled c-di-GMP was rapidly converted into a new nucleotide species (Fig. 2B). HPLC analysis (Fig. 2A) and mass spectrometry identified this compound as the linearized diguanylate derivative pGpG (Fig. 2C, *m/z* = 689.0, for c-di-GMP and *m/z* = 707.0 for pGpG). Although the conversion of c-di-GMP into pGpG was relatively rapid (turnover rate: 2.42 ± 0.28 min⁻¹), GMP appeared as a secondary product of the reaction at an about 10-fold slower rate (Table I). Thus, CC3396 specifically and rapidly cleaves c-di-GMP into its linear form, whereas the formation of GMP might be a nonspecific byproduct of the enzymatic reaction. The PDE activity of CC3396 is highly specific for the cyclic dimer of GMP and showed no significant affinity for monocyclic nucleotides cGMP and cAMP (data not shown). Also, whereas Mg²⁺ ions were critical for PDE activity, Ca²⁺ showed a strong inhibitory effect on the hydrolysis of c-di-GMP (Table II). Under no conditions were we able to detect DGC activity of the purified protein, arguing that the GGDEF domain of CC3396 is not a DGC (Table I).

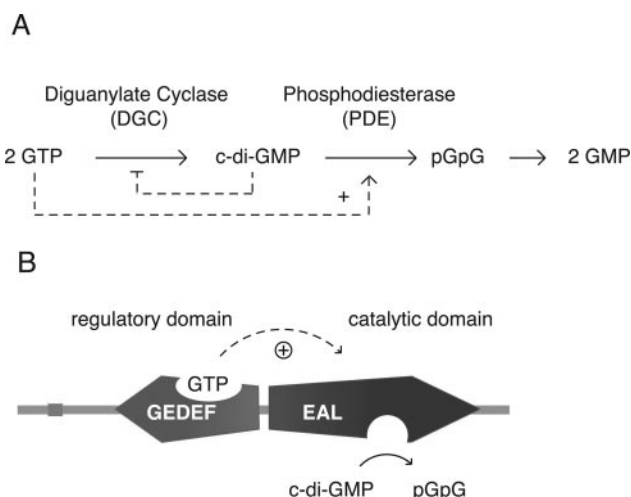


FIG. 1. Schematic of c-di-GMP synthesis and degradation (A) and model for GTP controlled PDE activity of CC3396 (B). A, the conversion of GTP into c-di-GMP is catalyzed by diguanylate cyclases that reside in the GGDEF domain (22, 41). Synthesis of c-di-GMP can be subject to negative allosteric feedback regulation (24) (indicated by the dashed line). Degradation of c-di-GMP into the linear form 5'-pGpG is catalyzed by the EAL domain and positively regulated by GTP (dashed line). The protein(s) responsible for the hydrolysis of pGpG into GMP have not been identified so far. B, the PDE activity of CC3396 is fully comprised within the EAL domain. The associated GGDEF domain with its altered active site motif (GEDEF) mediates activation of the C-terminal PDE by GTP. This domain lacks DGC activity but presumably binds GTP in a similar way, like the catalytic active GGDEF domains (22). We postulate that this novel role for GGDEF is either caused by the selective loss of DGC catalytic activity because of a slightly altered active site pocket formed by the GDEEF motif or is the result of an altered interaction surface of the DGC that prevents dimerization.

Stimulation of the c-di-GMP-specific PDE Activity of CC3396 by GTP—The activity of monocyclic PDEs is controlled by binding small effector molecules (including cAMP or cGMP) to N-terminal regulatory domains (5). To test the possibility that CC3396 could also be allosterically regulated, we measured the c-di-GMP-specific PDE activity of CC3396 in the presence or absence of different nucleotides (Table II). cAMP, cGMP, and dibutyryl-cGMP did not affect PDE activity of CC3396. Similarly, AMP, ATP, GMP, and GDP showed no effect. However, when the reaction mixture was supplemented with GTP (100 μM) the initial rate of the reaction increased by about 40-fold to 106.8 ± 1.5 μmol of c-di-GMP formed per μmol of protein and minute (Table II, Fig. 2B). The same positive effect was observed for an equimolar mixture of either GTP and GDP or GTP and GMP, arguing that both GDP and GMP do not counteract the positive effect of GTP. Interestingly, the GTP-activated form of CC3396 quantitatively converted c-di-GMP into the linear form pGpG, but failed to produce substantial amounts of GMP (Fig. 2, A and B, Table I). Together this suggested that the enzymatic activity of CC3396 responsible for the cleavage of c-di-GMP into pGpG is positively controlled

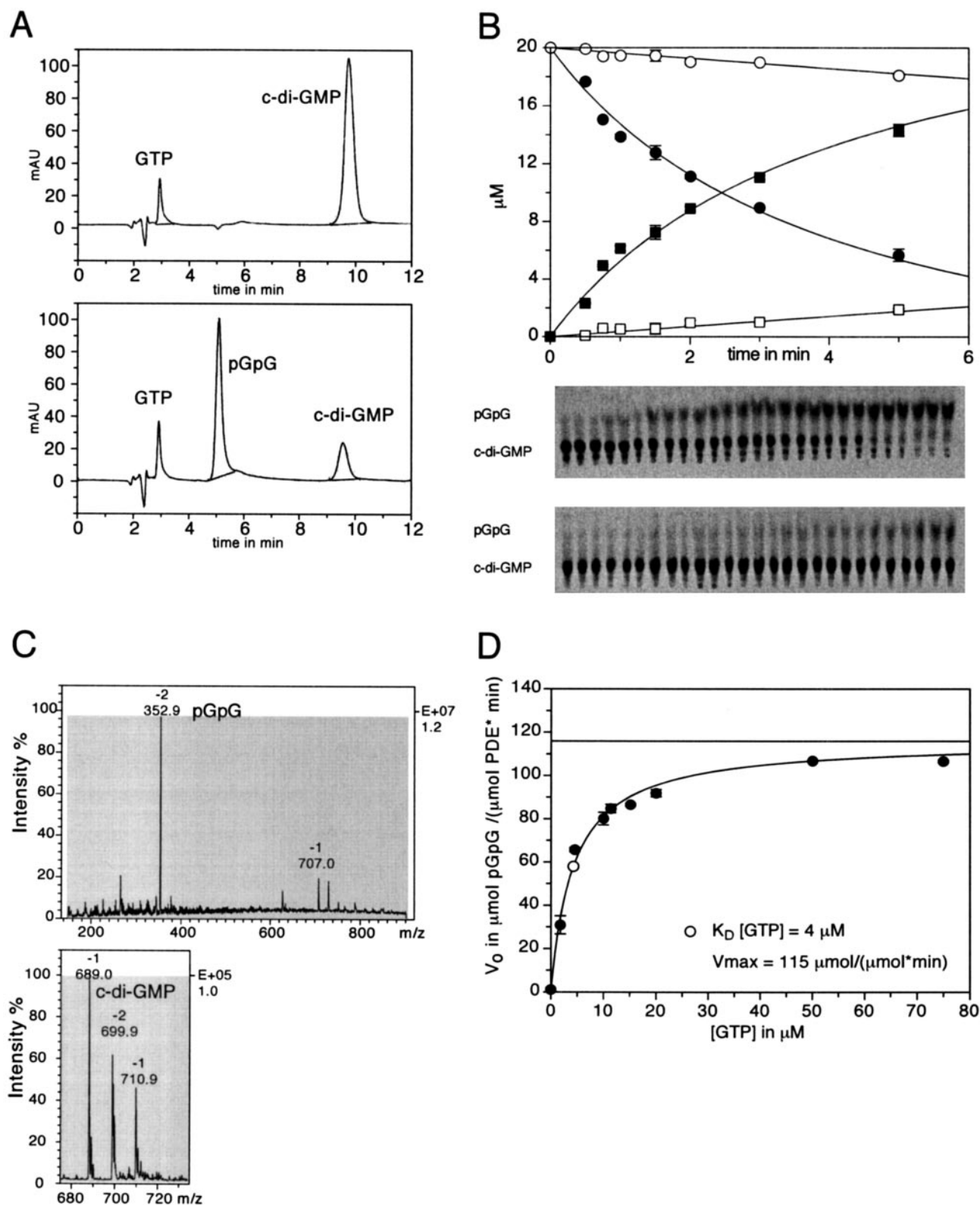


FIG. 2. *C. crescentus* protein CC3396 is a phosphodiesterase. **A**, HPLC analysis of the PDE reaction products. Purified CC3396 protein (5 μM) was incubated for 1 min with 100 μM *c*-di-GMP, and 4 μM GTP. Nucleotides were separated on a RP-18 column before (top panel) and after the enzymatic reaction (bottom panel), and fractions were analyzed by ESI-MS. GTP, which was added to activate the reaction, was not hydrolyzed. **B**, PDE activity of CC3396 in the absence (open symbols) or presence of GTP (4 μM GTP, closed symbols). The *c*-di-GMP hydrolysis activity of purified CC3396 is indicated as a function of the absolute concentrations of *c*-di-GMP (circles) and pGpG (squares) as determined by thin layer chromatography. Reactions included 150 nM purified CC3396 protein and 20 μM *c*-di-GMP and were incubated at 30 $^{\circ}\text{C}$ in buffer as described under "Materials and Methods." The polyethyleneimine-cellulose thin layer chromatogram with the raw data is shown below the graph with each time point spotted in triplicate (upper panel, with GTP; lower panel without GTP). **C**, mass spectrometry analysis of the reaction products of the CC3396 PDE. Mass spectrometry analysis of the reaction product of the PDE (top panel) and *c*-di-GMP (bottom panel) as shown in **A** and **B**. Top panel, ESI-MS of pGpG (m/z -) 352.9 (pGpG) $^{2-}$, and 707.0 (pGpG) $^{-}$. Bottom panel, ESI-MS of *c*-di-GMP m/z - 689.0 [*c*-di-GMP*H] $^{-}$, m/z - 699.9 [(*c*-di-GMP) $_{2}$ *H*Na] $^{2-}$, m/z - 710.9 [*c*-di-GMP*Na] $^{-}$. **D**, determination of the equilibrium constant for GTP. Initial velocities of the PDE reaction were measured at increasing concentrations of GTP and $V_{\text{max}}/2$ was determined to be 4 μM .

TABLE II
Activation of c-di-GMP-specific PDE by GTP

Specific activity (initial velocities) of purified CC3396 was determined in the presence of 10 μM c-di-GMP and one additional nucleotide (100 μM). All reaction mixtures (except the no Mg^{2+} control) contained 10 mM Mg^{2+} and 10 mM Ca^{2+} that were used to show PDE inhibition by calcium ions.

Nucleotide	PDE activity $\mu\text{mol c-di-GMP}/\mu\text{mol min}$
AMP	1.93 \pm 0.08
ATP	2.09 \pm 0.22
cAMP	1.17 \pm 0.46
cGMP	2.13 \pm 0.32
dibu-cGMP ^a	1.79 \pm 0.18
GMP	1.87 \pm 0.20
GDP	1.92 \pm 0.40
GTP	106.8 \pm 1.5
GTP + GDP	113.2 \pm 1.9
GTP + GMP	97.2 \pm 1.5
GTP, no Mg	0.23 \pm 0.10
GTP + Ca	1.61 \pm 0.37

^a 200 μM .

by GTP, whereas the consecutive hydrolysis step, which generates GMP is probably a nonspecific side reaction and not subject to allosteric control by GTP. It is important to note that we found no indication for GTP hydrolysis during the enzymatic reaction in the presence of the inducer (Fig. 2A).

When logarithmically growing cells were analyzed by nucleotide extraction and HPLC, the internal concentration of c-di-GMP was determined to be 1.1 μM (\pm 0.11 μM) (data not shown). This is well below the K_m for c-di-GMP, which was determined for the basal level PDE activity of CC3396 ($>$ 100 μM). To test if GTP activation substantially lowers the K_m for c-di-GMP to a physiologically relevant level, PDE activity was determined at different substrate concentrations. The K_m for c-di-GMP in the presence of 4 μM GTP (at half-maximal PDE activity, see below) was determined to be 420 nM, close to the cellular concentration of c-di-GMP measured in growing cells.

The intracellular concentration of GTP in bacterial cells growing exponentially in rich medium is in the submillimolar range (29, 30) but can drop by 70–80% upon entry into stationary phase (29). To find out if the concentration of GTP required for activation of CC3396 is physiologically relevant, the K_D for GTP was determined at saturating substrate concentrations. Half-maximal induction of CC3396 was found to occur at a GTP concentration of 4 μM , well below the GTP concentrations normally found in bacterial cells (Fig. 2D). The V_{max} of the GTP-activated protein was 115 \pm 4 $\mu\text{mol}/(\mu\text{mol min})$ (Fig. 2D). This argues that under physiological conditions promoting cell growth and division, the PDE activity of CC3396 is likely to be fully induced.

The PDE Activity of CC3396 Resides in the C-terminal EAL Domain—The observation that CC3396 harbors PDE but lacks DGC activity raised the question of whether the enzymatic activity is entirely comprised within the GGDEF or the EAL domain, or is maybe the result of a catalytic interaction between the two domains. To distinguish between these possibilities, we attempted to separate the two domains by a limited tryptic digest of the full-length CC3396 protein and to determine the enzymatic activities of the individual domains. Treatment with trypsin resulted in the specific cleavage of CC3396 into two distinct peptide fragments of \sim 30 and 27 kDa in size, according to their migration behavior in polyacrylamide gels (Fig. 3A). Separation of these two cleavage products by gel filtration, followed by mass spectrometry analysis (Fig. 3, C and D) revealed that the slightly larger peptide corresponds to the N-terminal portion of CC3396, which includes the entire GGDEF domain (amino acids 1–279; fractions 8 and 9 in Fig.

3C), whereas the smaller peptide corresponds exactly to the C-terminal EAL domain (amino acids 280–554; fractions 10 and 11 in Fig. 3C). The cleavage site mapped to the Arg²⁷⁹ residue positioned in the center of the linker that connects the GGDEF and the EAL domain (Fig. 3D). It is reasonable to assume that the two domains can be separated by proteolysis because this charged residue is easily accessible for the protease because of its position in the flexible inter-domain linker.

PDE activity was found exclusively in fractions 10 and 11 of the gel filtration column used to separate the tryptic digest of CC3396 (Fig. 3C). Because fractions 10 and 11 contain the C-terminal EAL fragment, this strongly supported the view that the c-di-GMP-specific PDE activity is fully contained within the EAL domain. As shown in Table III, the specific activity of the separated EAL domain is similar to the activity found for the full-length CC3396 protein, arguing that the overall PDE activity is not significantly reduced upon separation of the catalytically active EAL from the GGDEF domain. Interestingly, when analyzing a CC3396 mutant with a mutation in the highly conserved aspartic acid residue of the EAL motive (E323Q), we found that both PDE activity and induction by GTP was not affected by this change (Table III). *In vivo* studies with the *Vibrio cholerae* EAL protein VieA had shown that a glutamate to alanine exchange at this position resulted in loss of activity (19). It is possible that the more conservative mutation chosen for CC3396 might still support PDE activity.

Allosteric Activation of the PDE Activity in EAL Through Binding of GTP to the GGDEF Domain—Whereas the EAL signature sequence of the C-terminal EAL domain is conserved in CC3396, the GGDEF domain has one of the highly conserved Gly residues of the active site (A-site) motif (24) replaced by Glu (GEDEF) (Fig. 3D). It is possible that this altered A-site in GGDEF is still able to bind GTP but cannot catalyze the diguanylate cyclase reaction. Such an altered domain might have been recruited as a regulatory module for the PDE activity residing in the C-terminal EAL domain. This would be in agreement with the observation that CC3396 has no apparent DGC activity (Table I). Also, a regulatory role for the GGDEF domain would be consistent with the finding that the isolated EAL domain almost fully retained the specific PDE activity of full-length CC3396, but in contrast to the intact protein could not be activated by GTP (Table III).

To obtain evidence in support of this idea we performed UV cross-link experiments with [³³P]c-di-GMP and [³³P]GTP using purified full-length CC3396 and the two individual domains separated by trypsin treatment (Fig. 3A). [³³P]c-di-GMP specifically bound to full-length CC3396 and to the C-terminal EAL domain, but not to the N-terminal GGDEF domain fragment (Fig. 4A). In contrast, [³³P]GTP, while also cross-linking to the full-length protein, did not bind to the EAL domain fragment but instead specifically reacted with the N-terminal GGDEF domain fragment (Fig. 4B). This suggested that GTP imposes allosteric control on the PDE enzyme activity of CC3396 by binding to its regulatory GGDEF domain.

Catalytically active GGDEF domains bind GTP in their A-site pocket, which in part is formed by a loop structure consisting of the highly conserved GGDEF (often GGEEF) motif (24). One possibility is that the slightly altered A-site motif (GEDEF) of the N-terminal domain of CC3396 has retained the ability to bind GTP and in response activates the associated EAL domain. To test this we generated a mutant CC3396 protein with the A-site motif changed to GQNEF. As shown in Table III, the mutant fully retained its PDE activity. But in contrast to the wild-type protein, the PDE activity was more or less constitutive with a 10-fold higher basal level activity in the absence of GTP as compared with wild-type (Table III). The

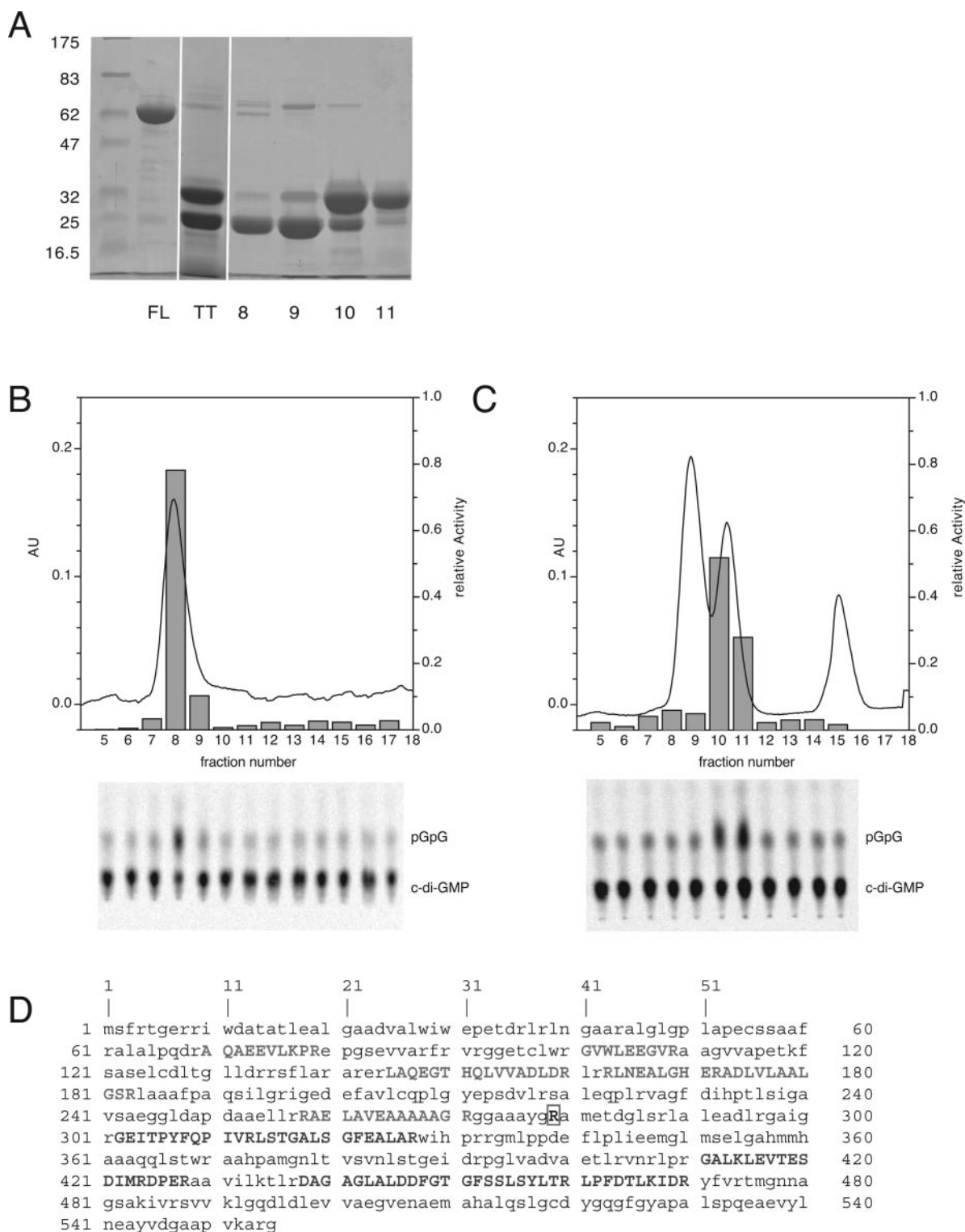


FIG. 3. The PDE activity of CC3396 resides in the C-terminal EAL domain. **A**, SDS-polyacrylamide gel with purified full-length CC3396 (*FL*), CC3396 after trypsin treatment (see “Materials and Methods”) (*TT*), and elution fractions 8–11 of the gel filtration column used to separate the tryptic fragments (see “Materials and Methods” and *panel C*). Note that *lane TT* was pasted from an independent gel. Samples of undigested (**B**) and trypsin-digested CC3396 protein (**C**) were separated by gel filtration (see “Materials and Methods.”) The TLC plates with the resolved reaction products originating from each fraction are shown *below* the graphs. The *bars* in the graphs indicate the relative activity measured for each fraction, and the *curve* shows the protein concentration as determined by UV spectrometry. The protein peak of fractions 8 and 9 in *panel C* corresponds to the N-terminal GGDEF domain of CC3396, and the protein peak of fractions 10 and 11 (**C**) corresponds to the C-terminal EAL domain of CC3396. Note that on the gel filtration column, the N-terminal GGDEF fragment runs at the position of a dimer, whereas the full-length CC3396 protein and the N-terminal EAL fragment run at the equivalent position of monomers. Fraction 15 corresponds to the cleaved C-terminal His tag, as determined by antibody staining with anti-His antibody. **D**, mass spectrometry analysis of the peptides originating from a tryptic digest of fractions 9 and 10 from *panel C*. A total of seven fragments of the GGDEF domain of CC3396 could be assigned to fraction 9, and a total of six fragments of the EAL domain could be assigned to fraction 10 digest. The corresponding fragments are highlighted in *capital letters*. LC-MS analysis of the undigested sample of fraction 10 revealed a mass of 29650.86 (Δ Da 4.16) (amino acids 280–554, theoretical mass: 29655.0). The proposed trypsin cleavage site (Arg²⁷⁹) is highlighted.

TABLE III
Activation of CC3396 wild-type and mutant forms by GTP

Protein	c-di-GMP-specific PDE activity ^a	
	10 μM c-di-GMP	4 μM GTP
CC3396	2.42 \pm 0.28	57.9 \pm 5.9
EAL domain ^b	1.32 \pm 0.33	2.54 \pm 1.10
E323Q	1.2 \pm 4.2	76.2 \pm 8.9
ED213QN	26.9 \pm 3.8	77.3 \pm 7.7

^a PDE activity (initial velocities) was measured in the presence of 10 μM c-di-GMP and in the presence or absence of 4 μM GTP.

^b The isolated EAL domain of CC3396 corresponds to fraction 10 of Fig. 3C.

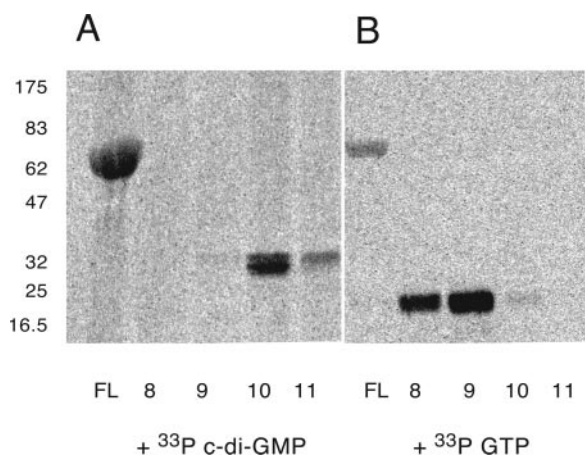


FIG. 4. GGDEF of CC3396 is a GTP binding regulatory domain. Full-length CC3396 (FL) and protein from elution fractions 8–11 of the gel filtration column used to separate the tryptic fragments were separated by SDS-PAGE (see Fig. 3A) and were used to UV cross-link with [³³P]c-di-GMP (A) or [³³P]GTP (B) as outlined under “Materials and Methods.” Samples were separated by SDS-PAGE, and the dried gels were analyzed by autoradiography.

addition of GTP resulted in an only 3-fold activation of the GQNEF mutant and resulted in similar activity as the GTP-induced wild-type protein (Table III). This implied that the amino acid changes in the A-site motif are able to switch this domain into the regulatory ON state and is consistent with the view that in CC3396 a catalytically inactive GGDEF domain imposes allosteric regulation by binding of GTP in its substrate binding pocket (A-site).

DISCUSSION

The pioneering work of the late Moshe Benziman and collaborators has not only identified dicyclic guanosine monophosphate as a signaling molecule involved in bacterial metabolism, but has also led to the recognition of proteins containing GGDEF and EAL domains as being involved in the synthesis and breakdown of c-di-GMP (reviewed in Ref. 6). Building on this foundation, an increasing number of genetic studies have in recent years highlighted a global role for c-di-GMP as a signaling molecule in bacteria. Most of these studies have reported mutant and/or overexpression phenotypes of proteins containing GGDEF or EAL domains (9–21). The common pattern appearing from these studies is that genetic changes associated with an increase of the cellular concentration of c-di-GMP negatively modulates cell motility and induce biofilm formation, whereas genetic modifications that led to a presumable decrease of c-di-GMP in the cell had the opposite effect. However, limited information is available on the downstream activities and possible targets of c-di-GMP and on the specific biochemical properties of enzymes involved in synthesis and hydrolysis of c-di-GMP. Genetic studies had predicted that GGDEF domains are DGCs and that EAL domains should harbor the c-di-GMP-specific PDE activity. But whereas many

of the several thousand bacterial GGDEF and EAL proteins listed in the non-redundant data bases have either a GGDEF or an EAL domain fused to other signaling domains, a large fraction combines both domains in the same polypeptide (31). A similar heterogeneity is found for cNMP (cAMP or cGMP)-specific cyclases and PDEs in eukaryotic cells, where several families of each enzyme class vary in ligand and co-factor specificities, in regulatory properties, and in tissue distribution (1, 4). This raised several important questions: Are the enzymatic activities responsible for the “make and break” of c-di-GMP really confined to these highly modular single domains? And if so, do all multidomain proteins that contain both a GGDEF and an EAL domain harbor both activities or have some of these proteins “specialized” in that they catalyze only the synthesis or degradation of c-di-GMP, respectively? The few examples studied so far have either been associated with DGC or PDE activity (25). No bifunctional enzyme has been described as yet. And finally, how would these activities be controlled if no obvious regulatory domains are fused to GGDEF or EAL?

Recent biochemical and structural studies have proposed a catalytic and regulatory mechanism for the synthesis of c-di-GMP by the GGDEF protein PleD (22, 24). Here we show that CC3396, a GGDEF-EAL protein of *C. crescentus* harbors c-di-GMP-specific PDE activity but lacks DGC activity. Analysis of the catalytic activities of the individual domains strongly suggested that the PDE activity of CC3396 is confined to the C-terminal EAL domain, and does not depend on the physical presence of the N-terminal GGDEF domain. To our knowledge, this is the first report that directly links an isolated EAL domain with the ability to catalyze the hydrolysis of c-di-GMP *in vitro*. Our data further propose a regulatory role for the N-terminal GGDEF domain of CC3396. The *in vitro* PDE activity of CC3396 is increased about 40-fold upon addition of GTP. Activation of the PDE activity seems to occur via the reduction of the K_m for c-di-GMP from above 100 μM in the absence of GTP to 420 nM when GTP was present. Several lines of evidence suggest that GGDEF mediates this allosteric control through an interaction with the associated EAL domain. (i) Whereas the basal level PDE activity of full-length CC3396 and the isolated EAL domain are comparable, GTP activation could only be detected if the GGDEF domain was present. (ii) Compared with the *bona fide* DGC PleD (22), the GGDEF domain of CC3396 has a slightly altered consensus sequence A-site motif (GEDEF). Consistent with this, CC3396 does not seem to possess diguanylate cyclase activity *in vitro*. (iii) GTP specifically binds to the GGDEF but not to the associated catalytic EAL domain. (iv) A defined mutation in the A-site motif of the GGDEF domain (GQNEF) abolished allosteric activation and resulted in a constitutive activity of the associated EAL domain. This last observation implies that the GGDEF domain of CC3396 is a GGDEF-like domain, which is still able to bind GTP in the A-site cavity with a relatively high affinity (K_D 4 μM) but does not catalyze the formation of c-di-GMP. If so, an original GGDEF domain might have been recruited as sensory domain for GTP through the loss of its catalytic function and the evolution of a regulatory interaction with EAL. If such a regulatory role of a GGDEF domain has indeed evolved from an enzymatically active GGDEF domain, two scenarios are possible. Either the GGDEF domain has lost DGC activity because key catalytic residues are missing, or because, in the context of the GGDEF-EAL composite protein, it is no longer able to form a dimeric structure required to condense two GTP molecules into c-di-GMP (24).

Thus, we propose that GGDEF domains, depending on their sequence conservation or on their oligomeric status, can have

two alternative biological activities and can play different roles in the controlled formation and hydrolysis of c-di-GMP. It is conceivable that at least a subgroup of the large family of bacterial GGDEF-EAL composite proteins represents PDEs with an associated regulatory GGDEF domain that can act as GTP sensor. At the same time, GGDEF-EAL proteins may exist that combine both a GGDEF-born DGC and an EAL-associated PDE activity. And finally it is equally possible that the EAL domain of GGDEF-EAL composite proteins also engages in a regulatory function by controlling the N-terminal DGC activity in response to the prevailing c-di-GMP concentration. Such a regulatory mechanism has been proposed recently for the DGC activity of the PleD response regulator, which is under tight negative allosteric control by its own product, c-di-GMP (24). A direct consequence of our findings is that each GGDEF or EAL domain will first have to be carefully analyzed biochemically before it can be assigned a catalytic or regulatory role.

The model that we propose for catalysis and regulation of the CC3396 PDE is shown in Fig. 1B. The protein architecture with an N-terminal regulatory and a C-terminal catalytic domain is reminiscent of cNMP-specific PDEs found in eukaryotes (e.g. PDE5, a phosphodiesterase highly specific for cGMP has two non-catalytic cGMP binding sites located at the N terminus). Binding of cGMP to these allosteric sites stimulates PDE activity, increases cGMP hydrolysis, and thus forms a negative feedback mechanism regulating the cellular cGMP concentration (32). Other N-terminal regulatory domains of cNMP-specific PDEs can serve as phosphorylation sites, can interact with transducing proteins, or act as an allosteric binding site for Ca^{2+} /calmodulin effectors (5). It is reasonable to assume that c-di-GMP-specific PDEs in bacteria are also tightly controlled and that the allosteric control of CC3396 reported here represents a general phenomenon of this class of enzymes.

PDE activity is likely to be a critical component of c-di-GMP signaling in bacterial cells. But why would phosphodiesterase activity be coupled to the cellular concentration of GTP? Römmling and colleagues (18) have reported that upon expression of the DGC protein AdrA in *Salmonella typhimurium*, the cellular GTP to c-di-GMP ratio reverses from about 100:1 to 1:10 (18). Thus, it is possible that when c-di-GMP synthesis is fully induced, uncontrolled hydrolysis of c-di-GMP to pGpG and GMP would deplete the cellular GTP pool. A massive reduction of the cellular GTP concentration has been reported as a consequence of the increased production of the "alarmone" pppGpp upon amino acid starvation in *Bacillus subtilis* (33). Similarly, the GTP concentration decreases considerably upon nitrogen starvation in *C. crescentus* (34). It is possible that to prevent drainage of the cellular GTP pool, specific PDEs are quickly turned off when the GTP concentration drops under a threshold level. Considering that the K_D for GTP of CC3396 is about 4 μM , one would expect such a threshold GTP concentration to be in the low micromolar range. Together with the observation that DGCs can be subject to tight allosteric feedback inhibition by their own product (24), this could be interpreted as a simple means for flux-controlled sensitivity, which would allow breaching the threshold for signal transduction by either increased production or decreased degradation of the second messenger. Alternatively, the prevailing GTP level of the cell itself could be used as a physiological signal to control the internal concentration of c-di-GMP through the controlled activity of PDEs. A drastic drop of the GTP concentration to the low micromolar range could lead to a rapid and substantial increase of the cellular c-di-GMP concentration through the inhibition of one or several key PDEs, which respond to GTP in a similar manner as observed for CC3396. Whereas such a regulatory role for GTP remains speculative, cellular GTP pools

are known to affect developmental transitions in bacteria. A decrease in the cellular GTP concentration, but not of other purine or pyrimidine nucleotides, correlates with the initiation of morphological differentiation during nutrient starvation of *B. subtilis* and *Streptomyces griseus* (29, 35, 36). The signal responsible for the induction of sporulation is the reduced GTP pool, rather than pppGpp, which is formed under the same starvation conditions (29). The cellular GTP concentration is sensed by CodY, a transcriptional repressor of several sporulation and motility genes, whose repression activity depends on binding of GTP with a K_D in the physiologically relevant millimolar range (37, 38). It remains to be shown if the GTP concentration plays a similar regulatory role in cellular c-di-GMP signaling.

Finally, what is the physiological role of CC3396? CC3396 substantially contributes to the PDE activity in the soluble fraction of actively growing *C. crescentus* cells. It is possible that this protein adds to a more or less constant and rapid degradation of the freely diffusible cytoplasmic pool of c-di-GMP and would only be turned off under severe depletion of GTP. The cellular concentration of c-di-GMP has been determined to be about 1 μM in growing *C. crescentus* cells (this study) or 5–10 μM in cellulose producing *Acetobacter xylinum* (39). This is in good agreement with a K_m for c-di-GMP of 420 nM, which was determined for the PDE activity of CC3396 in the presence of GTP. It has been argued that specifically localized DGCs might act as "local pacemakers" of metabolic reactions resulting in cellular gradients of c-di-GMP (6, 40). In such a model, c-di-GMP synthesis and signaling would be locally confined and one would imagine that a strong and constitutive PDE activity is critical to spatially confine different c-di-GMP signaling pathways. Further studies are needed to test this idea more thoroughly.

Acknowledgments—We thank Tilman Schirmer and Helma Wennemers for helpful discussions, Thomas Augst and Paul Jenö for mass spectrometry analysis, and Nicholas Amiot for providing a sample of c-di-GMP.

REFERENCES

- Lucas, K. A., Pitari, G. M., Kazeroonian, S., Ruiz-Stewart, I., Park, J., Schulz, S., Chepenik, K. P., and Waldman, S. A. (2000) *Pharmacol. Rev.* **52**, 375–414
- Kaupp, U. B., and Seifert, R. (2002) *Physiol. Rev.* **82**, 769–824
- Essayan, D. M. (2001) *J. Allergy Clin. Immunol.* **108**, 671–680
- Houslay, M. D., and Milligan, G. (1997) *Trends Biochem. Sci.* **22**, 217–224
- Conti, M., and Jin, S. L. (1999) *Prog. Nucleic Acids Res. Mol. Biol.* **63**, 1–38
- Jenal, U. (2004) *Curr. Opin. Microbiol.* **7**, 185–191
- D'Argenio, D. A., and Miller, S. I. (2004) *Microbiology* **150**, 2497–2502
- Ross, P., Weinhouse, H., Aloni, Y., Michaeli, D., Weinberger-Ohana, P., Mayer, R., Braun, S., de Wroom, E., van der Marel, G. A., van Boom, J. H., and Benziman, M. (1987) *Nature* **325**, 279–281
- Spiers, A. J., Kahn, S. G., Bohannon, J., Trivisano, M., and Rainey, P. B. (2002) *Genetics* **161**, 33–46
- Drenkard, E., and Ausubel, F. M. (2002) *Nature* **416**, 740–743
- Aldridge, P., Paul, R., Goymer, P., Rainey, P., and Jenal, U. (2003) *Mol. Microbiol.* **47**, 1695–1708
- Huang, B., Whitechurch, C. B., and Mattick, J. S. (2003) *J. Bacteriol.* **185**, 7068–7076
- Bomchil, N., Watnick, P., and Kolter, R. (2003) *J. Bacteriol.* **185**, 1384–1390
- Guvener, Z. T., and McCarter, L. L. (2003) *J. Bacteriol.* **185**, 5431–5441
- Thomas, C., Andersson, C. R., Canales, S. R., and Golden, S. S. (2004) *Microbiology* **150**, 1031–1040
- Garcia, B., Latasa, C., Solano, C., Garcia-del Portillo, F., Gamazo, C., and Lasa, I. (2004) *Mol. Microbiol.* **54**, 264–277
- Choy, W. K., Zhou, L., Syn, C. K., Zhang, L. H., and Swarup, S. (2004) *J. Bacteriol.* **186**, 7221–7228
- Simm, R., Morr, M., Kader, A., Nitz, M., and Römmling, U. (2004) *Mol. Microbiol.* **53**, 1123–1134
- Tischler, A. D., and Camilli, A. (2004) *Mol. Microbiol.* **53**, 857–869
- Kirilina, O., Fetherston, J. D., Bobrov, A. G., Abney, J., and Perry, R. D. (2004) *Mol. Microbiol.* **54**, 75–88
- Johnson, M. R., Montero, C. I., Connors, S. B., Shockley, K. R., Bridger, S. L., and Kelly, R. M. (2005) *Mol. Microbiol.* **55**, 664–674
- Paul, R., Weiser, S., Amiot, N. C., Chan, C., Schirmer, T., Giese, B., and Jenal, U. (2004) *Genes Dev.* **18**, 1715–1727
- Galperin, M. Y., Nikolskaya, A. N., and Koonin, E. V. (2001) *FEMS Microbiol. Lett.* **203**, 11–21
- Chan, C., Paul, R., Samoray, D., Amiot, N. C., Giese, B., Jenal, U., and

- Schirmer, T. (2004) *Proc. Natl. Acad. Sci. U. S. A.* **101**, 17084–17089
25. Tal, R., Wong, H. C., Calhoun, R., Gelfand, D., Fear, A. L., Volman, G., Mayer, R., Ross, P., Amikam, D., Weinhouse, H., Cohen, A., Sapir, S., Ohana, P., and Benziman, M. (1998) *J. Bacteriol.* **180**, 4416–4425
26. Chang, A. L., Tuckerman, J. R., Gonzalez, G., Mayer, R., Weinhouse, H., Volman, G., Amikam, D., Benziman, M., and Gilles-Gonzalez, M. A. (2001) *Biochemistry* **40**, 3420–3426
27. Galperin, M. Y., Natale, D. A., Aravind, L., and Koonin, E. V. (1999) *J. Mol. Microbiol. Biotechnol.* **1**, 303–305
28. Ely, B. (1991) *Methods Enzymol.* **204**, 372–384
29. Lopez, J. M., Marks, C. L., and Freese, E. (1979) *Biochim. Biophys. Acta* **587**, 238–252
30. Bochner, B. R., and Ames, B. N. (1982) *J. Biol. Chem.* **257**, 9759–9769
31. Galperin, M. Y. (2004) *Environ. Microbiol.* **6**, 543–545
32. Corbin, J. D., and Francis, S. H. (1999) *J. Biol. Chem.* **274**, 13729–13732
33. Ochi, K., Kandala, J., and Freese, E. (1982) *J. Bacteriol.* **151**, 1062–1065
34. Chiaverotti, T. A., Parker, G., Gallant, J., and Agabian, N. (1981) *J. Bacteriol.* **145**, 1463–1465
35. Freese, E., Heinze, J. E., and Galliers, E. M. (1979) *J. Gen. Microbiol.* **115**, 193–205
36. Ochi, K. (1987) *J. Bacteriol.* **169**, 3608–3616
37. Ratnayake-Lecamwasam, M., Serror, P., Wong, K. W., and Sonenshein, A. L. (2001) *Genes Dev.* **15**, 1093–1103
38. Bergara, F., Ibarra, C., Iwamasa, J., Patarroyo, J. C., Aguilera, R., and Marquez-Magana, L. M. (2003) *J. Bacteriol.* **185**, 3118–3126
39. Weinhouse, H., Sapir, S., Amikam, D., Shilo, Y., Volman, G., Ohana, P., and Benziman, M. (1997) *FEBS Lett.* **416**, 207–211
40. Ross, P., Mayer, R., and Benziman, M. (1991) *Microbiol. Rev.* **55**, 35–58
41. Ryjenkov, D. A., Tarutina, M., Moskvina, O. V., and Gomelsky, M. (2005) *J. Bacteriol.* **187**, 1792–1798

3.4 Genetic Analysis of a Novel Pathway for D-xylose Metabolism in *Caulobacter crescentus*

C. Stephens, B. Christen, T. Fuchs, V. Sundaram, K. Watanabe, and U. Jenal
J. Bacteriol. 2007 189: 2181-2185. [Epub ahead of print] December 15, 2006

Summary

In this paper, we characterized the pathway for D-xylose metabolism in *C. crescentus* by genetic and biochemical methods. We used a saturated transposon screen to define an operon consisting of five genes, essential for xylose degradation. Further, bioinformatic and biochemical approaches were applied to predict possible conversion pathways and to prove enzymatic functions. Taken together we postulate that *C. crescentus* metabolize D- xylose over a similar pathway as recently described for L-arabinose degradation of *A. brasilense*.

Statement of my work

I contributed to this work by performing a large scale transposon screen and identified mutants defective in xylose uptake, metabolism and regulation.

Genetic Analysis of a Novel Pathway for D-Xylose Metabolism in *Caulobacter crescentus*[∇]

Craig Stephens,^{1*} Beat Christen,² Thomas Fuchs,^{2†} Vidyodhaya Sundaram,¹
Kelly Watanabe,¹ and Urs Jenal²

Biology Department, Santa Clara University, 500 El Camino Real, Santa Clara, California 95053,¹ and Biozentrum, University of Basel, Klingelbergstrasse 70, 4054 Basel, Switzerland²

Received 11 September 2006/Accepted 6 December 2006

Genetic data suggest that the oligotrophic freshwater bacterium *Caulobacter crescentus* metabolizes D-xylose through a pathway yielding α -ketoglutarate, comparable to the recently described L-arabinose degradation pathway of *Azospirillum brasilense*. Enzymes of the *C. crescentus* pathway, including an NAD⁺-dependent xylose dehydrogenase, are encoded in the xylose-inducible *xylXABCD* operon (CC0823-CC0819).

D-Xylose (“wood sugar”) is the primary constituent of xylans that make up the bulk of hemicellulose in plant cell walls and is one of the more abundant carbohydrates in the biosphere. Two routes for D-xylose degradation in microorganisms have been described. Numerous bacteria, including *Escherichia coli* (15), *Bacillus* species (24, 25), and *Lactobacillus* species (16), use xylose isomerase to convert D-xylose to xylulose, which is then phosphorylated to enter the pentose phosphate pathway. Although some fungi have recently been shown to use this “bacterial” pathway (11), fungi more commonly transform D-xylose into xylitol by using xylose reductase and xylitol dehydrogenase (13). The freshwater bacterium *Caulobacter crescentus*, which readily uses D-xylose as a carbon and energy source, expresses an NAD-dependent xylose dehydrogenase (XDH) activity, suggesting that xylose metabolism occurs through a distinct pathway (21).

Prior to this work, the only known mutation affecting D-xylose utilization in *C. crescentus* was a Tn5-*lacZ* insertion that eliminated growth on xylose and exhibited strong xylose-dependent induction of β -galactosidase expression (18). The gene in which this insertion is located, designated “*xyIX*” by Meisenzahl et al. (18) and later “CC0823” in the *C. crescentus* genome annotation (19), does not closely resemble any gene of known function. *xyIX* is the first gene in a xylose-inducible operon (CC0823-CC0819) (12), referred to here as the *xyI* operon. We show that all of the genes in this operon are involved in xylose metabolism and propose a metabolic pathway employing these gene products.

Genetic analysis of D-xylose metabolism. To identify genes required for D-xylose utilization, *C. crescentus* NA1000 was mutagenized with a kanamycin-resistant mini-Tn5 transposon (9). Insertion strains were selected on peptone-yeast extract (PYE) medium containing kanamycin (20 μ g ml⁻¹). Mutants in which xylose metabolism is defective were identified by patching Kan^r colonies onto M2 minimal media

(10) with glucose (M2G) or xylose as a carbon source. We also patched colonies on M2 medium containing both glucose and xylose to identify strains for which xylose had become toxic [*xyI*(Tox)]. Roughly 20,000 Kan^r isolates were screened. Using chromosomal DNA as the template and primers derived from the Tn5 sequence, mutants with growth defects were analyzed by cycle sequencing to determine the location of the transposon insertion in comparison with that of the *C. crescentus* genome sequence (19). Strains unable to use glucose but unaffected in xylose utilization had mutations in genes previously implicated in glucose catabolism (12), including components of the Entner-Doudoroff (E-D) pathway (Fig. 1) (12, 22). The only gene identified here that was not previously associated with *C. crescentus* glucose catabolism is CC3065, which encodes a putative LacI superfamily transcription factor of unknown function.

Twenty-two *xyI* mutants were isolated. Insertions were found in 11 genes, including 4 of the 5 genes of the *xyI* operon (CC0823-CC0819) (Table 1). No insertions were identified in the CC0820 coding region, but one was found upstream, between CC0821 and CC0820. Six genes yielding the *xyI* mutant phenotype were found in multiple independent isolates, suggesting that the mutagenesis was approaching saturation and that these represent most, if not all, of the genes required specifically for xylose metabolism. None of the *xyI* mutant strains had a mutation in a putative transcriptional activator, consistent with previous suggestions (12, 18) that *C. crescentus* xylose metabolism genes are controlled by an as-yet-unidentified repressor. In addition, no genes resembling transporters were identified in this screen. Perhaps there are multiple transport systems capable of importing xylose into *C. crescentus*, as there are in *E. coli* (1, 8), so that a single mutation cannot sufficiently impair xylose uptake to block growth.

The previously unnamed genes of the *xyI* operon are hereafter designated *xyIA* (CC0822), *xyIB* (CC0821), *xyIC* (CC0820), and *xyID* (CC0819). Because transposon insertions in upstream genes of the operon (which is transcribed in the order *xyIX-xyIA-xyIB-xyIC-xyID*) could have polar effects, the role of each gene was assessed independently by constructing nonpolar in-frame deletions, using a PCR-based strategy (29). Deletion of any of the five genes rendered strains incapable of growth with

* Corresponding author. Mailing address: Biology Department, Santa Clara University, 500 El Camino Real, Santa Clara, CA 95053. Phone: 408-551-1898. Fax: 408-554-2710. E-mail: cstevens@scu.edu.

† Present address: Synthes Biomaterials, Guterstrasse 5, 2544 Betlach, Switzerland.

[∇] Published ahead of print on 15 December 2006.

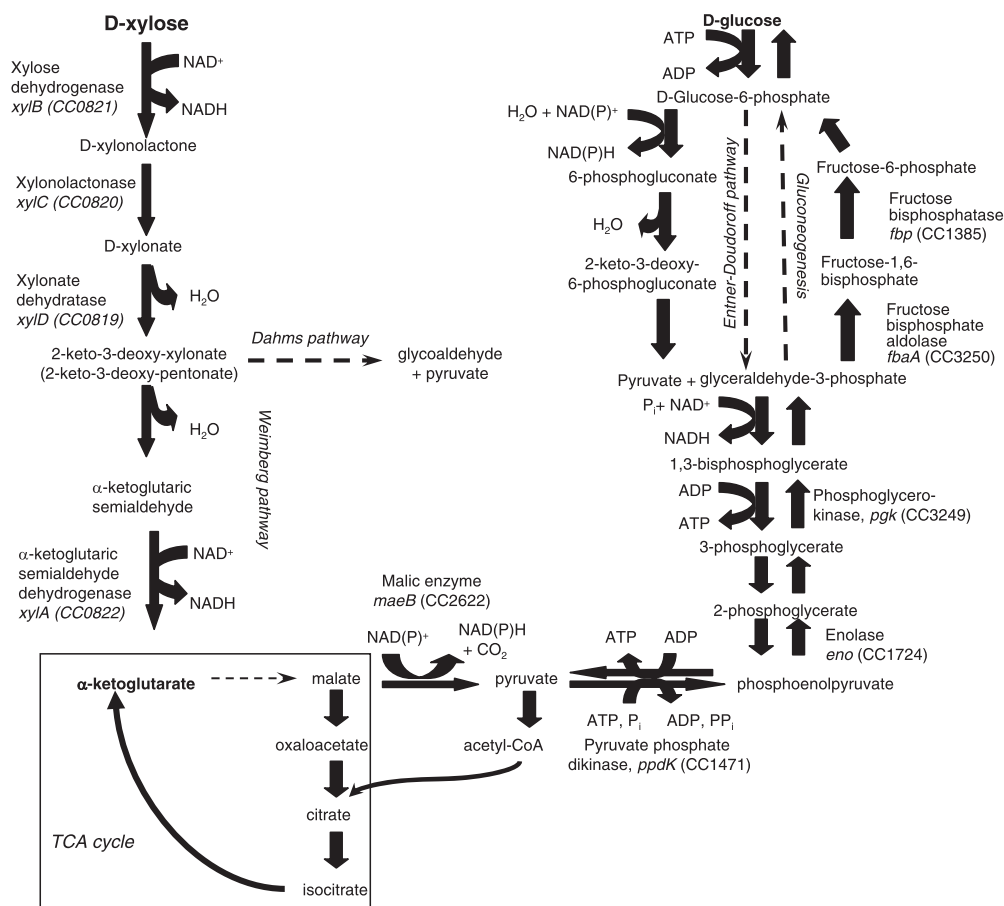


FIG. 1. Proposed pathway for D-xylose metabolism in *C. crescentus*. The reactions shown are based on biochemically confirmed degradation pathways for D-xylose metabolism in pseudomonads (7, 27). Both D-xylose and L-arabinose produce 2-keto-3-deoxy-pentionate. In the Dahms pathway (7), this compound is converted by an aldolase to pyruvate and glycoaldehyde. In an alternative reaction first demonstrated by Weimberg (27) and confirmed by Watanabe et al. (25, 26), for L-arabinose degradation in *A. brasilense*, a dehydratase produces α -ketoglutarate semialdehyde, which is then oxidized to α -ketoglutarate. The genes identified (through mutation) in this work as necessary for growth on D-xylose (Table 1) and the enzymes they encode are shown beside the appropriate reaction. The Entner-Doudoroff pathway and alternative reactions used in gluconeogenesis are shown at the upper right. TCA cycle reactions (in the box on the lower left, not shown in detail) are expected to be necessary for both D-xylose and D-glucose metabolism; genes encoding these enzymes were probably not found in this screen because they are also necessary for growth on PYE medium.

D-xylose as the sole carbon source, confirming that all five genes are necessary for xylose utilization.

All strains with an insertion in one of the genes of the *xyl* operon exhibited a *xyl*(Tox) phenotype on M2G agar plates, with colony formation blocked by inclusion of 10 mM D-xylose in the medium. In logarithmically growing M2G broth cultures, all the mutant strains exhibited reduced growth rates following the addition of D-xylose (data not shown), but only the $\Delta xylD$ and $\Delta xylX$ strains suffered a loss of viability. Xylose toxicity was generally reduced on complex PYE medium, with the effects on growth rate and colony appearance being less pronounced. The exception was the $\Delta xylD$ strain, which generated no colonies on PYE plus xylose agar medium and still lost viability after the addition of xylose to PYE broth culture.

Analysis of D-xylose dehydrogenase activity. Poindexter (21) observed D-xylose dehydrogenase activity in some *C. crescentus* strains grown in the presence of xylose. To determine whether any of the genes of the *xyl* operon encode this enzyme, XDH activity was assayed in extracts from wild-type and mutant

strains. Cultures were grown in PYE broth at 30°C with constant shaking to an optical density at 600 nm of approximately 0.5, at which time xylose was added to a final concentration of 1 mM. After 2 h, cells were harvested by centrifugation and disrupted by sonication. XDH activity in cell extracts was measured by following the xylose-dependent reduction of NAD^+ , as indicated by an increase in absorption at 340 nm (21). Assays were carried out in a 1-ml quartz cuvette containing 50 mM phosphate buffer (pH 8), 5 mM D-xylose, and 4 mM NAD^+ . If present, xylose-independent NADH production ("background activity," measured in control assays without xylose) was subtracted out. XDH activity was easily detectable in the wild-type strain induced with xylose (31.7 nmol NADH generated min^{-1} mg protein $^{-1}$) but was not observable above background in cultures grown without xylose. The enzyme was unable to use NADP^+ as the electron acceptor, as found by Poindexter (21). XDH activity was observed in extracts from the $\Delta xylX$, $\Delta xylC$, and $\Delta xylD$ mutant strains but was conspicuously absent from the $\Delta xylA$ and $\Delta xylB$ strains.

TABLE 1. Results of Tn5 mutant screen for *C. crescentus* *xyl* and *xyl*(Tox) mutants

Phenotype ^a	Interrupted gene	No. of isolates	Annotation	Proposed function
Xyl ⁻ Gluc ⁺ [Xyl(Tox)]	<i>xylX</i> (CC0823)	2	Conserved hypothetical protein	Unknown
	<i>xylA</i> (CC0822)	2	Aldehyde dehydrogenase	α-Ketoglutaric semialdehyde dehydrogenase
	<i>xylB</i> (CC0821)	1	Oxidoreductase, short-chain dehydrogenase/reductase family	Xylose dehydrogenase
	<i>xylC</i> (CC0820) upstream region ^b	1	CC0820: "SMP/Cgr family"	Xylonolactonase
	<i>xylD</i> (CC0819)	1	Dehydratase (IlvD/Edd family)	Xylonate dehydratase
	<i>fbp</i> (CC1385)	1	Fructose-1,6-bisphosphatase (EC 3.1.3.11)	Gluconeogenesis
Xyl ⁻ Gluc ⁺	<i>ppdK</i> (CC1471)	4	Pyruvate phosphate dikinase (EC 2.7.9.1)	Gluconeogenesis
	<i>maeB</i> (CC2622)	1	NADP-dependent malic enzyme (EC 1.1.1.40)	Gluconeogenesis
	<i>fbpA</i> (CC3250)	2	Fructose-bisphosphate aldolase (EC 4.1.2.13)	Gluconeogenesis
	CC3364	1	Homoserine kinase (EC 2.1.7.13)	Unknown
Xyl ⁻ Gluc ⁻	<i>eno</i> (CC1724)	2	Enolase (EC 4.2.1.11)	Glycolysis and gluconeogenesis
	<i>pgk</i> (CC3249)	4	Phosphoglycerate kinase (EC 2.7.2.3)	Glycolysis and gluconeogenesis
Xyl ⁺ Gluc ⁻	<i>zwf</i> (CC2057)	1	Glucose-6-phosphate 1-dehydrogenase (EC 1.1.1.49)	Entner-Doudoroff pathway
	CC2056	1	6-Phospho-glucono-lactonase (EC 3.1.1.31)	Entner-Doudoroff pathway
	<i>ppc</i> (CC1493)	2	Phosphoenolpyruvate carboxylase (EC 4.1.1.31)	Anaplerotic function
	CC3065	1	Transcriptional regulator, LacI family	Unknown
Xyl ⁺ Gluc ⁻ [Gluc(Tox)]	<i>eda</i> (CC1495)	1	4-Hydroxy-2-oxoglutarate aldolase (EC 4.1.2.14)	Entner-Doudoroff pathway

^a The "Xyl⁻" phenotype refers to strains that were unable to grow on M2 medium containing 10 mM D-xylose as the sole carbon source. The "Gluc⁻" phenotype refers to strains that were unable to grow on M2 medium containing 10 mM D-glucose as the sole carbon source. The "Xyl(Tox)" phenotype refers to strains that were sensitive to the presence of D-xylose in the medium, i.e., strains that were able to grow on M2G but that did not form colonies when 10 mM D-xylose was added to M2G.

^b Tn5 insertion was between the CC0821 and CC0820 coding regions.

The *xylA* gene product was annotated by the *C. crescentus* genome project as a "short-chain aldehyde dehydrogenase," while the *xylB* product was annotated as an "oxidoreductase" (19). To determine whether XDH activity is attributable to one of these gene products, the PCR-amplified coding regions were cloned separately into the pCR-CT-T7-Topo expression vector to allow production of C-terminal His-tagged proteins in *E. coli* strain BL21(λDE3) pLysS (Invitrogen). Cloning was carried out and protein expression was measured according to the manufacturer's protocols. Extracts from the *E. coli* strain expressing the cloned *C. crescentus xylB* gene displayed XDH activity (48.1 nmol NADH min⁻¹ mg protein⁻¹), which was absent from both the *E. coli* host strain and the strain expressing *xylA*. A 30-kDa polypeptide with XDH activity was purified from the *xylB*-expressing strain by Ni-affinity chromatography (Pharmacia nickel-nitrilotriacetic acid [nickel-NTA] column, developed with a 0 to 300 mM imidazole gradient in 50 mM sodium phosphate-50 mM NaCl-1 mM EDTA buffer on a Pharmacia fast protein liquid chromatography system). This polypeptide was confirmed as the XylB-His₆ fusion protein by liquid chromatography-mass spectrometry analysis (Midwest Bio Services, Overland Park, KS). Affinity-purified XylB-His₆ was at least 95% pure, based on sodium dodecyl sulfate-polyacrylamide gel electrophoresis analysis. XylB is thus responsible for XDH catalytic activity. It is not clear why the Δ*xylA* strain lacked XDH activity; one possibility is that the *xylA* deletion may have somehow affected *xylB* expression, even though it was designed to be nonpolar.

Purified recombinant XDH has a strong preference for D-xylose as a substrate. At sugar concentrations of up to 50 mM, D-arabinose, L-xylose, D-ribose, D-galactose, D-glucose, or

D-glucose-6-phosphate produced little or no NADH. L-Arabinose was active as a substrate, but analysis of XDH activity over a range of substrate concentrations (0.1 to 500 mM D-xylose or L-arabinose) showed that the enzyme strongly prefers D-xylose as a substrate (for D-xylose, $K_m = 0.76$ mM, $V_{max} = 27.5$ μmol NADH min⁻¹ mg⁻¹; for L-arabinose, $K_m = 166$ mM, $V_{max} = 20.5$ μmol NADH min⁻¹ mg⁻¹). Preliminary analysis of partially purified native *C. crescentus* XDH (to be described elsewhere) showed an even lower K_m for D-xylose of 70 μM, suggesting that the recombinant XylB-His₆ is not completely native in structure when produced in *E. coli*, perhaps due to additional amino acids at the N and C termini introduced for expression and purification.

A few bacterial species have been shown to express XDH activity (3, 6, 28, 30), but only one dehydrogenase with high specificity for D-xylose has been identified genetically (14), in the halophilic archeon *Haloarcula marismortui*. A pairwise BLAST comparison identified no significant similarity between the *H. marismortui* XDH and the *C. crescentus* XylB polypeptide sequences.

Pathway for D-xylose degradation. The two proposed pathways for xylose metabolism initiated by xylose dehydrogenase are identical through the production of 2-keto-3-deoxyxylonate (Fig. 1) (5, 7, 28). The initial series of reactions is analogous to the Entner-Doudoroff pathway, particularly the archaeal version of the E-D pathway in which glucose is not phosphorylated (23). One component of the Entner-Doudoroff and xylose degradation pathways appears to be evolutionarily related, since *C. crescentus* XylD (GenBank accession no. AAK22804) is notably similar in sequence to bacterial 6-phosphogluconate dehydratases (e.g., *E. coli* Edd; GenBank acces-

sion no. AAA23722; 31% identity over 446 amino acids with XylD) (4). Based on this, we hypothesize that XylD catalyzes the dehydration of D-xylo-2,5-dione to 2-keto-3-deoxyxylonate.

Watanabe et al. (26, 27) have recently shown that L-arabinose degradation in *Azospirillum brasilense* follows the pathway Weimberg proposed for L-arabinose and D-xylose (28). L-Arabinose and D-xylose are structurally related pentoses, and the L-arabinose in arabinogalactan polymers also contributes substantially to hemicellulose. Although the L-arabinose dehydrogenase cloned by Watanabe et al. (26) is unrelated by amino acid sequence to the *C. crescentus* XylB D-xylose dehydrogenase, other potential pathway components are related. *Caulobacter crescentus* XylC (GenBank accession no. AAK22805) aligns well with *A. brasilense* arabinolactonase (GenBank accession no. AB241136.1; 34% identity over 285 amino acids with XylC) and is thus a good candidate to catalyze the conversion of D-xylo-2,5-dione to D-xylo-2,5-dione- γ -lactone to D-xylo-2,5-dione. 2-Keto-deoxyxypentolate is produced by the subsequent dehydration reaction, which as noted above is predicted to be catalyzed by XylD. In the Weimberg pathway (28), 2-keto-deoxyxypentolate is dehydrated to α -ketoglutarate semialdehyde and oxidized to α -ketoglutarate by α -ketoglutarate semialdehyde dehydrogenase. The *C. crescentus* XylA sequence (GenBank accession no. AAK22807) aligns well with the *A. brasilense* α -ketoglutarate semialdehyde dehydrogenase (GenBank accession no. AB241137; 32% identity over 475 amino acids with XylA), suggesting that it executes this reaction (Fig. 1).

This strategy for D-xylose metabolism in *C. crescentus* could explain the requirement for malic enzyme (*maeB*; CC2622) for growth on xylose (Table 1; Fig. 1). This enzyme would divert some malate (produced ultimately from α -ketoglutarate) to generate pyruvate, which is necessary for a variety of anabolic functions, including gluconeogenesis. The requirement for malic enzyme would be difficult to rationalize if *C. crescentus* metabolized D-xylose via the Dahms pathway (Fig. 1), because pyruvate would be generated by aldolase cleavage of 2-keto-deoxyxylonate (7). Gluconeogenesis presumably continues from pyruvate to phosphoenolpyruvate via pyruvate phosphate dikinase (*ppdK*; CC1471) (Table 1). *Sinorhizobium meliloti*, a close relative of *C. crescentus*, can use malic enzyme and PPK to support gluconeogenesis during growth on tricarboxylic acid (TCA) cycle intermediates (20), which is comparable to what *C. crescentus* would experience if xylose metabolism proceeded via α -ketoglutarate. Other gene products required for growth on xylose, and likely identified in our screen because of gluconeogenic function, include enolase (*eno*; CC1724) and phosphoglycerate kinase (*pgk*; CC3249), which catalyze reversible reactions also required for glucose catabolism (Table 1). Fructose biphosphate aldolase (*fabA*; CC3250) also catalyzes a reversible reaction but is not necessary for growth on glucose because the Entner-Doudoroff pathway bypasses the fructose biphosphate intermediate of glycolysis.

Given the similarity of the proposed *C. crescentus* D-xylose degradation pathway to the *A. brasilense* L-arabinose pathway and the fact that the *xylB*-encoded XDH can utilize L-arabinose as a substrate (albeit poorly), we examined whether this pathway has a role in L-arabinose metabolism. Wild-type *C. crescentus* strain CB15 grows very poorly in liquid M2 medium with L-arabinose as the sole carbon source but forms colonies on M2 agar containing L-arabinose. Growth levels of CB15 and the Δ *xylA*, Δ *xylB*, Δ *xylC*, and Δ *xylD* mutants were compared on

M2 agar plates with either D-glucose, D-xylose, or L-arabinose (all at 10 mM) as the sole carbon sources. The strains grew similarly on glucose (i.e., 1-mm colonies within 3 days), and none of the mutants grew with xylose. CB15 produced 1-mm colonies within 3 to 4 days on xylose, and after 5 to 6 days, had formed 1-mm colonies on L-arabinose. The Δ *xylA*, Δ *xylB*, and Δ *xylC* strains formed smaller "microcolonies" (≤ 0.5 mm) on L-arabinose after 5 to 6 days and thus appear to be defective for growth on this substrate. Curiously, growth of the Δ *xylD* strain was similar to that of the parental strain CB15 on L-arabinose, indicating that the *xylD* product is dispensable for growth on L-arabinose. Deficiencies in growth on L-arabinose among the other *xyl* mutant strains were confirmed using Biolog phenotype microarray plates PM1 and PM2 (2) to examine carbon source utilization (data not shown). Thus, with the exception of the XylD-catalyzed step, the *C. crescentus* D-xylose degradation pathway probably contributes to L-arabinose degradation in vivo, but there may be an additional route for L-arabinose utilization.

Genes necessary for growth on D-xylose to which we cannot assign a role include *xylX* (CC0823) and CC3364. The *xylX* product falls into COG3970, the fumarylacetoacetate hydrolase family. CC3364 is annotated as a "homoserine kinase" due to weak similarity to the *Pseudomonas aeruginosa* *thrB* gene product. Functional characterization of these genes is an important future goal for understanding D-xylose metabolism in *C. crescentus*.

The basis for growth inhibition by xylose in strains with mutations in the *xyl* operon is not known. Interruption of a metabolic pathway can lead to toxicity if harmful intermediates accumulate. The Δ *xylD* mutant suffers the most severe effects in the presence of D-xylose, which could conceivably be due to the accumulation of D-xylo-2,5-dione, but we have no direct evidence at present to support that hypothesis. Excessive uptake of a nonmetabolized sugar, or the effects of xylose on gene expression, could also result in metabolic alterations that are harmful in the absence of metabolite flux through the xylose catabolic pathway. For example, xylose increases isocitrate lyase expression in *C. crescentus* (12). During growth on glucose in the absence of productive xylose metabolism, an increase in isocitrate lyase activity could excessively channel isocitrate into the glyoxylate bypass at the expense of critical TCA cycle intermediates, such as α -ketoglutarate, that are no longer being generated (directly or indirectly) from D-xylose. Potential explanations of the *xyl*(Tox) phenotype must also take into account the observation that growth inhibition is less severe in the complex PYE medium than in the defined M2 medium. If a metabolic imbalance is leading to growth inhibition, the diversity of organic metabolites present in PYE may alleviate some of the problems.

This route of D-xylose metabolism is not unique to *C. crescentus*, having been identified originally in a *Pseudomonas* strain (28), but a preliminary survey of other sequenced genomes suggests that this pathway is not common. Using BLAST, we were able to identify only three other bacteria containing possible operons with component genes closely related to most or all of the *C. crescentus* *xyl* operon genes: *Caulobacter* strain K31 (a freshwater α -proteobacterium isolated from chlorophenol-contaminated groundwater) (17), *Burkholderia xenovorans* strain LB400 (a PCB-degrading β -proteobacterium isolated from a landfill), and *Chro-*

mohalobacter salexigens strain DSM 3043 (a halophilic γ -proteobacterium). These three genome sequences have not been described in publications but are available through the U.S. Department of Energy's Joint Genome Institute website (http://genome.jgi-psf.org/mic_home.html). *Caulobacter* strain K31 expresses D-xylose-inducible XDH activity (data not shown), but to our knowledge, xylose metabolism has not been further examined in these diverse species. We speculate that they share with *C. crescentus* a common pathway for D-xylose degradation, encoded in a gene cluster that may have been horizontally transferred in aquatic and/or soil habitats.

This work was supported by National Science Foundation grant MCB-0317037 to C.S. and Swiss National Science Foundation fellowship 3100A0-108186 to U.J.

We gratefully acknowledge the students of the 2003 and 2004 advanced bacterial genetics courses at Cold Spring Harbor Laboratory and the 2003 microbiology block course at the University of Basel who isolated the transposon mutants, as well as several Santa Clara University undergraduates who generated knockout strains in the recombinant DNA technology course (Desiree Yang, Naomi Arana, Nicole Robledo, Sarah Arriola, and Dennie Magcase). We also thank Angel Islas for advice on protein expression and purification and Minna Manisto (Finnish Forest Research Institute, Rovaniemi, Finland) for providing *Caulobacter* strain K31.

REFERENCES

- Ahlem, C., W. Huisman, G. Nestlund, and A. S. Dahms. 1982. Purification and properties of a periplasmic D-xylose-binding protein from *Escherichia coli* K-12. *J. Biol. Chem.* **257**:2926–2931.
- Bochner, B. R. 2003. New technologies to assess genotype-phenotype relationships. *Nat. Rev. Genet.* **4**:309–314.
- Buchert, J., L. Viikari, M. Linko, and P. Markkanen. 1986. Production of xylonic acid by *Pseudomonas fragi*. *Biotechnol. Lett.* **8**:541–546.
- Carter, A. T., B. M. Pearson, J. R. Dickinson, and W. E. Lancashire. 1993. Sequence of the *Escherichia coli* K-12 *edd* and *eda* genes of the Entner-Doudoroff pathway. *Gene* **130**:155–156.
- Dagley, S., and P. W. Trudgill. 1965. The metabolism of galactarate, D-glucarate and various pentoses by species of *Pseudomonas*. *Biochem. J.* **95**:48–58.
- Dahms, A. S., and J. Russo. 1982. D-xylose dehydrogenase. *Methods Enzymol.* **89D**:226–228.
- Dahms, A. S. 1974. 3-Deoxy-D-pentulosonic acid aldolase and its role in a new pathway of D-xylose degradation. *Biochem. Biophys. Res. Commun.* **60**:1433–1439.
- Davis, E. O., and P. J. F. Henderson. 1987. The cloning and DNA sequence of the gene *xylE* for xylose-proton symport in *Escherichia coli* K12. *J. Biol. Chem.* **262**:13928–13932.
- de Lorenzo, V., M. Herrero, U. Jakubzik, and K. N. Timmis. 1990. Mini-Tn5 transposon derivatives for insertion mutagenesis, promoter probing, and chromosomal insertion of cloned DNA in gram-negative eubacteria. *J. Bacteriol.* **172**:6568–6572.
- Ely, B. 1991. Genetics of *Caulobacter crescentus*. *Methods Enzymol.* **204**:372–384.
- Harhangi, H. R., A. S. Akhmanova, R. Emmens, C. van der Drift, W. T. de Laet, J. P. van Dijken, M. S. Jetten, J. T. Pronk, and H. J. Op den Camp. 2003. Xylose metabolism in the anaerobic fungus *Piromyces* sp. strain E2 follows the bacterial pathway. *Arch. Microbiol.* **180**:134–141.
- Hottes, A. K., M. Meewan, D. Yang, N. Arana, P. Romero, H. H. McAdams, and C. Stephens. 2004. Transcriptional profiling of *Caulobacter crescentus* during growth on complex and minimal media. *J. Bacteriol.* **186**:1448–1461.
- Jeffries, T. W. 1983. Utilization of xylose by bacteria, yeasts, and fungi. *Adv. Biochem. Eng. Biotechnol.* **27**:1–32.
- Johnsen, U., and P. Schönheit. 2004. Novel xylose dehydrogenase in the halophilic archaeon *Haloarcula marismortui*. *J. Bacteriol.* **186**:6198–6207.
- Lawlis, V. B., M. S. Dennis, E. Y. Chen, D. H. Smith, and D. J. Henner. 1984. Cloning and sequencing of the xylose isomerase and xylulose kinase genes of *Escherichia coli*. *Appl. Environ. Microbiol.* **47**:15–21.
- Lokman, B. C., P. Van Santen, J. C. Verdoes, J. Kruse, R. J. Leer, M. Posno, and P. H. Pouwels. 1991. Organization and characterization of three genes involved in D-xylose catabolism in *Lactobacillus pentosus*. *Mol. Gen. Genet.* **230**:161–169.
- Mannisto, M. K., M. A. Tirola, M. S. Salkinoja-Salonen, M. S. Kulomaa, and J. A. Puhakka. 1999. Diversity of chlorophenol-degrading bacteria isolated from contaminated boreal groundwater. *Arch. Microbiol.* **171**:189–197.
- Meisenzahl, A. C., L. Shapiro, and U. Jenal. 1997. Isolation and characterization of a xylose-dependent promoter from *Caulobacter crescentus*. *J. Bacteriol.* **179**:592–600.
- Nierman, W. C., T. V. Feldblyum, M. T. Laub, I. T. Paulsen, K. E. Nelson, J. Eisen, J. F. Heidelberg, M. R. Alley, N. Ohta, J. R. Maddock, I. Potocka, W. C. Nelson, A. Newton, C. Stephens, N. D. Phadke, B. Ely, R. T. DeBoy, R. J. Dodson, A. S. Durkin, M. L. Gwinn, D. H. Haft, J. F. Kolonay, J. Smit, M. B. Craven, H. Khouri, J. Shetty, K. Berry, T. Utterback, K. Tran, A. Wolf, J. Vamathevan, M. Ermolaeva, O. White, S. L. Salzberg, J. C. Venter, L. Shapiro, and C. M. Fraser. 2001. Complete genome sequence of *Caulobacter crescentus*. *Proc. Natl. Acad. Sci. USA* **98**:4136–4141.
- Osteras, M., B. T. Driscoll, and T. M. Finan. 1997. Increased pyruvate orthophosphate dikinase activity results in an alternative gluconeogenic pathway in *Rhizobium (Sinorhizobium) meliloti*. *Microbiology* **143**:1639–1648.
- Poindexter, J. S. 1964. Biological properties and classification of the *Caulobacter* group. *Bacteriol. Rev.* **28**:231–295.
- Riley, R. G., and B. J. Kolodziej. 1976. Pathway of glucose catabolism in *Caulobacter crescentus*. *Microbios* **16**:219–226.
- Romano, A. H., and T. Conway. 1996. Evolution of carbohydrate metabolic pathways. *Res. Microbiol.* **147**:448–455.
- Rygas, T., A. Scheler, R. Allmansberger, and W. Hillen. 1991. Molecular cloning, structure, promoters and regulatory elements for transcription of the *Bacillus megaterium* encoded regulon for xylose utilization. *Arch. Microbiol.* **155**:535–542.
- Scheler, A., T. Rygas, R. Allmansberger, and W. Hillen. 1991. Molecular cloning, structure, promoters and regulatory elements for transcription of the *Bacillus licheniformis*-encoded regulon for xylose utilization. *Arch. Microbiol.* **155**:526–534.
- Watanabe, S., T. Kodaki, and M. Keisuke. 2006. Cloning, expression and characterization of bacterial L-arabinose 1-dehydrogenase involved in an alternative pathway of L-arabinose metabolism. *J. Biol. Chem.* **281**:2612–2623.
- Watanabe, S., T. Kodaki, and K. Makino. 2006. A novel alpha-ketoglutaric semialdehyde dehydrogenase: evolutionary insight into an alternative pathway of bacterial L-arabinose metabolism. *J. Biol. Chem.* **281**:28876–28888.
- Weimberg, R. 1961. Pentose oxidation by *Pseudomonas fragi*. *J. Biol. Chem.* **236**:629–635.
- West, L., D. Yang, and C. Stephens. 2002. Use of the *Caulobacter crescentus* genome sequence to develop a method for systematic genetic mapping. *J. Bacteriol.* **184**:2155–2166.
- Yamanaka, K., M. Gino, and R. Kaneda. 1977. A specific NAD-D-xylose dehydrogenase from *Arthrobacter* sp. *Agric. Biol. Chem.* **41**:1493–1499.

4 Unpublished results

4.1 Isolation of *S. enterica* Transposon Mutants Impaired in c-di-GMP Dependent EPS Production.

4.1.1 Introduction

One fundamental characteristic of bacterial behavior is the elaborate adaptation to various environments. Bacteria dominate extreme niches such as hot springs, highly acidic stockpiles or live inside hosts, under steady confrontation with the host immune system (48). Under such conditions, bacteria often switch from a unicellular, dispersal into a multicellular, sedentary lifestyle (49) (Figure 3), whereby cells are physically protected by a self-secreted shelter made of extracellular polymeric substances (EPS) (50). The biofilm EPS are composed of polysaccharides (51-53) but may also comprise fimbriae, pili (54) or even DNA (55).

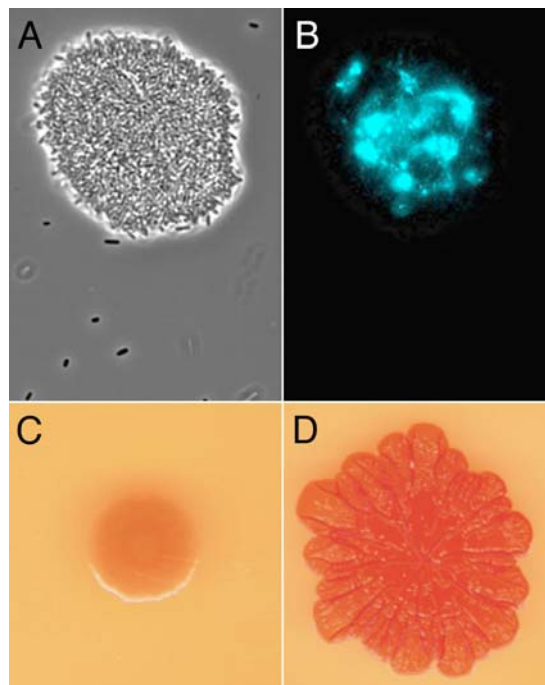


Figure 3: *S. enterica* phenotypic changes upon conversion from planktonic to biofilm state.

A) Biofilm formation in liquid culture, phase contrast microscopy. B) EPS in the core of the biofilm visualized by polysaccharide specific calcofluor staining, fluorescent microscopy. C) Smooth and white morphotype of *S. enterica* with low cellular levels of c-di-GMP on Congo Red plates D) Red, dry and rough morphotype of *S. enterica* with high cellular levels of c-di-GMP on Congo Red plates.

Recent studies have demonstrated that the novel bacterial second messenger c-di-GMP orchestrates the developmental transition between the two lifestyles (56,57). The enzymes diguanylate cyclase and phosphodiesterase, which synthesize and degrade the second messenger c-di-GMP have been characterized down to the molecular level (26,58-61). High intracellular c-di-GMP levels induce dramatic phenotypic changes such as massive production of EPS and inhibition

of flagella and pili based motility (46,56,62). However, the nature of effector proteins and signaling mechanisms involved have not been studied.

4.1.2 Results and Discussion

Identification of transposon mutants blocked in c-di-GMP dependent EPS production - To define how c-di-GMP controls EPS production in *S. enterica* serovar Typhimurium, a genetic screen for transposon mutants blocked in c-di-GMP dependent EPS production was designed. A strain with a constitutive active diguanylate cyclase under the control of the arabinose promoter was constructed. Induction with arabinose caused an elevated cellular c-di-GMP level, as detected by total nucleotide measurements using HPLC methods, and results in a dramatic upregulation of EPS secretion. Under these conditions, colonies develop a red, dry and rough (rdar) morphotype (33-35,63) on reporter plates containing the EPS binding dye Congo Red (Figure 3C and D).

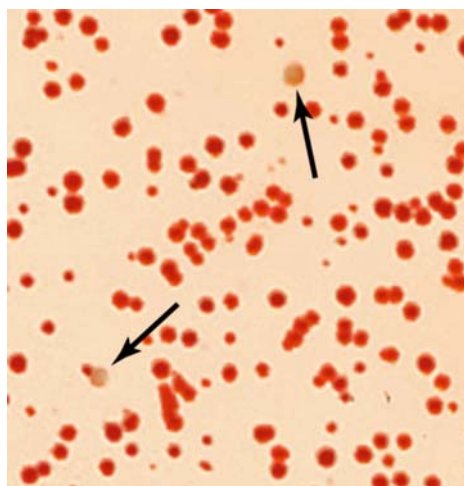


Figure 4: *S. enterica* Tn10dTc mutant screened on Congo Red plates

The morphotype red, dry and rough (rdar) produce massive amounts of EPS whereas transposon mutants with a smooth and white (saw) morphotype are deficient in EPS production.

20'000 independent Tn10dTc (64) insertion mutants were visually screened on Congo Red plates (Figure 4). Thereof, 25 mutants, presumably deficient in c-di-GMP dependent EPS production, were detected by their smooth and white colony morphotype. Co-transduction experiments followed by sequencing transposon boundaries revealed three distinct mutant classes. In the first class, 11 out of 25 Tn10dTc mutants were linked to the arabinose locus. These mutants abolished ectopic expression the constitutive diguanylate cyclase (*dgcA*) and had insertions in the

transcriptional regulator *araC* or in the arabinose promoter P_{BAD} . The second mutant class (2 out of 25) mapped to an *astA* homolog, coding for a putative arylsulfate sulfotransferase (*stm4098*). This enzyme catalyzes the transfer of sulfate groups from phenylsulfate esters to phenolic compounds (65) and was identified in *Edwardsiella tarda* in a screen for mutants defective in virulence and siderophore production (66). The exact role of *astA* in c-di-GMP dependent EPS production remains unclear. Either *astA* is involved in EPS modification or it interferes directly or indirectly with a component essential for EPS production. The third mutant class (12 out of 25) mapped to the bacterial cellulose synthase (*bcs*) locus.

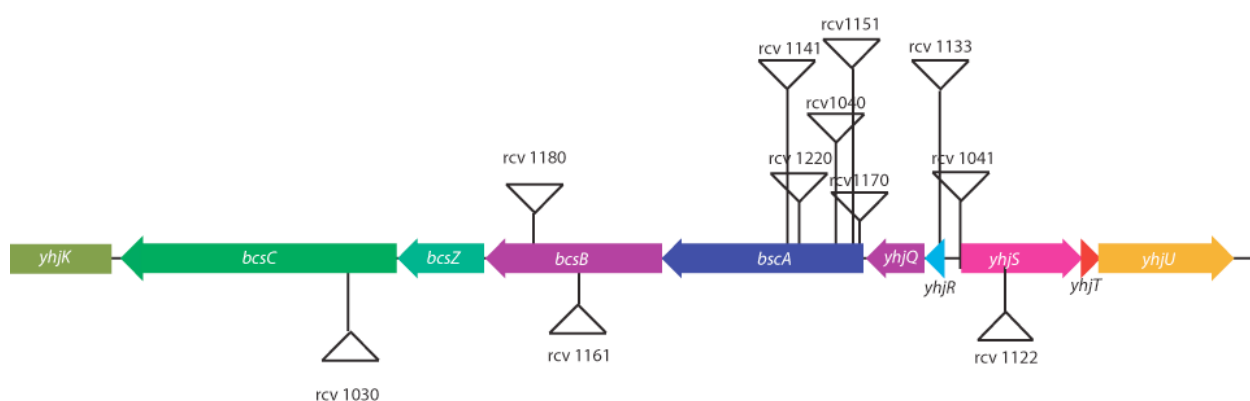


Figure 5: Components involved in c-di-GMP dependent cellulose production in *S. enterica*.

Tn *10dTc* insertion mutants defect in cellulose synthesis. *yjhH* putative diguanylate cyclase/phosphodiesterase domain 3, *kdgK* ketodeoxygluconokinase, *yhjJ* putative Zn-dependent peptidase, *dctA* DAACS family, C4-dicarboxylic acids transport protein, *yhjK* putative diguanylate cyclase/phosphodiesterase, *bcsC* Cellulose synthase operon protein C, *bcsZ* Cellulose synthase operon protein Z endo 1,4-D-glucanase, *bcsB* Cellulose synthase operon protein B, *bcsA* Cellulose synthase operon protein A glycosyltransferase, *yhjQ* putative ATPase involved in chromosome partitioning, *yhjR* putative cytoplasmic protein, *yhjS* putative cytoplasmic protein, *yhjT* putative inner membrane protein, *yhjU* putative inner membrane protein.

Some of these mutants were entirely smooth and white and had insertions in *bcsA*, *bcsB* and *bcsC*. All of these genes code for essential subunits of the bacterial cellulose synthase complex. Three mutants only showed the smooth and white morphotype at the rim of the colony. These transposon insertions are located upstream of the *bcs*-operon in *yhjR* and *yhjS* both annotated as putative cytoplasmic proteins. Whereas *yhjS* shows weak homology to a putative protease, the function of *yhjR* remain elusive. Since EPS production was only reduced but not completely abolished, *yhjR* and *yhjS* presumably define auxiliary or regulatory rather than essential components for EPS production. Despite near saturation of the genetic screen, most transposon insertions mapped to the cellulose synthase locus. This strongly suggests that in *S. enterica*

serovar Typhimurium, the cellulose synthase complex is activated by c-di-GMP and that cellulose is the main EPS component that binds Congo Red, leading to a red, dry and rough morphotype. This model is consistent with the findings from *G. xylinum*, where c-di-GMP was initially biochemically isolated as an allosteric regulator of the cellulose synthase complex (67).

Cellulose synthesis and motility are controlled via independent pathways - The c-di-GMP controlled transition from the unicellular lifestyle into biofilm mode is not only characterized by massive production of EPS, but also by a block of flagella and pili based motility (57). In principle inhibition of cell motility could be explained by two models. Either increased EPS secretion makes the cells sticky and physically blocks motility or c-di-GMP inhibits flagella-based motility via a second, EPS independent pathway. If increased cellulose production rendered cells nonmotile, mutants deficient in cellulose synthesis would consequently regain motility despite a high intracellular c-di-GMP level. Swimming behaviour of two *S. enterica* strains both ectopically expressing a constitutive diguanylate cyclase, in either wild type or mutated *bcsA* background, was analysed. The *bcsA* mutant as well as the control strain were nonmotile, suggesting that c-di-GMP blocks motility over a cellulose synthase independent pathway.

4.1.3 Material and Methods

*Ectopic expression of the diguanylate cyclase *dgcA* under P_{BAD}* - A linear DNA fragment containing the *C. crescentus* diguanylate cyclase allele *dgcA* flanked by 40bp homologous to the *araBAD* locus was PCR amplified and electroporated into the recombinogenic *S. enterica* strain TH6706 *araB::Tn10dTc* / pKD46. Double homologous recombinants replacing the entire *araBAD::Tn10dTc* with the *dgcA* allele were selected by *tetRA* counter selection on fusaric acid plates. TetS recombinants were screened onto Congo Red plates supplemented with arabinose for correctly inserted *dgcA* alleles under control of the arabinose promoter P_{BAD} . One strain with an arabinose dependent red dry and rough morphotype was isolated, and named BC478 (LT2 $P_{BAD}::dgcA$).

Transposon mutagenesis using Tn10dTc - Plasmid pNK2880 expressing transposase was transduced into BC478 by standard P22 phage transduction. Tn10dTc elements were delivered via a second P22 transduction from the donor strain TH338 $\Delta proAB47$ / F' Pro Lac *zzf1831::Tn10dTc*. Transposon insertions in strain BC478 were selected on LA plates supplemented with Tetracycline (10µg/ml), EGTA (1mM), Arabinose (0.2%), Congo Red (50µg/ml) and putative EPS deficient mutants were visual identified by their smooth and white colony morphology.

*Identification of transposon insertions with deficient *dgrA* expression* – Smooth and white transposon mutants were transduced into *S. enterica* LT2 and analysed on minimal arabinose plates. Transposon mutants that abolish *dgcA* expression because of insertions in *araC*, P_{BAD} or *dgcA* are linked to the defective *araBAD* locus (*araB::dgcA*) and were identified as Ara⁻ transductants and discarded.

Mapping of Transposon mutants deficient in c-di-GMP dependent EPS production – exact insertion sites of transposon mutants not linked to the *araBAD* locus were sequenced by arbitrary PCR technique.

4.2 Genetic Identification of the Xylose Repressor *xyIR* and the Xylose Operator *xyIO* site

4.2.1 Introduction

C. crescentus is an oligotroph and metabolize various monosaccharides such as glucose, xylose, galactose and mannose (68). While glucose is catabolized via the Entner-Doudoroff pathway to pyruvate (69,70), xylose is probably degraded through a pathway yielding α -ketoglutarate (71), similar to the L-arabinose degradation pathway of *A. brasilense* (72). Biochemical studies showed that *C. crescentus* induce NAD-linked xylose dehydrogenase activity is specifically induced when xylose is present in the growth media (68). Recently, xylose dehydrogenase was allocated to the *xyIB* gene that together with other genes essential for xylose degradation forms the *xyIXABCD* operon (71). Global transcriptome analysis (70) as well as *lacZ* reporter studies (73) revealed that transcription of the *xyIXABCD* operon is repressed when xylose is absent, but so far no regulatory components affecting the xylose dependent promoter (P_{xyl}) were identified. Here, we demonstrated that the *xyIXABCD* operon is tightly control via a LacI like repressor and define determinants of the xylose operator *xyIO* critical for repressor operator interactions.

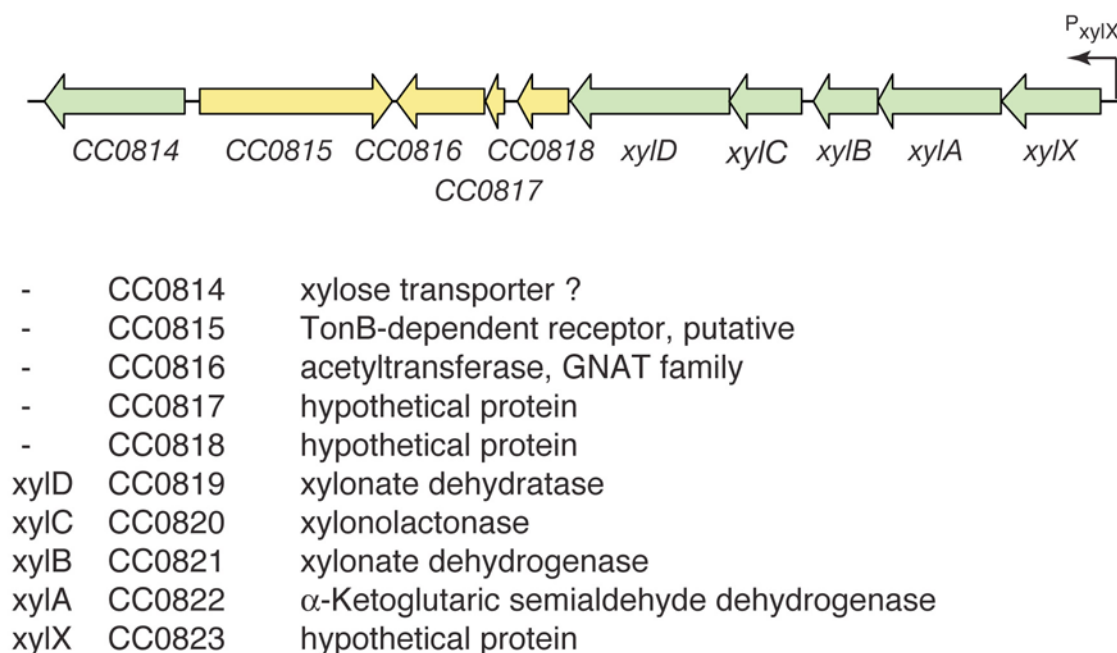
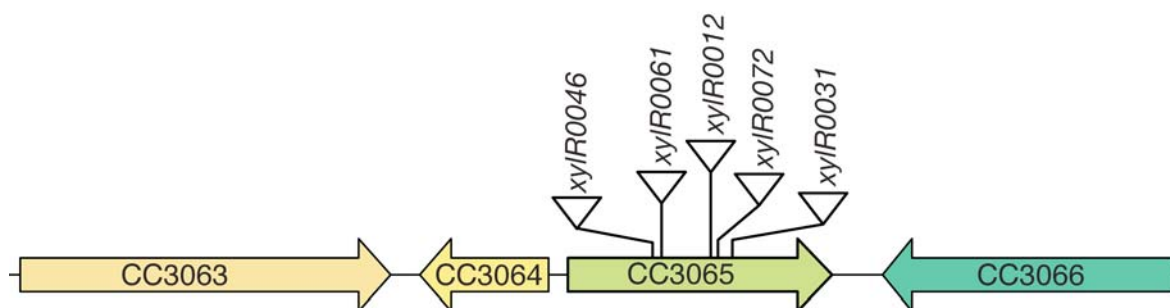


Figure 6: Organization of the xylose operon *xyIXABCD*

Xylose induced genes high lighted in green as determined by microarray analysis (70). The xylose inducible promoter P_{xylX} is positioned 70 bp upstream of *xyIX*

4.2.2 Results and Discussion

In order to genetically identify the xylose repressor (*xyIR*) gene as well as the xylose operator (*xyIO*) element, a *C. crescentus* strain was engineered, that expressed the only copy of *clpX* ectopically from the xylose promoter P_{xyIX} . Because ClpX is essential for cell cycle progression (74), the resulting strain was conditional lethal and required xylose for growth. In a first attempt, putative transposon insertions in *xyIR* were isolated by selecting for growth in absence of the inducer xylose. Five independent transposon mutants that showed a strict linkage of the transposon resistance to the xylose independent growth phenotype were mapped to gene CC3065 (Figure 7).



CC3063 - sulfite reductase (NADPH) flavoprotein alpha-component

CC3064 - hypothetical protein

CC3065 - *xyIR* transcriptional regulator, LacI family

CC3066 - *argJ* bifunctional ornithine acetyltransferase/N-acetylglutamate synthase protein

Figure 7: Tn5 insertion sites in *xyIR*

Five independent miniTn5 insertions isolated from the xylose repressor selection were mapped to CC3065 that codes for a LacI like repressor protein

CC3065, renamed *xyIR*, codes for a LacI-like transcriptional repressor with an N-terminal LacI DNA binding domain and a C-terminal sugar binding domain. To validate the hypothesis that XyIR is responsible for the repression of the *xyIXABCD* operon, LacZ reporter studies were performed in a *xyIR::Tn5* mutant strain (UJ3002). A *lacZ* operon fusion to *xyIX* was derepressed even when xylose was absent, whereas wild type showed tight repression under these (Figure 8). These data suggested that *xyIR* encodes a repressor of the xylose operon.

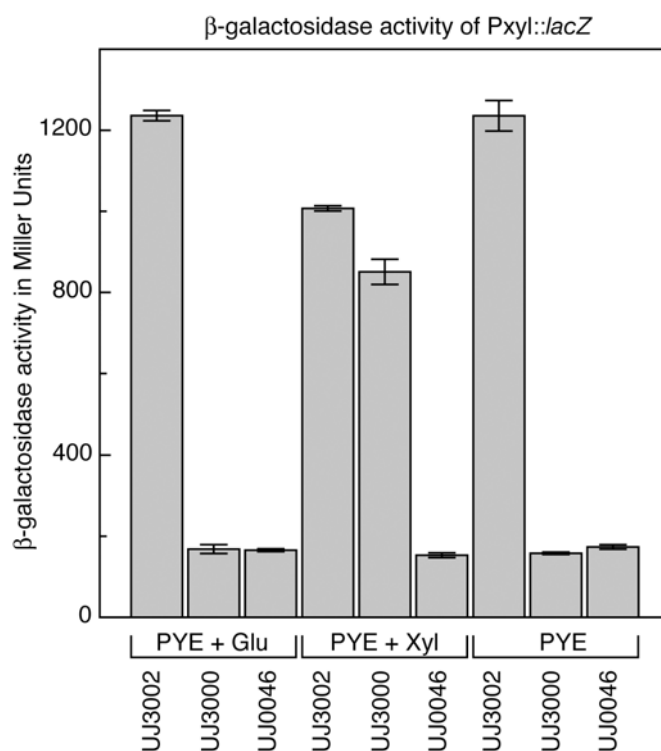


Figure 8: β-galactosidase activity of $P_{xyI}::lacZ$ reporter construct

The β-galactosidase activity of a $xyI::lacZ$ gene fusion (pCS225) was determined in a wild type $xyIR$ (UJ3000) or $xyIR::Tn5$ mutant strain (UJ3002) and compared to basal β-galactosidase activity of a control strain (UJ0046, NA1000 / pLac290). All strains were analysed in triplicates when grown in normal PYE, PYE supplemented with 0.2% glucose (PYE + Glu) or PYE supplemented with 0.2% xylose (PYE + Xyl).

To further define the XylR repressor binding site within the xylose promoter region, rare point mutants in the xylose operator ($xyIO$) allowing xylose independent growth of the $P_{xyI}::clpX \Delta clpX$ strain were selected and further separated from spontaneous $xyIR$ loss of function mutations by chromosomal linkage cross as described in materials and methods (see section 4.2.3). Sequencing the xylose promoter region revealed that four discrete point mutations close to the annotated transcriptional start site of xyI were independently isolated several times (Figure 9A). Interestingly, all point mutants identified reside in a 12 bp nearly palindromic DNA region that partially overlaps with the annotated Pribnow box. This makes this region a good candidate for the xylose operator $xyIO$, where XylR binds DNA, an idea that is supported by the fact that the isolated point mutations were not exclusively symmetrically distributed within the palindrome. For instance both point mutations at the 5th and 8th position in the $xyIO$ motif miss their symmetrical counterpart (10th and 7th position, see Figure 9A) arguing that these non mutated positions are essential for promoter function and probably constitute part of the Pribnow box.

A

<i>xylO</i> wt	TGTTAGCGCTACCA
<i>xylO0601</i>	TATTAGCGCTACCA
<i>xylO0612</i>	TGTTGGCGCTACCA
<i>xylO0607</i>	TGTTAGCACTACCA
<i>xylO0608</i>	TGTTAGCACTACCA
<i>xylO0512</i>	TGTTAGCACTACCA
<i>xylO0422</i>	TATTAGCGCTACCA
<i>xylO0423</i>	TATTAGCGCTACCA
<i>xylO0304</i>	TATTAGCGCTACCA
<i>xylO0305</i>	TGTTAGCGCTACTA
<i>xylO0306</i>	TGTTAGCGCTACTA
<i>xylO0309</i>	TGTTGGCGCTACCA
<i>xylO0116</i>	TGTTAGCGCTACTA
<i>xylO0114</i>	TGTTGGCGCTACCA
<i>xylO</i> motif	TGTTAGCGCTACCA

B

-35 BOX	<i>xylO</i> site	-10 BOX	+1
AACCTACTTGCCGTCCCCACATGTTAGCGCTACCAAGTGCCGACGAACGCGCGC			
		SD	START
CGCCGACGGTGTCTGGCGCTTCAGACGCTCGAGTTTTGGGGAGACGACGCCGTG			

Figure 9: Overview of *xylO* suppressor mutations

Independently isolated point mutations in the upstream region of *xylX* were mapped to a 14 bp nearly palindromic region, palindromic sites (7th and 10th position) that were not mutated are framed, mutated residues are high lighten in red (A). the xylose operator *xylO* overlaps with the annotated -10 Box of the xylose dependent promoter of *xylX* (B).

The genetically defined *xylO* element provided an excellent opportunity to predict other putative members of the xylose regulon. 14 putative *xylR* binding sites were detected by blastn search whereof 12 were located in intergenic regions of the *C. crescentus* genome (Figure 10). To validate these predicted *xylO* elements *in vivo* and define further XylR controlled genes, the global transcriptome of wt and *xylR* mutant was compared.

Microarray analysis revealed that over 30 genes were at least 3-fold derepressed in a *xylR* mutant strain compared to wild type (Table 2), including the *xylXABCD* operon and two additional genes from this gene cluster, which were strongly up regulated (3-40 fold) confirming the *xylX::lacZ*

reporter studies. In addition, 4 genes (CC0505, CC2152, CC2804 and CC2805) harboring a predicted *xyIO* element in their upstream region, were 2-4 fold stronger expressed in the *xyIR::Tn5* mutant background (Figure 10).

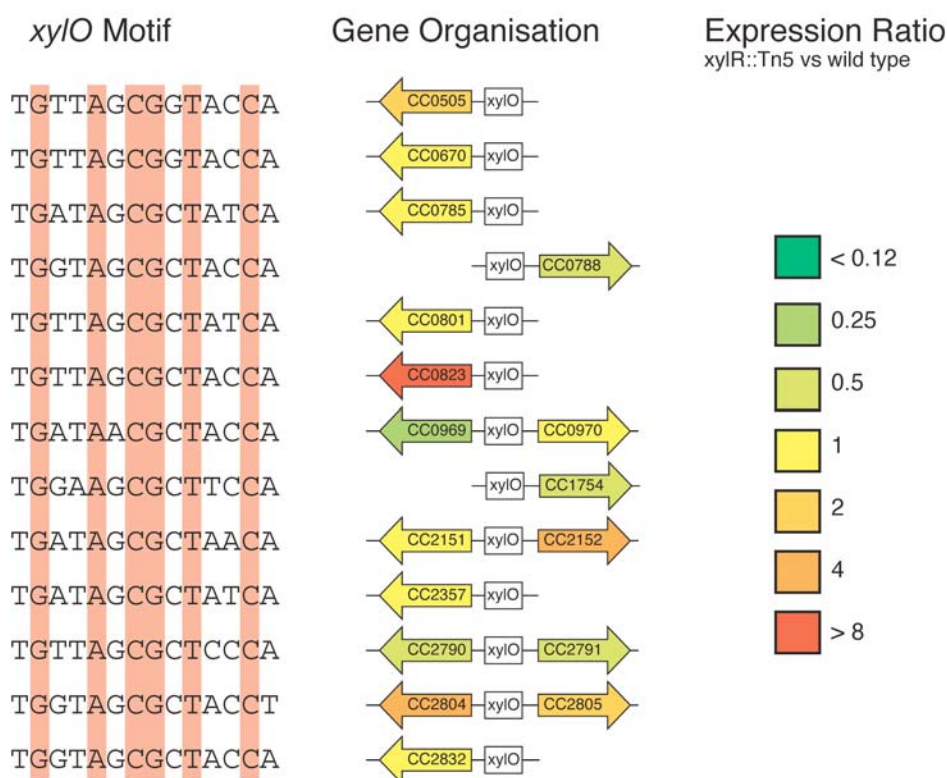


Figure 10: predicted *xyIO* elements

Putative *xyIO* boxes were identified based on following assumptions: 1) the genetically defined critical residues for *xyIR* binding should be 100% conserved (highlighted in Red), 2) other nucleotides in the putative *xyIO* box should show 80% similarity to the *xyIO* motif upstream of *xyIX*. 3) The putative *xyIO* box should be located not more that 400bp upstream of an annotated gene. The ratio of expression change, as determined by MA analysis. is color coded according to the left panel.

The exact role of CC0505, CC2152, CC2804 and CC2805 in xylose metabolism remains to be determined. These findings argue that XylR not only acts as a repressor of the *xyIXABCD* operon but in addition adjusts the expression of other genes of the xylose regulon. Based on the presented genetic, bioinformatic and microarray data we propose the following model: The xylose repressor XylR binds as a dimer to the xylose operator site when xylose is absent and prevents RNA-polymerase from binding to the promoter region. If xylose is present XylR no longer binds to *xyIO* allowing transcription initiation (Figure 11). Biochemical foot printing analysis and mobility shift experiments with the purified XylR repressor could be useful to verify and refine the proposed

model and enable the accurate design of a tight xylose inducible expression system for *C. crescentus*.

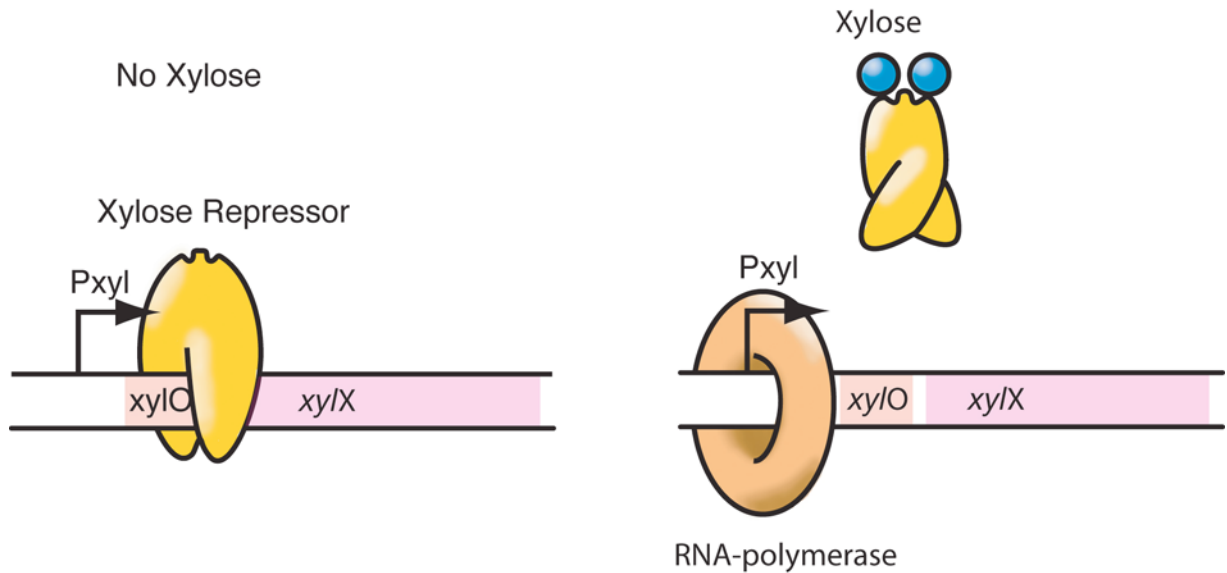


Figure 11: Model for xylose dependent repression of the *xyI**XABCD* operon:

The xylose repressor XylR (in yellow) binds as a dimer to the xylose operator (*xyI/O*) site when xylose is absent and prevents RNA-polymerase from transcription initiation. Only if xylose is present, XylR no longer binds to *xyI/O* and RNA polymerase (in fawn) starts transcribing the xylose regulon

Table 2: Global transcriptom comparison of *xylR*::Tn5 mutant strain versus a *xylR* wild type strain

Xylose Metabolism and Regulation

Name	allele	function	ration ¹
CC0821	<i>xyIB</i>	Xylonate dehydratase	42.4
CC0822	<i>xyIA</i>	a-Ketoglutaric semialdehyde dehydrogenase	32
CC0823	<i>xyIX</i>	hypothetical protein	10.1
CC0814	-	MFS transporter, sugar:H ⁺ symporter	8.3
CC0819	<i>xyID</i>	Xylonate dehydratase	6.7
CC0820	<i>xyIC</i>	Xylonolactonase	5.3

Sugar metabolism Pathway Genes

Name	allele	function	ration
CC2057	<i>zwf</i>	glucose-6-phosphate 1-dehydrogenase	9
CC3054	<i>xarB</i>	xylosidase/arabinosidase	6.8
CC2055	<i>edd</i>	phosphogluconate dehydratase	6.4
CC1724	<i>eno</i>	enolase	3.2
CC2056	<i>pgl</i>	6-phospho-glucono-lactonase	2.7

Other genes

Name	allele	function	ration
CC0874	-	conserved hypothetical protein	6.8
CC3028	-	transcriptional regulator, ArsR family	6.8
CC3079	-	hypothetical protein	6.8
CC3663	-	conserved hypothetical protein	6.8
CC3681	-	putative tellurium resistance protein	6.8
CC0536	-	GntR family transcriptional regulator	6.6
CC0682	-	hypothetical protein	6.4
CC0718	-	hypothetical protein	6.2
CC2838	-	hypothetical protein	6.1
CC0163	-	hypothetical protei	4.3
CC0366	<i>atpF'</i>	ATP synthase F0, B' subunit	4.1
CC1343	-	hypothetical protein	3.9
CC2804	-	TonB-dependent receptor	3.9
CC0360	-	putative ornithine decarboxylase	3.5
CC1344	-	FF domain protein	3.4
CC2152	-	hypothetical protein	3.3
CC3063	-	sulfite reductase (NADPH	0.06

¹ Ratio: *xylR*::Tn5 versus wildtype

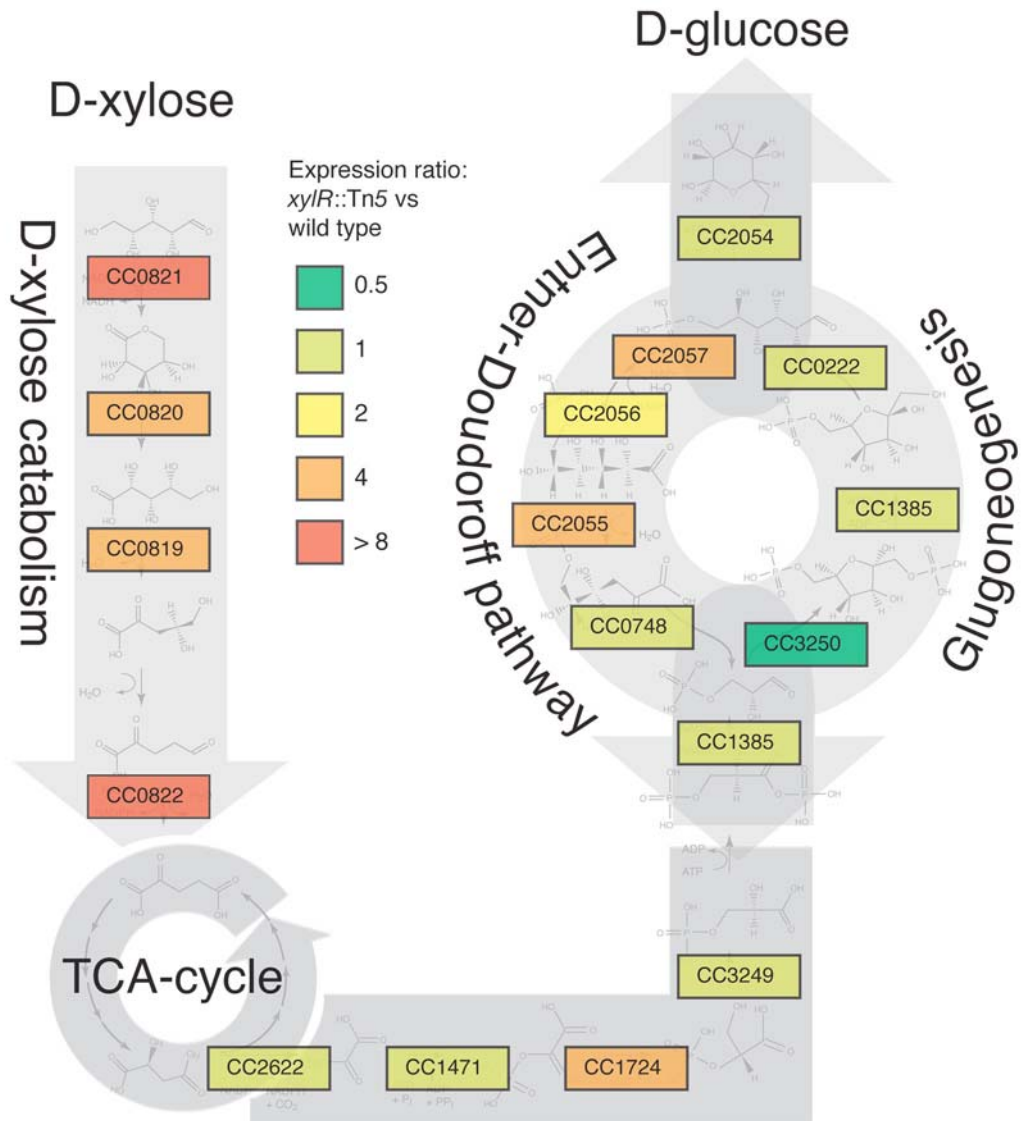


Figure 12: Effect of *xyIR* on expression of sugar conversion pathways genes:

Beside the *xyIXABCD* operon, genes defining the Entner-Doudoroff pathway are up regulated in a *xyIR* mutant strain compared to wild type grown on PYE.

4.2.3 Material and Methods

*Construction of a conditional *clpX* mutant strain* - Two artificial xylose auxotrophic strains (UJ200 and UJ270, (74)) were constructed by inserting either the suicide plasmid pUJ174 (Tet) or pUJ167 (Km), both carrying a translational *clpX* fusion to the first 18 base pairs of *xyIX*, into the *xyIX* locus and deleting the chromosomal wild type *clpX* locus as described in (74).

*Transposon mutagenesis to define the xylose repressor *xyIR** - The miniTn5 Transposon was delivered on a suicide plasmid (pUT_Km1) into UJ200 by conjugation. Transposon insertion mutants were selected on PYE plates supplemented with nalidixic acid (20µg/ml) and kanamycin (20µg/ml). Potential *xyIR*::Tn5 insertions were verified by transducing the Tn5 marker into strain LS1280 harboring a *xyIX*::*gusA* insertion and assaying for glucuronidase activity in the absence of xylose. The Tn5 insertion site of transductants with derepressed *gusA* were mapped by cycle sequencing out of the Tn5 with primer 699 (5'-TAC CGA GCT CGA ATT CGG-3') using genomic DNA as template.

*Isolation of suppressor mutations in *xyIO** - Spontaneous xylose independent mutants were isolated by plating 10^8 - 10^9 cells to PYE plates lacking xylose. Point mutations in *xyIO* that disable binding of XylR were expected to be rare compared to spontaneous *xyIR* loss of function mutations. To distinguish between these 2 classes, spontaneous xylose-independent-mutants were transduced into strain UJ200 in a chromosomal linkage cross using the tetracycline resistance of the inserted pUJ174 as a *xyIO* linked selection marker. Xylose-independent, tetracycline-resistant colonies were isolated and suppressor mutations in *xyIO* were identified by PCR amplifying their *xyIX* promoter region using primers 920 (5'-CAG GTC GTC GTG GTC CAG CA-3') and 921 (5'-CCA GGA CTT CGC AGA TTT CG-3') and sequencing the PCR product using primer 922 (5'-CTT TCC GCA GAA AGA GCA GT-3').

*β-galactosidase activity assay of *xyIX*::*lacZ* reporter strains* - Three independent *xyIR*::Tn5 insertions were transduced with phage CR30 into NA1000 wild type strain carrying a *xyIX*::*lacZ* fusion on plasmid pCS225 (73). LacZ activity was determined by the standard Miller assay and compared to NA1000 / pCS225 wild type strain in presence or absence of xylose and glucose. Background *lacZ* activity of *C. crescentus* was determined using a NA1000 wild type strain harboring a nontranscribed *lacZ* copy on plasmid pLac290.

Microarray analysis - mRNA of *C. crescentus* wild type strain and a *xyIR*::Tn5 mutant strain was extracted from PYE log phase cultures with RNeasy Kit (Roche). mRNA was reverse transcribed

by Superscript II Kit (Invitrogen) and direct labeled with either Cy3-dCTP or Cy5-dCTP. mRNA was degraded via NaOH hydrolysis and cDNA was purified over a QiaQuick column (Qiagen). Labeled cDNA from both conditions were hybridized onto oligo based *C. crescentus* Microarray slides and analyzed as reported in (75).

5 Discussion

Cellular homeostasis requires the ability to react on environmental and physiological changes continuously with metabolic and developmental adjustments. Therefore signaling cascades have to sense external and internal signals by a wide variety of receptors and transmit information to regulatory components that accomplish an adequate cellular response. Frequently receptors do not directly interact with their downstream regulators but instead affect the synthesis and turnover of small diffusible molecules called second messengers. This signaling principle allows information propagation between spatially separated signaling components and enable beside signal integration also signal amplification. Beside the well described cAMP and ppGpp signaling systems involved in carbon source catabolism (6) and stringent response (7,8), bacteria widely use the nucleotide derivative c-di-GMP as a second messenger to orchestrate biofilm formation (46,57,62,76,77). Based on our recent data and findings, we will postulate a comprehensive c-di-GMP signaling model, provide insights into essential signaling components on a molecular level and discuss general principles of signal conversion, signal transduction and modulation.

c-di-GMP is synthesized by diguanylate cyclases – Biochemical and structural studies demonstrated that the GGDEF domain harbors diguanylate cyclase activity (26,45) and perform the condensation of two GTP molecules into c-di-GMP. Like guanylate and adenylate cyclases (GC, AC), DGC's possess a similar domain architecture but in contrast to, catalyse the intramolecular nucleophilic attack of the 3' hydroxyl group on the α -phosphate of a nucleoside triphosphate. While AC's and GC's build heterodimers, DGC's form homodimers, with a GTP molecule bound within the catalytic core of each DGC monomer. Residues of the highly conserved GGDEF motif and a close by Asp on the opposing β -sheet, form the enzymatic active-site (A-site) by coordinating two Mg^{2+} cations involved in catalysis (26,45).

c-di-GMP specific phosphodiesterase hydrolyse c-di-GMP – Intracellular signaling molecule should only be transiently present if a perceived stimuli afore has activated the corresponding signaling pathway. Therefore signal inactivation is a fundamental principle of signaling cascades crucial for information transfer. We showed that CC3396, a GGDEF-EAL composite protein of *C. crescentus* harbors c-di-GMP-specific phosphodiesterase (PDE) activity and catalyse the cleavage of c-di-GMP into the linear dinucleotide pGpG. Biochemical characterization of the individual domains demonstrated that the PDE activity of CC3396, responsible for second messenger inactivation, is confined to the C-terminal EAL domain, and does not dependent on the physical presence of the N-terminal GGDEF domain (59). The solved crystal structure of Ykul from *B.subtilis* suggested that

the EAL domain possess a TIM barrel fold consisting of eight α -helices and eight parallel β -strands alternating along the peptide backbone . The active site, catalyzing the Mg^{2+} dependent hydrolysis of c-di-GMP, is presumably located in the central core and build by the EAL motif and other nearby located negatively charged residues.

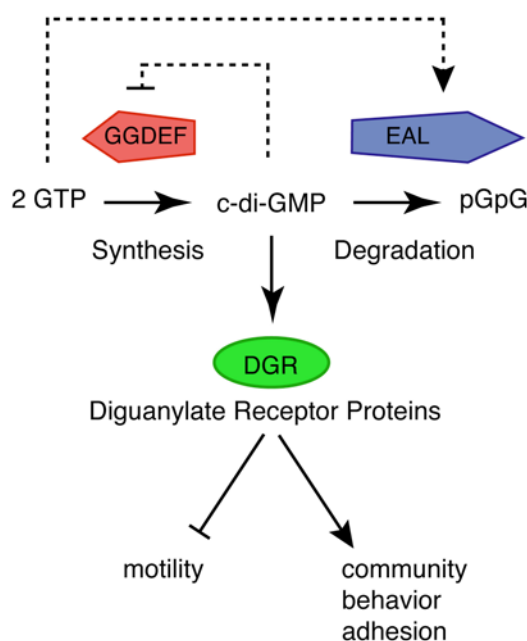


Figure 13: Overview of the c-di-GMP signaling pathway

Synthesis of c-di-GMP out of two GTP is catalyzed by diguanylate cyclases activity residing within the GGDEF domain (in red) and degraded by the action of c-di-GMP-specific phosphodiesterases activity constrained to the EAL, domain (in blue) into the linear dinucleotide pGpG respectively. The second messenger is sensed via a diguanylate receptor (DGR) module (in green) that mediate diverse output functions as inhibition of flagellar motor function and activation of EPS synthesis.

Allosteric control mechanisms - The existence of multiple GGDEF and EAL domain proteins within the same bacterial species and the occurrence of GGDEF-EAL composite proteins pose the question how c-di-GMP turnover is regulated and wasteful hydrolysis of GTP is circumvented. Often GGDEF and EAL domains are fused to various sensory domains arguing that the activity of both DGC's and PDE's are tightly controlled by diverse signaling input. In principles a perceived stimuli could either modulate DGC or PDE activity by lowering the substrate affinity, induce conformational changes that liberate the catalytic pocket or in the case of DGC's change dimerization properties. Furthermore the c-di-GMP circuitry has adopted allosteric regulation and feedback control mechanisms that link the degradation of c-di-GMP to the cellular GTP pool or increase signaling robustness.

Diguanylate cyclases are subjected to allosteric feedback inhibition - We showed by genetic, biochemical and bioinformatic approaches that noncompetitive product inhibition is a general regulatory principle of DGC's. High affinity binding of c-di-GMP to an inhibition site (I-site) distant from the catalytic pocket efficiently blocks enzymatic activity. The I-site pocket is formed by a conserved RXXD motif whereby the Arg and Asp residue participate directly in ligand recognition. The RXXD motif is positioned within a turn at the end of a short five amino acid β -sheet that directly connects the I-site with the conserved catalytic GGDEF motif. Molecular dynamic calculation supported the idea that balance like movements of the interconnecting five amino acid β -sheet cause, upon binding of c-di-GMP at the I-site, a repositioning of active site residues and thereby possibly alter DGC activity. The fact that the I-site motif is highly conserved among GGDEF domain proteins with biochemically verified DGC activity argues that negative feedback inhibition is a regulatory key feature of DGC's (78). Using highly active DGC's with an implemented negative feedback loop could potentially increase signaling robustness, decrease the rise-time of the signaling system and enable accurate adjustment of the intracellular second messenger concentration.

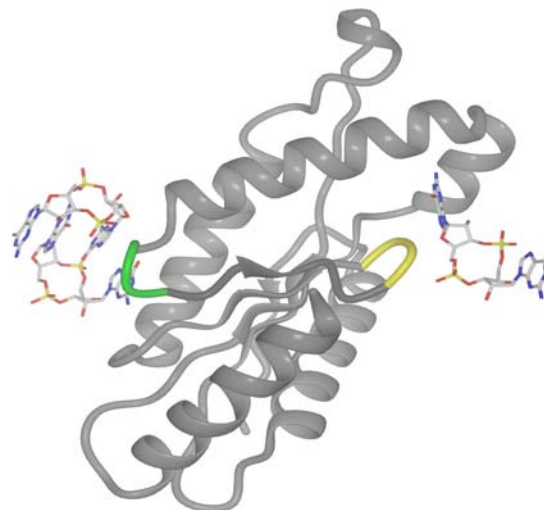


Figure 14: Model for the allosteric feedback inhibition of DGC's

Binding of a c-di-GMP dimer to the I-site motif RXXD (green) cause structural changes at the active site loop (gold) through balance like rearrangement of the interconnecting 5 amino acid spanning β -sheet.

c-di-GMP specific phosphodiesterase activity is regulated by GTP - Beside DGC's also PDE enzymes are subjected to an allosteric control mechanism. The biochemical characterization of the PDE CC3396 from *C. crescentus* suggested that a subgroup of the large family of bacterial GGDEF-EAL composite proteins represents PDE's with an associated regulatory GGDEF domain that can act as GTP sensor but has lost DGC activity. Thereby the sensory GGDEF domain activates the neighboring EAL domain, only if the cellular GTP concentration is above a certain threshold level, probably by increasing the K_M for c-di-GMP hydrolysis (59). What could be the regulatory reason to couple PDE activity to the availability of GTP? First, In case both DGC's and PDE's are simultaneously active, the above-mentioned allosteric activation mechanism could circumvent the rapidly exhaustion of the cellular GTP pool. Second, a drastic drop of the GTP concentration could lead to a rapid and substantial increase of the cellular c-di-GMP concentration. This would provide the opportunity to cross connect the c-di-GMP signaling system with other signaling systems, as for example the stringent response, known to affect the cellular GTP pool.

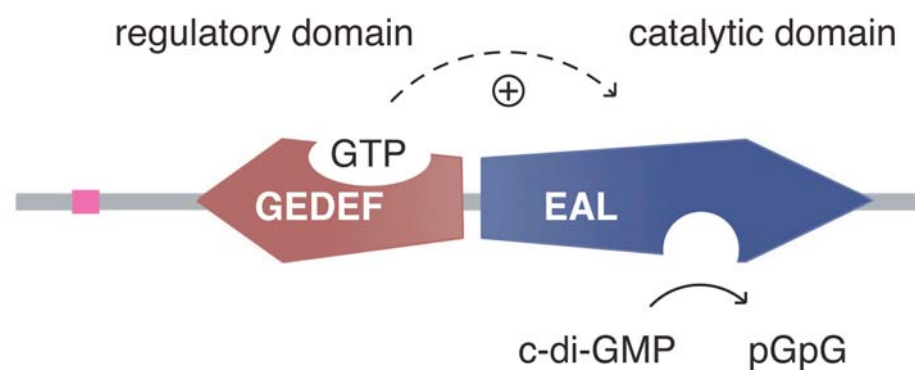


Figure 15: Model for the allosteric regulation of PDE activity by GTP

The PDE activity of CC3396 is fully comprised within the EAL domain. The associated, enzymatic inactive, GGDEF domain with its altered active site motif (GEDEF) mediates allosteric activation of the C-terminal PDE by GTP.

Diguanylate receptor proteins sense the intracellular c-di-GMP concentration - C-di-GMP influences flagellar motility as a function of growth (79) or adaptation to surfaces (22), affects pili assembly (80), and controls the production of surface structures like fimbria and exopolysaccharide matrices (62,81-83). The wide variety of cellular functions that are orchestrated by c-di-GMP calls for divergent signaling output architecture and multiple receptors. Using affinity chromatography we have isolated several c-di-GMP binding proteins from *C. crescentus*. One of these proteins, DgrA, is a PilZ homolog and function as a negative regulator of flagellar motility. Whereby the c-di-GMP

bound form of DgrA cause inhibition of flagellar motor function probably over a posttranscriptional mechanism affecting FliL expression . In *C. crescentus* the FliL protein is not part of the flagellar structure but is required for flagellar rotation (84). Biochemical and structural analysis of DgrA and homolog from *C. crescentus*, *S. enterica* and *P. aeruginosa* demonstrated that this family of diguanylate receptor is able to bind specifically an intercalated dimer of c-di-GMP with high affinity.

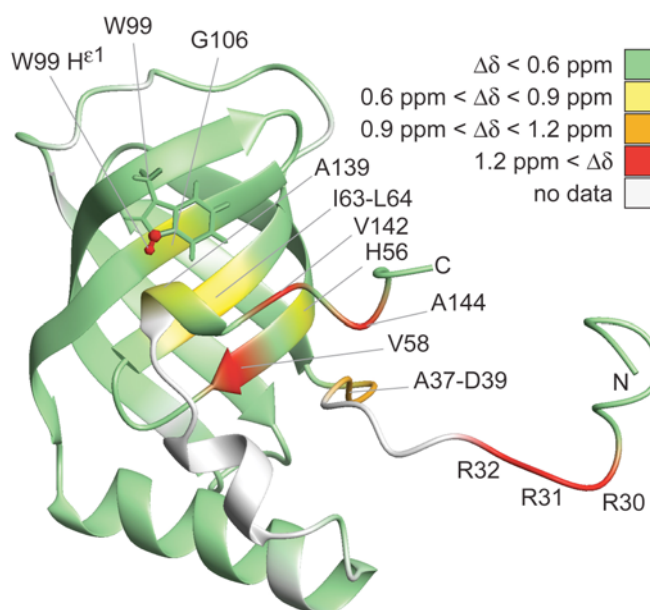


Figure 16: NMR shift map of PA4608 between free and c-di-GMP bound form






Combined amide 1H and 15N shift differences between PA4608 in its free and ligand-bound form are color-coded on the structure of free PA4608 (PDB 1YWU, model 12). Combined chemical shift differences were calculated as

$$\Delta\delta = \sqrt{[(\Delta\delta_H)^2 + ((\Delta\delta_N / 5)^2)] / 2}.$$

NMR and site directed mutagenesis experiments revealed that the diguanylate receptor function is contained within a six-stranded anti-parallel β -barrel flanked by three helices whereby the binding site is probably built by conserved key residues, clustered within a discrete patch at the surface of the β -barrel. C-di-GMP dependent motility control is not unique to *C. crescentus*. Also in *S. enterica* the YcgR protein (85), harboring an N-terminal DgrA-like domain, regulates motor function and specifically binds c-di-GMP, thus suggesting that c-di-GMP dependent motility control is generally exerted via similar diguanylate receptor proteins. Beside inhibition of flagellar based motility, c-di-GMP has also been identified as an activator of EPS production (10,11,23,86-88). Interestingly the DgrA-like c-di-GMP effector module is a component of the glycosyltransferases BcsA and neighboring *alg44* responsible for cellulose respective alginate synthesis in Enterobacteriaceae and Pseudomonades (89). Often multiple versions of this receptor type are encoded within the same

bacteria species either as single domain proteins or fused to a variety of accessory domains, thus giving the possibility to control various output functions in a modular way over a common signal transduction mechanism.

Table 3: Domain organization of diguanylate receptors

Domain Organization	Organism	K_D in nM	ΔK_D	Output function	
	DgrA	<i>C. crescentus</i>	<50	14	motor function
	DgrB	<i>C. crescentus</i>	132	36	motor function
	PA4608	<i>P. aeruginosa</i>	<50	27	unknown
	YcgR	<i>S. enterica</i>	182	29	motor function
	BcsA	<i>S. enterica</i>	N.D		cellulose synthesis

K_D = binding constant for c-di-GMP in nM

Flexibility of c-di-GMP signaling – Often bacteria encode multiple DGC and PDE enzymes and possess several DgrA-like effectors. In principle two different signaling architectures could be used to transfer information. In a first model, different stimuli would be perceived and integrated by a convergent signaling architecture. Thereby the input information from different DGC's or PDE's could not be discerned and the diguanylate receptors would only sense the overall cellular level of c-di-GMP. In a second signaling model, subsets of DGC's and PDE's would process information in parallel pathways only toward discrete receptors. For instance DGC's characterized by different product inhibition constants could be used to increase stepwise the cellular c-di-GMP level. Depending on different binding affinities, various diguanylate receptors could be consecutively activated. Furthermore, allosteric regulation mechanisms could also be adopted to convert stimuli information into oscillating c-di-GMP levels whereby certain diguanylate receptors would only respond to defined frequency modes. Alternative recognition specificity could be achieved if c-di-GMP is directly delivered from DGC's to specific receptors but would require specially restricted

signaling systems. Further studies will be used to discriminate between these models and will unravel the complexity of c-di-GMP signaling systems.

6 Outlooks

The presented studies allow for the first time a detailed view on fundamental aspects and mechanisms of the c-di-GMP signaling circuitry. Beside the characterization of key components regulating c-di-GMP turnover and the specification of all relevant protein ligand interactions on a molecular level we describe a diguanylate receptor module involved in sensing the intracellular c-di-GMP concentration and mediating diverse output functions. To acquire a profound understanding about signal transduction, signal specificity and cross connectivity to other signaling systems, and to determine the role of c-di-GMP signaling in virulence, it will be crucial to implement our established genetic and biochemical tools on various model organisms and address the following outstanding questions:

- What kind of stimuli are perceived and integrated by the c-di-GMP signaling network?
- How are DGC's and PDE's activated in general?
- Do bifunctional composite GGDEF-EAL domain proteins exist, what is their activation mode?
- Are other enzymes involved in c-di-GMP metabolism?
- Do beside the DgrA-like receptors also other c-di-GMP effectors exist?
- What is the function of catalytically inactive EAL and GGDEF domains?
- What is the underlying signaling architecture of the c-di-GMP signaling circuitry, do parallel signal transduction pathway exist, how signal specificity is ensured?
- What is the output function of DgrA-like receptors. Do these receptors mediate protein-protein interactions? What is the nature of interaction partners?
- What is the spacial organization of DGC, PDE and DGR components?
- How does the c-di-GMP signaling cascade affect the cellular nucleotide pool?
- How are other signaling cascades cross connected to the c-di-GMP system.
- How does the second messenger c-di-GMP orchestrate biofilm formation and affect virulence of pathogenic bacteria.

7 Appendix

List of Strains

Strain	Genotype	Reference
BC425	<i>S. enterica</i> LT2 <i>trp::T7RNAP</i>	Christen unpublished
BC428	<i>E. coli</i> S17-1/ pAS22:: <i>pdeA</i>	Christen et al 2005, JBC
BC430	<i>E. coli</i> S17-1/ pNPTS138:: <i>KO</i> <i>dgcA</i>	Christen et al 2006, JBC
BC431	<i>E. coli</i> S17-1/ pNPTS138:: <i>KO</i> <i>pdeA</i>	Christen et al 2005, JBC
BC432	<i>E. coli</i> S17-1/ pUJ142:: <i>dgcA</i>	Christen et al 2006, JBC
BC433	<i>E. coli</i> S17-1/ pAS22:: <i>dgcA</i>	Christen et al 2006, JBC
BC434	<i>E. coli</i> S17-1/ pUJ142:: <i>pdeA</i>	Christen et al 2006, JBC
BC478	<i>S. enterica</i> LT2 <i>araBAD::dgcA</i>	Christen et al 2006, JBC
BC480	<i>S. enterica</i> LT2/ pET42b:: <i>dgcA5002-his6</i>	Christen unpublished
BC482	<i>S. enterica</i> LT2 <i>trp::T7RNAP</i> / pET42b:: <i>dgcA5002-his6</i>	Christen unpublished
BC498	<i>S. enterica</i> LT2 <i>araBAD::dgcA bcsA::Tn10dTc</i>	Christen unpublished
BC500	<i>S. enterica</i> LT2 <i>araBAD::dgcA bcsA::Tn10dTc</i>	Christen unpublished
BC506	<i>E. coli</i> BL21(DE3)/ pET42b:: <i>ycgR</i>	Christen et al 2007, PNAS
BC512	<i>E. coli</i> BL21(DE3)/ pET42b:: <i>dgrAD38A</i>	Christen et al 2007, PNAS
BC514	<i>E. coli</i> BL21(DE3)/ pET42b:: <i>dgrARR11AA</i>	Christen et al 2007, PNAS
BC516	<i>E. coli</i> S17-1/ pBBR:: <i>dgrA-his6</i>	Christen et al 2007, PNAS
BC517	<i>E. coli</i> S17-1/ pBBR:: <i>dgrB-his6</i>	Christen et al 2007, PNAS
BC535	<i>C. crescentus</i> CB15ATCC/ pBBR:: <i>dgrA-his6</i>	Christen et al 2007, PNAS
BC538	<i>C. crescentus</i> CB15ATCC/ pBBR:: <i>dgrB-his6</i>	Christen et al 2007, PNAS
BC541	<i>C. crescentus</i> CB15ATCC/ pBBR	Christen et al 2007, PNAS

Strain	Genotype	Reference
BC546	<i>E. coli</i> S17-1/ pNPTS138::KODgrA	Christen et al 2007, PNAS
BC547	<i>E. coli</i> S17-1/ pNPTS138::KODgrB	Christen et al 2007, PNAS
BC548	<i>E. coli</i> DH10B/ pBBR::dgrA-his6	Christen et al 2007, PNAS
BC558	<i>E. coli</i> S17-1/ pBBR::dgrA-his6	Christen et al 2007, PNAS
BC559	<i>E. coli</i> S17-1/ pBBR::dgrB-his6	Christen et al 2007, PNAS
BC562	<i>C. crescentus</i> CB15ATCC Δ dgrB	Christen et al 2007, PNAS
BC568	<i>C. crescentus</i> CB15ATCC Δ dgrA	Christen et al 2007, PNAS
BC680	<i>C. crescentus</i> CB15ATCC Δ dgrA Δ dgrB	Christen et al 2007, PNAS
BC695	<i>S. enterica</i> LT2 <i>trp</i> ::T7RNAP/ pET42b	Christen et al 2006, JBC
BC719	<i>C. crescentus</i> CB15ATCC/ pBBR::dgrAV74A-his6	Christen et al 2007, PNAS
BC777	<i>C. crescentus</i> CB15ATCC/ pUJ142	Christen et al 2007, PNAS
BC779	<i>C. crescentus</i> CB15ATCC/ pAS22::dgrA	Christen et al 2007, PNAS
BC827	<i>E. coli</i> BL21(DE3)/ pET42b::dgrAW75A	Christen et al 2007, PNAS
BC831	<i>E. coli</i> S17-1/ pBBR::dgrAW75A-his6	Christen et al 2007, PNAS
BC834	<i>E. coli</i> S17-1/ pBBR::dgrA-his6	Christen et al 2007, PNAS
BC862	<i>E. coli</i> S17-1/ pBBR::dgrARR11AA-his6	Christen et al 2007, PNAS
BC864	<i>E. coli</i> S17-1/ pBBR::dgrAD41A-his6	Christen et al 2007, PNAS
BC867	<i>E. coli</i> S17-1/ pBBR::dgrAW75A-his6	Christen et al 2007, PNAS
BC871	<i>C. crescentus</i> CB15ATCC/ pUJ142::dgcA	Christen et al 2007, PNAS
BC877	<i>C. crescentus</i> CB15ATCC Δ dgrA/ pUJ142::dgcA	Christen et al 2007, PNAS
BC880	<i>C. crescentus</i> CB15ATCC Δ dgrA/ pAS22::dgcA	Christen et al 2007, PNAS
BC883	<i>C. crescentus</i> CB15ATCC Δ dgrB/ pUJ142::dgcA	Christen et al 2007, PNAS

Strain	Genotype	Reference
BC886	<i>C. crescentus</i> CB15ATCC $\Delta dgrB$ / pAS22:: <i>dgcA</i>	Christen et al 2007, PNAS
BC889	<i>C. crescentus</i> CB15ATCC $\Delta dgrA \Delta dgrB$ / pUJ142:: <i>dgcA</i>	Christen et al 2007, PNAS
BC892	<i>C. crescentus</i> CB15ATCC $\Delta dgrA \Delta dgrB$ / pAS22:: <i>dgcA</i>	Christen et al 2007, PNAS
BC913	<i>E. coli</i> S17-1/ pBBR:: <i>dgrARR11AA-his6</i>	Christen et al 2007, PNAS
BC915	<i>C. crescentus</i> CB15ATCC/ pBBR:: <i>dgrARR11AAV74A-his6</i>	Christen et al 2007, PNAS
BC918	<i>C. crescentus</i> CB15ATCC/ pBBR:: <i>dgrAD38A-his6</i>	Christen et al 2007, PNAS
BC921	<i>C. crescentus</i> CB15ATCC/ pBBR:: <i>dgrAW75A-his6</i>	Christen et al 2007, PNAS
BC939	<i>C. crescentus</i> NA1000 $\Delta recA$ / pBBR:: <i>dgrA-his6</i>	Christen et al 2007, PNAS
BC940	<i>C. crescentus</i> NA1000 $\Delta recA$ / pBBR:: <i>dgrA-his6</i>	Christen et al 2007, PNAS
BC941	<i>C. crescentus</i> NA1000 $\Delta recA$ / pBBR:: <i>dgrA-his6</i>	Christen et al 2007, PNAS
BC942	<i>C. crescentus</i> NA1000 $\Delta recA$ / pBBR:: <i>dgrA-his6</i>	Christen et al 2007, PNAS
BC943	<i>C. crescentus</i> NA1000 $\Delta recA$ / pBBR:: <i>dgrA-his6</i>	Christen et al 2007, PNAS
BC944	<i>C. crescentus</i> NA1000 $\Delta recA$ / pBBR:: <i>dgrA-his6</i>	Christen et al 2007, PNAS
BC945	<i>C. crescentus</i> NA1000 $\Delta recA$ / pBBR:: <i>dgrA-his6</i>	Christen et al 2007, PNAS
BC946	<i>C. crescentus</i> NA1000 $\Delta recA$ / pBBR:: <i>dgrA-his6</i>	Christen et al 2007, PNAS
BC947	<i>C. crescentus</i> NA1000 $\Delta recA$ / pBBR:: <i>dgrA-his6</i>	Christen et al 2007, PNAS
BC948	<i>C. crescentus</i> NA1000 $\Delta recA$ / pBBR:: <i>dgrA-his6</i>	Christen et al 2007, PNAS
BC949	<i>C. crescentus</i> NA1000 $\Delta recA$ / pBBR:: <i>dgrA-his6</i>	Christen et al 2007, PNAS
BC950	<i>C. crescentus</i> NA1000 $\Delta recA$ / pBBR:: <i>dgrA-his6</i>	Christen et al 2007, PNAS
BC951	<i>C. crescentus</i> NA1000 $\Delta recA$ / pBBR:: <i>dgrA-his6</i>	Christen et al 2007, PNAS
BC952	<i>C. crescentus</i> NA1000 $\Delta recA$ / pBBR:: <i>dgrA-his6</i>	Christen et al 2007, PNAS
BC953	<i>C. crescentus</i> NA1000 $\Delta recA$ / pBBR:: <i>dgrA-his6</i>	Christen et al 2007, PNAS

Strain	Genotype	Reference
BC954	<i>C. crescentus</i> NA1000 Δ <i>recA</i> / pBBR:: <i>dgrA-his6</i>	Christen et al 2007, PNAS
BC955	<i>C. crescentus</i> NA1000 Δ <i>recA</i> / pBBR:: <i>dgrA-his6</i>	Christen et al 2007, PNAS
BC956	<i>C. crescentus</i> NA1000 Δ <i>recA</i> / pBBR:: <i>dgrA-his6</i>	Christen et al 2007, PNAS
BC961	<i>C. crescentus</i> CB15ATCC/ pBBR:: <i>dgrAR11AA-his6</i>	Christen et al 2007, PNAS
BC965	<i>E. coli</i> S17-1/ pMR10::CC2058-CC2069	Christen unpublished
BC966	<i>E. coli</i> S17-1/ pMR10::fliLM	Christen unpublished
BC972	<i>C. crescentus</i> NA1000 ::Tn5Tc <i>rpsAH323R</i> / pBBR:: <i>dgrA-his6</i>	Christen et al 2007, PNAS
BC973	<i>C. crescentus</i> NA1000 ::Tn5Tc <i>rpsAH323R</i> / pBBR:: <i>dgrA-his6</i>	Christen et al 2007, PNAS
BC974	<i>C. crescentus</i> NA1000 ::Tn5Tc <i>rpsAH323R</i> / pBBR:: <i>dgrA-his6</i>	Christen et al 2007, PNAS
BC975	<i>C. crescentus</i> NA1000 ::Tn5Tc <i>rpsAH323R</i> / pBBR:: <i>dgrA-his6</i>	Christen et al 2007, PNAS
BC976	<i>C. crescentus</i> NA1000 ::Tn5Tc <i>rpsAH323R</i> / pBBR:: <i>dgrA-his6</i>	Christen et al 2007, PNAS
BC977	<i>C. crescentus</i> NA1000 ::Tn5Tc	Christen et al 2007, PNAS
BC978	<i>C. crescentus</i> NA1000 ::Tn5Tc	Christen et al 2007, PNAS
BC979	<i>C. crescentus</i> NA1000 ::Tn5Tc	Christen et al 2007, PNAS
BC980	<i>C. crescentus</i> NA1000 ::Tn5Tc	Christen et al 2007, PNAS
BC981	<i>C. crescentus</i> NA1000 ::Tn5Tc	Christen et al 2007, PNAS
BC995	<i>E. coli</i> BL21(DE3)/ pET21c:: <i>dgcA</i>	Christen et al 2006, JBC
BC997	<i>E. coli</i> BL21(DE3)/ pET21c:: <i>pdeA</i>	Christen et al 2005, JBC
BC999	<i>E. coli</i> BL21(DE3)/ pET21c:: <i>dgcB</i>	Christen unpublished
BC1000	<i>E. coli</i> BL21(DE3)/ pET21c:: <i>pdpA</i>	Christen unpublished
BC1001	<i>E. coli</i> BL21(DE3)/ pET21c::CC3148	Christen unpublished
BC1002	<i>E. coli</i> BL21(DE3)/ pET15:: <i>pleDΔ1-290</i>	Christen et al 2006, JBC

Strain	Genotype	Reference
BC1003	<i>E. coli</i> BL21(DE3)/ pET21:: <i>pleD</i> Δ 1-290	Christen et al 2006, JBC
BC1004	<i>E. coli</i> BL21(DE3)/ pET21b	Christen et al 2005, JBC
BC1005	<i>E. coli</i> BL21(DE3)/ pET21c	Christen et al 2005, JBC
BC1007	<i>E. coli</i> BL21(DE3)	Christen unpublished
BC1008	<i>E. coli</i> BL21(DE3)/ pET42b:: <i>pdeAE323Q</i>	Christen et al 2005, JBC
BC1009	<i>E. coli</i> BL21(DE3)/ pET21c:: <i>pdeAED213QN</i>	Christen et al 2005, JBC
BC1010	<i>E. coli</i> BL21(DE3)/ pET21c:: <i>pdeA</i> thrb	Christen et al 2005, JBC
BC1011	<i>E. coli</i> BL21(DE3)/ pET21c:: <i>pdeA</i> Δ 1-112	Christen et al 2005, JBC
BC1012	<i>E. coli</i> BL21(DE3)/ pET21c:: <i>pdeA</i> hybrid	Christen unpublished
BC1013	<i>E. coli</i> BL21(DE3)/ pET21c:: <i>dgrA</i>	Christen et al 2007, PNAS
BC1014	<i>E. coli</i> BL21(DE3)/ pET21c:: <i>dgrB</i>	Christen et al 2007, PNAS
BC1015	<i>E. coli</i> BL21(DE3)/ pET15::PA4608	Christen unpublished
BC1016	<i>E. coli</i> BL21(DE3)/ pET21::CC0095short	Christen unpublished
BC1017	<i>E. coli</i> BL21(DE3)/ pET21c:: <i>flmA</i> short	Christen unpublished
BC1018	<i>E. coli</i> BL21(DE3)/ pET21c:: <i>ppx</i>	Christen unpublished
BC1019	<i>E. coli</i> BL21(DE3)/ pET42b:: <i>cheYII</i>	Christen unpublished
BC1020	<i>E. coli</i> BL21(DE3)/ pET42b:: <i>flmA</i>	Christen unpublished
BC1021	<i>E. coli</i> BL21(DE3)/ pET42b:: <i>pdeB</i>	Christen unpublished
BC1022	<i>E. coli</i> BL21(DE3)/ pET42b:: <i>dgcA0207</i>	Christen et al 2006, JBC
BC1023	<i>E. coli</i> BL21(DE3)/ pET42b:: <i>dgcA0230</i>	Christen et al 2006, JBC
BC1024	<i>E. coli</i> BL21(DE3)/ pET42b:: <i>dgcA0244</i>	Christen et al 2006, JBC
BC1025	<i>E. coli</i> BL21(DE3)/ pET42b:: <i>dgcA0306</i>	Christen et al 2006, JBC

Strain	Genotype	Reference
BC1026	<i>E. coli</i> BL21(DE3)/ pET42b:: <i>dgcA0347</i>	Christen et al 2006, JBC
BC1027	<i>E. coli</i> BL21(DE3)/ pET42b:: <i>dgcA0427</i>	Christen et al 2006, JBC
BC1028	<i>E. coli</i> BL21(DE3)/ pET42b:: <i>dgcA0613</i>	Christen et al 2006, JBC
BC1029	<i>E. coli</i> BL21(DE3)/ pET42b:: <i>dgcA0617</i>	Christen et al 2006, JBC
BC1030	<i>E. coli</i> BL21(DE3)/ pET42b:: <i>dgcA0642</i>	Christen et al 2006, JBC
BC1031	<i>E. coli</i> BL21(DE3)/ pET42b:: <i>dgcA0646</i>	Christen et al 2006, JBC
BC1032	<i>E. coli</i> BL21(DE3)/ pET42b:: <i>dgcA0913</i>	Christen et al 2006, JBC
BC1033	<i>E. coli</i> BL21(DE3)/ pET42b:: <i>dgcA1007</i>	Christen et al 2006, JBC
BC1034	<i>E. coli</i> BL21(DE3)/ pET42b:: <i>dgcA1040</i>	Christen et al 2006, JBC
BC1035	<i>E. coli</i> BL21(DE3)/ pET42b:: <i>dgcA1229</i>	Christen et al 2006, JBC
BC1036	<i>E. coli</i> BL21(DE3)/ pET42b:: <i>dgcA1230</i>	Christen et al 2006, JBC
BC1037	<i>E. coli</i> BL21(DE3)/ pET42b:: <i>dgcA1231</i>	Christen et al 2006, JBC
BC1038	<i>E. coli</i> BL21(DE3)/ pET42b:: <i>dgcA1300</i>	Christen et al 2006, JBC
BC1039	<i>E. coli</i> BL21(DE3)/ pET42b:: <i>dgcA1301</i>	Christen et al 2006, JBC
BC1040	<i>E. coli</i> BL21(DE3)/ pET42b:: <i>dgcA1307</i>	Christen et al 2006, JBC
BC1041	<i>E. coli</i> BL21(DE3)/ pET42b:: <i>dgcA1311</i>	Christen et al 2006, JBC
BC1043	<i>E. coli</i> BL21(DE3)/ pET42b:: <i>dgcA1406</i>	Christen et al 2006, JBC
BC1044	<i>E. coli</i> BL21(DE3)/ pET42b:: <i>dgcA1524</i>	Christen et al 2006, JBC
BC1045	<i>E. coli</i> BL21(DE3)/ pET42b:: <i>dgcA1529</i>	Christen et al 2006, JBC
BC1046	<i>E. coli</i> BL21(DE3)/ pET42b:: <i>dgcA1724</i>	Christen et al 2006, JBC
BC1047	<i>E. coli</i> BL21(DE3)/ pET42b:: <i>dgcA1733</i>	Christen et al 2006, JBC
BC1048	<i>E. coli</i> BL21(DE3)/ pET42b:: <i>dgcA1840</i>	Christen et al 2006, JBC

Strain	Genotype	Reference
BC1049	<i>E. coli</i> BL21(DE3)/ pET42b:: <i>dgcA3011</i>	Christen et al 2006, JBC
BC1050	<i>E. coli</i> BL21(DE3)/ pET42b:: <i>dgcA3016</i>	Christen et al 2006, JBC
BC1051	<i>E. coli</i> BL21(DE3)/ pET42b:: <i>dgcA3018</i>	Christen et al 2006, JBC
BC1052	<i>E. coli</i> BL21(DE3)/ pET42b:: <i>dgcA3123</i>	Christen et al 2006, JBC
BC1053	<i>E. coli</i> BL21(DE3)/ pET42b:: <i>dgcA3200</i>	Christen et al 2006, JBC
BC1054	<i>E. coli</i> BL21(DE3)/ pET42b:: <i>dgcA3203</i>	Christen et al 2006, JBC
BC1055	<i>E. coli</i> BL21(DE3)/ pET42b:: <i>dgcA0751</i>	Christen et al 2006, JBC
BC1056	<i>E. coli</i> BL21(DE3)/ pET42b:: <i>dgcA1250</i>	Christen et al 2006, JBC
BC1057	<i>E. coli</i> BL21(DE3)/ pET42b:: <i>dgcA2006</i>	Christen et al 2006, JBC
BC1058	<i>E. coli</i> BL21(DE3)/ pET42b:: <i>dgcAwt</i>	Christen et al 2006, JBC
BC1059	<i>E. coli</i> BL21(DE3)/ pET42b:: <i>dgcAΔRES</i>	Christen et al 2006, JBC
BC1060	<i>E. coli</i> S17-1/ pPHU281:: <i>filLM</i>	Christen unpublished
BC1110	<i>C. crescentus</i> CB15ATCC <i>dgrAW75A</i>	Christen et al 2007, PNAS
BC1113	<i>C. crescentus</i> CB15ATCC <i>dgrAW75A</i> / pUJ142:: <i>dgcA</i>	Christen et al 2007, PNAS
BC1116	<i>C. crescentus</i> CB15ATCC <i>dgrAW75A</i> / pAS22:: <i>dgcA</i>	Christen et al 2007, PNAS
BC1119	<i>S. enterica</i> LT2 P _{BAD} :: <i>dgcA bcsC</i> ::Tn10dTc (<i>rcv1030</i>)	Christen unpublished
BC1120	<i>S. enterica</i> LT2 P _{BAD} :: <i>dgcA yhjS</i> ::Tn10dTc (<i>rcv1041</i>)	Christen unpublished
BC1121	<i>S. enterica</i> LT2 P _{BAD} :: <i>dgcA yhjS</i> ::Tn10dTc (<i>rcv1122</i>)	Christen unpublished
BC1122	<i>S. enterica</i> LT2 P _{BAD} :: <i>dgcA yhjR</i> ::Tn10dTc (<i>rcv1133</i>)	Christen unpublished
BC1123	<i>S. enterica</i> LT2 P _{BAD} :: <i>dgcA bcsA</i> ::Tn10dTc (<i>rcv1141</i>)	Christen unpublished
BC1124	<i>S. enterica</i> LT2 P _{BAD} :: <i>dgcA bcsA</i> ::Tn10dTc (<i>rcv1151</i>)	Christen unpublished
BC1125	<i>S. enterica</i> LT2 P _{BAD} :: <i>dgcA bcsB</i> ::Tn10dTc (<i>rcv1161</i>)	Christen unpublished

Strain	Genotype	Reference
BC1126	<i>S. enterica</i> LT2 P _{BAD} :: <i>dgcA bcsA</i> ::Tn10dTc (<i>rcv1170</i>)	Christen unpublished
BC1127	<i>S. enterica</i> LT2 P _{BAD} :: <i>dgcA bcsB</i> ::Tn10dTc (<i>rcv1132</i>)	Christen unpublished
BC1128	<i>S. enterica</i> LT2 P _{BAD} :: <i>dgcA stm4098</i> ::Tn10dTc (<i>rcv1191</i>)	Christen unpublished
BC1130	<i>S. enterica</i> LT2 P _{BAD} :: <i>dgcA stm4098</i> ::Tn10dTc (<i>rcv1132</i>)	Christen unpublished
UJ2505	<i>C. crescentus</i> NA1000 <i>clpX</i> :: Ω <i>xyiX</i> :: <i>pUJ175 xyiR0012</i> ::Tn5	Christen unpublished
UJ2506	<i>C. crescentus</i> NA1000 <i>clpX</i> :: Ω <i>xyiX</i> :: <i>pUJ175 xyiR0042</i> ::Tn5	Christen unpublished
UJ2507	<i>C. crescentus</i> NA1000 <i>clpX</i> :: Ω <i>xyiX</i> :: <i>pUJ175 xyiR0046</i> ::Tn5	Christen unpublished
UJ2510	<i>C. crescentus</i> NA1000 <i>clpX</i> :: Ω <i>xyiX</i> :: <i>pUJ175 xyiO0304</i>	Christen unpublished
UJ2511	<i>C. crescentus</i> NA1000 <i>clpX</i> :: Ω <i>xyiX</i> :: <i>pUJ175 xyiO0305</i>	Christen unpublished
UJ2512	<i>C. crescentus</i> NA1000 <i>clpX</i> :: Ω <i>xyiX</i> :: <i>pUJ175 xyiO0512</i>	Christen unpublished
UJ2513	<i>C. crescentus</i> NA1000 <i>clpX</i> :: Ω <i>xyiX</i> :: <i>pUJ175 xyiO0601</i>	Christen unpublished
UJ2514	<i>C. crescentus</i> NA1000 <i>clpX</i> :: Ω <i>xyiX</i> :: <i>pUJ175 xyiO0607</i>	Christen unpublished
UJ2515	<i>C. crescentus</i> NA1000 <i>clpX</i> :: Ω <i>xyiX</i> :: <i>pUJ175 xyiO0612</i>	Christen unpublished
UJ3000	<i>C. crescentus</i> NA1000 / <i>pCS225</i>	Christen unpublished
UJ3002	<i>C. crescentus</i> NA1000 <i>xyiR0012</i> ::Tn5 / <i>pCS225</i>	Christen unpublished
UJ3003	<i>C. crescentus</i> NA1000 <i>xyiR0042</i> ::Tn5 / <i>pCS225</i>	Christen unpublished
UJ3004	<i>C. crescentus</i> NA1000 <i>xyiR0046</i> ::Tn5 / <i>pCS225</i>	Christen unpublished

References

1. Benenson, Y., Paz-Elizur, T., Adar, R., Keinan, E., Livneh, Z., and Shapiro, E. (2001) *Nature* **414**(6862), 430-434
2. Ulrich, L. E., Koonin, E. V., and Zhulin, I. B. (2005) *Trends Microbiol* **13**(2), 52-56
3. Stock, A. M., Robinson, V. L., and Goudreau, P. N. (2000) *Annu Rev Biochem* **69**, 183-215
4. Lucas, K. A., Pitari, G. M., Kazerounian, S., Ruiz-Stewart, I., Park, J., Schulz, S., Chepenik, K. P., and Waldman, S. A. (2000) *Pharmacol Rev* **52**(3), 375-414
5. Schwartz, J. H. (2001) *Proc Natl Acad Sci U S A* **98**(24), 13482-13484
6. Harman, J. G. (2001) *Biochimica Et Biophysica Acta-Protein Structure and Molecular Enzymology* **1547**(1), 1-17
7. Reiness, G., Yang, H. L., Zubay, G., and Cashel, M. (1975) *Proceedings of the National Academy of Sciences of the United States of America* **72**(8), 2881-2885
8. Paul, B. J., Berkmen, M. B., and Gourse, R. L. (2005) *Proceedings of the National Academy of Sciences of the United States of America* **102**(22), 7823-7828
9. Jenal, U. (2004) *Curr Opin Microbiol* **7**(2), 185-191
10. Ross, P., Aloni, Y., Weinhouse, H., Michaeli, D., Weinberger-Ohana, P., Meyer, R., and Benziman, M. (1985) *FEBS Lett* **186**(2), 191-196
11. Ross, P., Aloni, Y., Weinhouse, H., Michaeli, D., Weinberger-Ohana, P., Mayer, R., and Benziman, M. (1986) *Carbohydrate Research* **149**(1), 101-117
12. Benziman, M., Aloni, Y., and Delmer, D. (1983) *Journal of Applied Polymer Science: Applied Polymer Symposium (1983)* **37**, 131-143
13. Tal, R., Wong, H. C., Calhoon, R., Gelfand, D., Fear, A. L., Volman, G., Mayer, R., Ross, P., Amikam, D., Weinhouse, H., Cohen, A., Sapir, S., Ohana, P., and Benziman, M. (1998) *J Bacteriol* **180**(17), 4416-4425
14. Ausmees, N., Jonsson, H., Hoglund, S., Ljunggren, H., and Lindberg, M. (1999) *Microbiology* **145**(Pt 5), 1253-1262
15. Rainey, P. B., and Travisano, M. (1998) *Nature* **394**(6688), 69-72
16. D'Argenio, D. A., Calfee, M. W., Rainey, P. B., and Pesci, E. C. (2002) *J Bacteriol* **184**(23), 6481-6489
17. Huang, B., Whitchurch, C. B., and Mattick, J. S. (2003) *J Bacteriol* **185**(24), 7068-7076
18. Friedman, L., and Kolter, R. (2004) *Mol Microbiol* **51**(3), 675-690
19. Spiers, A. J., Bohannon, J., Gehrig, S. M., and Rainey, P. B. (2003) *Mol Microbiol* **50**(1), 15-27
20. Vallet, I., Olson, J. W., Lory, S., Lazdunski, A., and Filloux, A. (2001) *Proc Natl Acad Sci U S A* **98**(12), 6911-6916
21. Drenkard, E., and Ausubel, F. M. (2002) *Nature* **416**(6882), 740-743
22. Boles, B. R., and McCarter, L. L. (2002) *J Bacteriol* **184**(21), 5946-5954
23. Rashid, M. H., Rajanna, C., All, A., and Karaolis, D. K. R. (2003) *Fems Microbiology Letters* **227**(1), 113-119

24. Bomchil, N., Watnick, P., and Kolter, R. (2003) *J Bacteriol* **185**(4), 1384-1390
25. Tischler, A. D., Lee, S. H., and Camilli, A. (2002) *J Bacteriol* **184**(15), 4104-4113
26. Paul, R., Weiser, S., Amiot, N. C., Chan, C., Schirmer, T., Giese, B., and Jenal, U. (2004) *Genes Dev* **18**(6), 715-727
27. Gronewold, T. M., and Kaiser, D. (2001) *Mol Microbiol* **40**(3), 744-756.
28. Kaiser, D. (2004) *Annual Review of Microbiology* **58**, 75-98
29. Jones, H. A., Lillard, J. W., Jr., and Perry, R. D. (1999) *Microbiology* **145** (Pt 8), 2117-2128
30. Romling, U., Rohde, M., Olsen, A., Normark, S., and Reinkoster, J. (2000) *Mol Microbiol* **36**(1), 10-23
31. Romling, U., Sierralta, W. D., Eriksson, K., and Normark, S. (1998) *Molecular Microbiology* **28**(2), 249-264
32. Hinnebusch, B. J., Perry, R. D., and Schwan, T. G. (1996) *Science* **273**(5273), 367-370
33. AllenVercoe, E., DibbFuller, M., Thorns, C. J., and Woodward, M. J. (1997) *Fems Microbiology Letters* **153**(1), 33-42
34. Anriany, Y. A., Weiner, R. M., Johnson, J. A., De Rezende, C. E., and Joseph, S. W. (2001) *Applied and Environmental Microbiology* **67**(9), 4048-4056
35. Zogaj, X., Nimtz, M., Rohde, M., Bokranz, W., and Romling, U. (2001) *Mol Microbiol* **39**(6), 1452-1463.
36. Wheeler, R., and Shapiro, L. (1999) *Molecular Cell* **4**(5), 683- 694
37. Sommer, J. M., and Newton, A. (1989) *J Bacteriol* **171**(1), 392-401
38. Newton, A. (1987) *Microbiol Sci* **4**(11), 338-341
39. Ohta, N., Lane, T., Ninfa, E. G., Sommer, J. M., and Newton, A. (1992) *Proc Natl Acad Sci USA* **89**(21), 10297-10301
40. Hecht, G. B., and Newton, A. (1995) *J Bacteriol* **177**(21), 6223-6229.
41. Aldridge, P., and Jenal, U. (1999) *Mol Microbiol* **32**(2), 379-391
42. Wheeler, R. T., Gober, J. W., and Shapiro, L. (1998) *Current Opinion in Microbiology* **1**, 636-642
43. Jacobs, C., Hung, D., and Shapiro, L. (2001) *Proc Natl Acad Sci U S A* **98**(7), 4095-4100.
44. Aldridge, P., Paul, R., Goymer, P., Rainey, P., and Jenal, U. (2003) *Mol Microbiol* **47**(6), 1695-1708
45. Chan, C., Paul, R., Samoray, D., Amiot, N. C., Giese, B., Jenal, U., and Schirmer, T. (2004) *Proc Natl Acad Sci U S A* **101**(49), 17084-17089
46. D'Argenio, D. A., and Miller, S. I. (2004) *Microbiology* **150**(Pt 8), 2497-2502
47. Galperin, M. Y., Nikolskaya, A. N., and Koonin, E. V. (2001) *FEMS Microbiol Lett* **203**(1), 11-21.
48. Matz, C., McDougald, D., Moreno, A. M., Yung, P. Y., Yildiz, F. H., and Kjelleberg, S. (2005) *Proceedings of the National Academy of Sciences of the United States of America* **102**(46), 16819-16824
49. O'Toole, G., Kaplan, H. B., and Kolter, R. (2000) *Annual Review of Microbiology* **54**, 49-79

50. Donlan, R. M., and Costerton, J. W. (2002) *Clinical Microbiology Reviews* **15**(2), 167-+
51. Sutherland, I. W. (2001) *Trends Microbiol* **9**(5), 222-227
52. Sutherland, I. (2001) *Microbiology* **147**(Pt 1), 3-9
53. Stewart, P. S., and Costerton, J. W. (2001) *Lancet* **358**(9276), 135-138
54. Ghigo, J. M. (2001) *Nature* **412**(6845), 442-445
55. Whitchurch, C. B., Tolker-Nielsen, T., Ragas, P. C., and Mattick, J. S. (2002) *Science* **295**(5559), 1487-1487
56. Jenal, U. (2003) *Curr Opin Microbiol In Press*
57. Jenal, U., and Malone, J. (2006) *Annual Review of Genetics* **40**(1)
58. Bobrov, A. G., Kirillina, O., and Perry, R. D. (2005) *FEMS Microbiol Lett* **247**(2), 123-130
59. Christen, M., Christen, B., Folcher, M., Schauerte, A., and Jenal, U. (2005) *J Biol Chem* **280**(35), 30829-30837
60. Schmidt, A. J., Ryjenkov, D. A., and Gomelsky, M. (2005) *J Bacteriol* **187**(14), 4774-4781
61. Tamayo, R., Tischler, A. D., and Camilli, A. (2005) *J Biol Chem* **280**, 33324-33323
62. Romling, U., Gomelsky, M., and Galperin, M. Y. (2005) *Mol Microbiol* **57**(3), 629-639
63. Zogaj, X., Bokranz, W., Nimtz, M., and Romling, U. (2003) *Infect Immun* **71**(7), 4151-4158
64. Hughes, K. T., and Roth, J. R. (1988) *Genetics* **119**(1), 9-12
65. Konishiimamura, L., Dohi, K., Sato, M., and Kobashi, K. (1994) *Journal of Biochemistry* **115**(6), 1097-1100
66. Mathew, J. A., Tan, Y. P., Rao, P. S. S., Lim, T. M., and Leung, K. Y. (2001) *Microbiology-Sgm* **147**, 449-457
67. Ross, P., Weinhouse, H., Aloni, Y., Michaeli, D., Weinbergerohana, P., Mayer, R., Braun, S., Devroom, E., Vandermarel, G. A., Vanboom, J. H., and Benziman, M. (1987) *Nature* **325**(6101), 279-281
68. Poindexter, J. S. (1964) *Bacteriol. Rev.* **28**, 231-295
69. Shedlarski, J., Jr. (1974) *Biochim Biophys Acta* **358**(1), 33-43
70. Hottes, A. K., Meewan, M., Yang, D., Arana, N., Romero, P., McAdams, H. H., and Stephens, C. (2004) *J Bacteriol* **186**(5), 1448-1461
71. Stephens, C., Christen, B., Fuchs, T., Sundaram, V., Watanabe, K., and Jenal, U. (2006) *J Bacteriol*
72. Watanabe, S., Kodaki, T., and Makino, K. (2006) *Journal of Biological Chemistry* **281**(39), 28876-28888
73. Meisenzahl, A. C., Shapiro, L., and Jenal, U. (1997) *J Bacteriol* **179**(3), 592-600
74. Jenal, U., and Fuchs, T. (1998) *EMBO J* **17**(19), 5658-5669
75. Laub, M. T., McAdams, H. H., Feldblyum, T., Fraser, C. M., and Shapiro, L. (2000) *Science* **290**(5499), 2144-2148
76. Ross, P., Mayer, R., Weinhouse, H., Amikam, D., Huggirat, Y., Benziman, M., de Vroom, E., Fidler, A., de Paus, P., Sliedregt, L. A., and et al. (1990) *J Biol Chem* **265**(31), 18933-18943.

77. Romling, U., and Amikam, D. (2006) *Curr Opin Microbiol* **9**(2), 218-228
78. Christen, B., Christen, M., Paul, R., Schmid, F., Folcher, M., Jenoe, P., Meuwly, M., and Jenal, U. (2006) *Journal of Biological Chemistry* **281**(42), 32015-32024
79. Choy, W. K., Zhou, L., Syn, C. K., Zhang, L. H., and Swarup, S. (2004) *J Bacteriol* **186**(21), 7221-7228
80. Kazmierczak, B. I., Lebron, M. B., and Murray, T. S. (2006) *Mol Microbiol* **60**(4), 1026-1043
81. Romling, U. (2002) *Res Microbiol* **153**(4), 205-212
82. Kader, A., Simm, R., Gerstel, U., Morr, M., and Romling, U. (2006) *Mol Microbiol* **60**(3), 602-616
83. Simm, R., Fetherston, J. D., Kader, A., Romling, U., and Perry, R. D. (2005) *J Bacteriol* **187**(19), 6816-6823
84. Jenal, U., White, J., and Shapiro, L. (1994) *J Mol Biol* **243**(2), 227-244
85. Ko, M., and Park, C. (2000) *J Mol Biol* **303**(3), 371-382
86. Romling, U. (2005) *Cellular and Molecular Life Sciences* **62**(11), 1234-1246
87. Bokranz, W., Wang, X. D., Tschape, H., and Romling, U. (2005) *Journal of Medical Microbiology* **54**(12), 1171-1182
88. Guvener, Z. T., and McCarter, L. L. (2003) *J Bacteriol* **185**(18), 5431-5441
89. Amikam, D., and Galperin, M. Y. (2006) *Bioinformatics* **22**(1), 3-6

List of figures

Figure 1: dynamic localization of PleD, PleC and DivJ over <i>C. crescentus</i> cell cycle	5
Figure 2: Crystal structure of PleD in complex with c-di-GMP:	7
Figure 3: <i>S. enterica</i> phenotypic changes upon conversion from planktonic to biofilm state.	82
Figure 4: <i>S. enterica</i> Tn 10dTc mutant screened on Congo Red plates	83
Figure 5: Components involved in c-di-GMP dependent cellulose production in <i>S. enterica</i>	84
Figure 6: Organization of the xylose operon xyIXABCD	88
Figure 7: Tn5 insertion sites in <i>xyIR</i>	89
Figure 8: β -galactosidase activity of P _{xyIX} :: <i>lacZ</i> reporter construct	90
Figure 9: Overview of <i>xy/O</i> suppressor mutations.....	91
Figure 10: predicted <i>xy/O</i> elements	92
Figure 11: Model for xylose dependent repression of the <i>xyIXABCD</i> operon:	93
Figure 12: Effect of <i>xyIR</i> on expression of sugar conversion pathways genes:	95
Figure 13: Overview of the c-di-GMP signaling pathway.....	100
Figure 14: Model for the allosteric feedback inhibition of DGC's	101
Figure 15: Model for the allosteric regulation of PDE activity by GTP	102
Figure 16: NMR shift map of PA4608 between free and c-di-GMP bound form	103

List of tables

Table 1: domain organization of different GGDEF and EAL proteins	4
Table 2: Global transcriptom comparison of <i>xyIR::Tn5</i> mutant strain versus a <i>xyIR</i> wild type strain	94
Table 3: Domain organization of diguanylate receptors	104

Acknowledgments

I would like to thank the following people:

My twin brother Matthias for teaching his profound knowledge about biochemistry and sharing his enthusiasm, visions and the lab during scientific fruitful three years.

Marc Folcher for sharing his expertise and teaching his art of science.

Prof Dr Kelly Hughes for introducing me into the fabulous world of Salmonella genetics, Prof Dr Markus Meuwly for his effort to teach me computational modeling approaches and Prof Dr Stephan Grzesiek for providing NMR facilities.

Assaf for his help and scientific discussions.

Martin Allan and Franziska Schmid for there substantial contribution to various scientific projects.

Flora Mauch and Marta Gerber for there enthusiasm and tremendous effort during there master thesis.

Further, I would like to thank

Sören Abel, Arnaud Basle, Carmen Chan, Wanda Dischert, Anna Dürig, Fabienne Hamburger, Jacob Malone, Michel Letzelter, Ralph Paul, Salvo San Paolo, Sherif Tawfilis, Paul Wassmann

Curriculum vitae

BEAT CHRISTEN

STRASSBURGER ALLEE 128, CH-4055 BASEL

PERSÖNLICHE DATEN

Geburtstag	20. März 1978
Heimatort	Basel
Zivilstand	ledig
Adresse	Strassburgerallee 128 Tel. 061 / 322 21 26 E-Mail: beat.christen@unibas.ch

AUSBILDUNG

Nov. 2003 – Feb. 2007	Doktorarbeit am Biozentrum der Universität Basel Institut für Mikrobiologie bei Prof. Dr. Urs Jenal
Oktober 1998 – März 2003	Biologiestudium an der Universität Basel
28.03.2003	Diplom
26.9.2000	2. Vordiplom
5.10.1999	1. Vordiplom
1994 – 1997	Gymnasium Oberwil Matura Typ. C
1990 – 1994	Progymnasium Therwil BL
1985 – 1990	Primarschule Oberwil BL

PUBLIKATIONEN

- [1] M. Christen[–], B. Christen[–], M. Allan, M. Folcher, S. Moes, P. Jenö, S. Grzesiek, U. Jenal (2006): DgrA is a member of a new family of cyclic di-GMP receptors and controls flagellar motor function in *Caulobacter crescentus* PNAS 2007
- [2] B. Christen[–], M. Christen[–], R. Paul, F. Schmid, M. Folcher, P. Jenö, M. Meuwly, U. Jenal (2006): Allosteric Control of Cyclic di-GMP Signaling *J Biol Chem*. October 20, 2006; 281 (42):32015-24. Epub August 21. 2006
- [3] M. Christen, B. Christen, M. Folcher, A. Schauerte, U. Jenal (2005): Identification and Characterization of a c-di-GMP Specific Phosphodiesterase and its Allosteric Control by GTP *J. Biol. Chem*. September 2, 2005; 280 (35):30829-37. Epub July 1, 2005
- [4] C. Stephens, B. Christen, T. Fuchs, V. Sundaram, K. Watanabe, and U. Jenal: Genetic Analysis of a Novel Pathway for D-xylose Metabolism in *Caulobacter crescentus* *J. Bacteriol*. 2007 189: 2181-2185. Epub December 15, 2006

VORTRÄGE / POSTERPRÄSENTATIONEN AN INTERNATIONALEN KONFERENZEN

2006

- [5] B. Christen[–], M. Christen[–] (2006): Mechanisms of c-di-GMP Signaling Seminar at Developmental Biology Department, *Stanford University School of Medicine, May 26, Stanford, CA USA*
- [6] B. Christen[–], M. Christen[–], R.Paul, M. Folcher, U. Jenal (2006) An Allosteric Control Mechanism Coordinates c-di-GMP Signalling *106st General ASM Conference May 21-25, 2006 Orlando, FL USA*
- [7] M. Christen[–], B. Christen[–], R.Paul, M. Folcher, S. Möes, P. Jenö, U. Jenal (2006) Isolation and Characterization of Diguanylate Receptor Proteins (DGRís) from *Caulobacter crescentus* *106st General ASM Conference May 21-25, 2006 Orlando, FL USA*
- [8] B. Christen[–], M. Christen[–], M. Allan, M. Folcher, S. Moes, P. Jenö, S. Grzesiek, U. Jenal (2006): The c-di-GMP receptor DgrA controls flagellar motor function in *Caulobacter crescentus* *Biozentrum Symposium, October 20, 2006 - Basel, Switzerland*

- [9] M. Folcher, M. Christen, B. Christen, I. Wiederkehr, S. Moes, P. Jenö, U. Jenal (2006): C-di-GMP regulate key enzyme in nucleotide biosynthesis pathway *Biozentrum Symposium, October 20, 2006 - Basel, Switzerland*
- [10] M. Allan, M. Christen, B. Christen, M. Folcher, S. Moes, P. Jenö, U. Jenal, S. Grzesiek (2006): Structural characterization of a cyclic di-GMP receptor protein. *Symposium core program structural biology and biophysics, June 16, 2006 - Basel, Switzerland*

2005

- [11] B. Christen, M. Christen, U. Jenal (2005) The Make and Break of c-di-GMP *Biozentrum Symposium 21. Oct 2005 Basel Switzerland*
- [12] B. Christen, M. Christen, M. Folcher, U. Jenal (2005) Biochemical and Genetic Identification of a c-di-GMP Binding Motif *2nd ASM Conference on Prokaryotic Development July 13 - 16, 2005 Vancouver Canada*
- [13] R. Paul, M. Christen, B. Christen, A. Schauerte, P. Jenö, U. Jenal (2005) The PleD Diguanylate Cyclase is Activated Through Dimerization and is Subject to Tight Allosteric Feedback Control *2nd ASM Conference on Prokaryotic Development July 13 - 16, 2005 Vancouver Canada*
- [14] M. Christen, B. Christen, M. Folcher, A. Schauerte, U. Jenal (2005) Identification and Characterization of a c-di-GMP Specific Phosphodiesterase and its Allosteric Control by GTP *2nd Caulobacter meeting July 11 - 13, 2005 Vancouver Canada*
- [15] B. Christen, M. Christen, R. Paul, T. Schirmer, P. Jenö, U. Jenal (2005): A Novel Regulatory Mechanism Controls the Production of c-di-GMP by Diguanylate Cyclases *SSM SGM annual Congress 31.3.-1.4 2005 Geneva Switzerland*
- [16] M. Christen, B. Christen, R. Paul, A. Schauerte, T. Schirmer, P. Jenö, U. Jenal (2005): A Novel Regulatory Mechanism Controls the Production of c-di-GMP *SWIMM Meeting 15-17 March 2005 ETH Zürich Switzerland*
- [17] M. Christen, B. Christen, M. Folcher, A. Schauerte, T. Schirmer, T. Augst, U. Jenal (2005): Identification of a c-di-GMP specific Phosphodiesterase & its allosteric control by GTP *SWIMM Meeting 15-17 March 2005 ETH Zürich Switzerland*

2004

- [18] M. Christen, R. Paul, B. Christen, A. Schauerte, P. Jenö, U. Jenal (2004): Characterization of the c-di-GMP binding site of the diguanylate cyclase (DGC) *PleD Biozentrum Symposium 14. Oct 2004 Basel Switzerland*
- [19] B. Christen, M. Christen, U. Jenal (2004): Interaction Map of two-Component Signal Transduction Proteins in *Caulobacter crescentus EuroConference on Inter- and Intracellular Signalling and Global Regulation in Bacteria 8-13 May 2004 Barcelona Spain*

2002

- [20] B. Christen, U. Jenal (2002): *Experimental evolution of development and morphology with Caulobacter crescentus 61th Assembly of SSM, Luzern Switzerland Feb 2002*
- [21] B. Christen, M. Ackermann, U. Jenal (2002): *The cause of morphological divergence in experimental evolution of Caulobacter crescentus*“, *Caulobacter Meeting, Ville de Lac-Delage, Québec, Canada*

ASSISTENZEN

Teaching assistantship in Microbiology block course 2004-2006 (2 weeks per year) *at the Biozentrum, **University of Basel**, Switzerland*

Teaching assistant at the Advanced Bacterial Genetic Course June 8-28, 2005, **Cold Spring Harbor Laboratory**, Long Island, New York

Teaching assistant at the Advanced Bacterial Genetic Course June 9-29, 2004, **Cold Spring Harbor Laboratory**, Long Island, New York

KURSE

Personal training in microarray techniques, November 6-20 2004, *Bauer Center for Genomics Research, **Harvard University**, Boston*

BETREUUNG UND KONZEPTIONIERUNG VON MASTERARBEITEN

F. Mauch (2006): Genetic Identification of Diguanylate Receptor Proteins Regulating Biofilm Formation in *Salmonella enterica* Serovar Typhimurium. *Masterthesis of F. Mauch supervised by B & M. Christen, Laboratory of Prof. Dr. Urs Jenal, Oktober 2005 - Oktober 2006 - Biozentrum University of Basel*

M. Gerber (2006): Designing Diguanylate Cyclase Inhibitors. *Masterthesis of M. Gerber supervised by M & B. Christen, Laboratory of Prof. Dr. Urs Jenal, Oktober 2005 - November 2006 - Biozentrum University of Basel*

M. Christen (2003): Overexpression of TocA - A Tocopherol Cyase from *Anabaena* sp. *Diplomathesis of M. Christen supervised by B. Christen, Laboratory of Prof. Dr. Urs Jenal, November 2002 - March 2003 - Biozentrum University of Basel*

DIPLOMARBEIT

B. Christen (2006): The cause of morphological divergence in experimental evolution of *Caulobacter crescentus*. *Diplomathesis of B. Christen supervised by M. Ackermann, Laboratory of Prof. Dr. Urs Jenal, August 2001 - August 2002 - Biozentrum University of Basel*

ANNERKENNUNG/AUSZEICHNUNG

Oktober 2004 Posterprize Biozentrum Symposium 2004

BERUFSERFAHRUNGEN WÄHREND DES STUDIUMS

May. 2002 – Jun. 2002

Gymnasium Oberwil

Stellvertretung in Physik

Mar. 1998 – Jun. 1999

DataLynx GmbH Basel

Informatikpraktikum

Web-Dienste/Server – Server design and hosting

Apr. 2001 – May. 2001

Sekundarschule Therwil

Stellvertretung in Mathematik, Biologie, Physik

SPRACHEN

Deutsch

Muttersprache

Englisch

mündlich und schriftlich

Französisch

mündlich und schriftlich

Spanisch

mündlich